Universidad Autónoma de Madrid

Programa de Doctorado en Biociencias Moleculares

Enhancing B and T cell immune responses against the HIV-1 envelope using protein and poxvirus based vaccines

SURESH CHITHATHUR RAMAN

MADRID, 2018

Departamento de Biología Molecular
Facultad de Ciencias
Universidad Autónoma de Madrid

Enhancing B and T cell immune responses against the HIV-1 envelope using protein and poxvirus based vaccines

Memoria de Tesis Doctoral presentada por **Suresh Chithathur Raman** (M.Biotech, B.Tech-Biotechnology) para optar al Grado de Doctor en Biología Molecular por la Universidad Autónoma de Madrid.

Director de Tesis: **Mariano Esteban Rodríguez**

Centro Nacional de Biotecnología (CNB-CSIC),

Madrid, 2018.

DECLARATION

I, Suresh Chithathur Raman, declare that the thesis entitled ``Enhancing B and T cell immune responses against the HIV-1 envelope using protein and poxvirus based vaccines ´´ and the work presented in it, carried out at CNB-CSIC under the guidance of Prof. Mariano Esteban Rodríguez, are my own. No part of this work has previously been submitted for a degree or any other qualification at this university or any other institution.

Suresh Chithathur Raman
Candidate

Prof. Mariano Esteban Rodríguez
Thesis Director

ACKNOWLEDGEMENTS

I have to thank a lot of people, all of whom have played a role, big or small, in this journey of mine. The following is a humble attempt at expressing my gratitude to all of you, albeit in no particular order.

I am very grateful to my supervisor Mariano Esteban for everything he has done – from accepting me into the lab, providing me with great guidance on the project and supporting me on this journey towards my Phd. Thank you, Mariano – without you, your excellent insight, patience and trust in me, none of this would have been possible.

My deepest gratitude goes out to the *La caixa* foundation for the wonderful financial support extended to me. Thanks to the scholarship, I was able to live in and enjoy one of the best cities in Europe during my PhD.

Amma, Appa and Raghav, I thank you for being there for me right from my day one. Words cannot describe the sense of gratitude and appreciation I have for all the sacrifices you have done for putting me where I am. I am extremely grateful to all of you and I love you all to bits!

Keerthi, I have to thank you from the bottom of my heart for being there for me da. You have no idea of how much your friendship has meant to me over these years. Thank you being there for me and my (our) family da mamae!

Dearest Carmen and Jas - we´ve been in this together literally from day one and I have enjoyed every minute of this experience, thanks to you guys! You have been a constant source of support throughout these years – something that only the best of friends can offer. I simply could not have done this without having the both of you by my side. Thank you for everything! And Raj, thank you for being such a great friend and companion – it was great to share a house, your wonderful cooking and countless coffee-moments with you!

Lore! You´ve made such a difference to my life during these years. I have had so many memorable moments with you and you always seem to bring a smile to my face. Thank you for adopting me as a part of your life and your family. I really appreciate everything you have done for me!

Bea, you have been a great source of support right from the day one, both inside the lab and otherwise, thank you for all that you have done for me! Carmen, I have learnt a lot from you and I greatly appreciate your insightful guidance whenever I have needed them – thank you for all your help! Aneesh, I am very grateful to you for all your help and support – I have learnt a lot from you and having you guiding me through the first steps of my project was of immense help indeed! Juan, thank you for helping me out in numerous occasions – without you, I wouldn´t have gotten a visa to come to Spain in the first place!

I thank Chogüi and Cristina for their excellent technical help with many of my experiments. Thank you, María, Patri and Adri for making my stay in this laboratory a memorable and enjoyable one and helping me out whenever I have needed the same.

My sincere thanks also goes out to ex-112 lab members Lucas, Mauro, Ana and Mariví for accepting me into the lab and helping me out, especially during the first few days of my stay here. I really appreciate your being there for me whenever I needed any help – thanks a ton!

Liliana, I have immensely enjoyed your love, support and guidance throughout these years and I hope to enjoy the same for years to come - thank you for everything!

I also have to thank a lot of people who have helped me a lot in carrying out the work presented in this thesis: César, thank you for all your invaluable help with the protein purifications – I have truly enjoyed and learnt a lot from all the conversations that we have had! Mar and Ana, thank you for all your wonderful help with the EM analysis – it has been a real pleasure collaborating with you. My gratitude also goes out to Dr. Magda Stadnik at the Netherlands Cancer Institute (NKI) for the excellent work with the bio-physical characterization of the proteins. I sincerely thank the Instruct integrating biology platform for providing the iNEXT structural audit grant for helping us collaborate with the NKI.

A special thanks to my family in Spain – Ani, Lute, Mari Carmen and Domingo for making me feel at-home in this new country. I have immensely enjoyed the time spent with all of you and I look forward to spending more of it in the future.

My deepest gratitude also goes out to my previous project supervisors – Dr. Ashok Kumar Manickraj, Dr. Ben Schulz and Prof. Ross Barnard for all the help, support and

guidance they have offered me during my formative years. I wouldn´t be here if it wasn´t for them – I thank them deeply for their trust in me and my abilities.

There are a lot of people I need to thank for being there for me and making this journey a memorable and enjoyable one: Soco, Iván, Carol, Santa, Marina, Mari Carmen, Marcos and the entire CNB support staff. Immanuel, Sugirtha, Srividya, Suhail and Viswa – thank you guys for everything you have done for me!

And my dearest Ernest - words fail me when I think of what to say to you! You have been an incredible support to me, within the lab and outside – being there for me whenever I needed your help, in the best and the worst of times. You have donned so many caps in your gracious efforts towards helping me – that of an excellent (and strict) teacher, a magnanimous friend and a caring brother - I cannot thank you enough for all that you have done for me. You are one of the best human beings that I know of and you deserve a lot of happiness and great success in life. To you, I dedicate this thesis.

PRESENTACIÓN

El objetivo del proyecto ha estado dirigido a establecer procedimientos de inmunización en el modelo de ratón incorporando una serie de inmunógenos que fueran capaces de inducir respuestas inmunes tanto humorales (anticuerpos) como celulares (linfocitos T $CD8^+$, Tfh y células B de centros germinales) con capacidad potencial para controlar la infección por el virus de la inmunodeficiencia humana tipo 1 (VIH-1).

La novedad del proyecto radica en la generación de una proteína de fusión compuesta por la glicoproteína GP120 del VIH-1 subtipo C (el subtipo más prevalente) fusionada en su extremo C-terminal con la proteína 14K (gen *A27L*) del virus vaccinia; el diseño se centra en mejorar la eficacia del antígeno GP120C mediante su oligomerización mediada por la sección de la proteína 14K. Las mejoras en la respuesta inmune obtenidas por la fusión de antígenos heterólogos con la proteína 14K del virus vaccinia, han sido previamente demostradas por el laboratorio del Dr. Esteban en el modelo de Malaria mediante la fusión de la proteína 14K a la proteína CS (circumsporozoito) de *Plasmodium falciparum.*

En el proyecto de Tesis se propuso generar tres tipos diferentes de inmunógenos: proteína purificada GP120C14K, vector de DNA expresando la proteína de fusión y vector viral MVA expresando la proteína de fusión. Al mismo tiempo se generaron vectores equivalentes pero expresando la proteína GP120C como control para los análisis estructurales, funcionales e inmunológicos.

Se ha realizado el diseño de las diferentes proteínas y la generación de líneas celulares CHO transfectadas de forma estable para la producción constitutiva de la proteína de fusión GP120C14K o de la proteína monomérica GP120C; ambas proteínas se han purificado mediante columnas de afinidad de lectina y cromatografía de exclusión por tamaño. Asímismo, se ha llevado a cabo la caracterización estructural, el análisis bioquímico y biofísico, microscopía electrónica y difracción de rayos X (en proceso).

Se ha generado el vector recombinante basado en el virus modificado de Ankara (MVA) expresando el antígeno GP120C14K siguiendo los protocolos estándar de recombinación homóloga. El virus MVA-GP120C14K resultante se ha caracterizado *in vitro,* habiéndose evaluado su capacidad de crecimiento, la estabilidad del antígeno

heterólogo y la calidad/cantidad del antígeno expresado comparándolo con el virus control MVA-GP120C.

Una vez generadas y caracterizadas las diferentes construcciones, se ha llevado a cabo la última parte del proyecto centrada en la evaluación inmunológica de estos vectores en el contexto de un protocolo de vacunación "prime-boost" en el modelo de ratón.

Se han realizado dos ensayos en el modelo de ratón orientados hacia el estudio del aumento potencial de la respuesta de células B y T en ratón por parte del antígeno GP120C14K comparado con el control monomérico GP120C mediante tres procedimientos de inmunización "prime-boost": 1) proteína-proteína; 2) vector MVA-proteína; 3) combinación vector DNA-vector MVA-proteína.

Los ensayos de inmunogenicidad se han realizado a partir de los esplenocitos, de las células de los nódulos linfáticos drenantes y del suero de los ratones inmunizados con los diferentes protocolos de vacunación. Se ha medido la expresión de citoquinas relevantes en el contexto de la inducción de una respuesta celular específica, la magnitud y fenotipo de las células B específicas, las células B de centros germinales específicos y las células Tfh o "T follicular helper" en el contexto de la vacunación frente a la Envuelta de VIH-1 y la presencia de anticuerpos frente a GP120C en las muestras de suero.

Los resultados obtenidos demuestran que la proteína de fusión GP120C14K forma oligómeros en forma de hexámeros y que éstos son solubles y superiores a la forma monomerica de GP120C en su capacidad para inducir respuestas inmunes humorales y celulares frente al VIH. Se ha valorado que los protocolos basados en la combinación de MVA/proteína y DNA/MVA/proteína confieren una mayor ventaja inmunogénica para la proteína de fusión sobre la no fusionada y se ha propuesto un modelo de acción inmune frente al VIH-1.

SUMMARY

The objective of this project was directed towards establishing immunization protocols in the mice model using a series of immunogens that are able to induce immune responses, both humoral and cellular, with the capacity to control the infection by the Human Immunodeficiency Virus type 1 (HIV-1).

The novelty of the work lies in the generation of a fusion protein comprised of the envelope glycoprotein GP120C of the HIV-1 clade C (the most prevalent subtype) fused in its C-terminal end with the protein 14K (A27L gene) from Vaccinia virus. The design is based on improving the immunogenicity of the GP120C protein through its oligomerization facilitated by the fused 14K protein.

The contribution of the vaccinia virus 14K protein in improving the immunogenicity of heterologous antigens has been previously demonstrated by the Esteban laboratory in the Malaria model where the circumsporozite or CS protein from *Plasmodium falciparum* was fused with the 14K protein.

As a part of this Thesis work, three different immunogens were generated: GP120C14K purified fusion protein, a DNA vector expressing the fusion protein and a viral vector MVA expressing the fusion protein. Simultaneously, equivalent vectors expressing the monomeric protein GP120C were developed as a control for structural, functional and immunological analyses.

The proteins were designed and produced by the generation of CHO cell lines stably transfected for the production of the fusion protein GP120C14K and the monomeric protein GP120C. Both the proteins were purified using lectin affinity columns and size exclusion chromatography. The structural characterization, biochemical and biophysical analysis, electron miscroscopy and X-ray diffraction studies (in process) of the fusion protein have been carried out.

A recombinant viral vector based on the modified Vaccinia virus Ankara (MVA) expressing the fusion antigen GP120C14K has been generated following standard homologous recombination protocols. The resulting virus – MVA-GP120C14K has been characterized *in vitro* for its growth and replication capacity, stability of the inserted heterologous antigen and the quality/quantity of the antigen expression compared with that of the control virus MVA-GP120C.

After developing the vectors expressing the fusion antigen, the final stage of the project i.e., the immunological evaluation of these vectors was carried out in a standard prime-boost vaccination protocol in mice. Two *in vivo* assays have been conducted to analyse the potential of the GP120C14K antigen in enhancing the B and T cell responses in comparison with the monomeric antigen GP120C through three different prime-boost protocols of immunization: 1) protein – protein, 2) MVA vector – protein and 3) DNA vector – MVA vector – protein.

The immunological assays performed on Splenocytes, cells from the draining Lymph Nodes and serum of the vaccinated mice included the monitoring of the expression of cytokines relevant to the vaccination by CD8 T cells, determination of the content of antigen specific B cells, analysis of Germinal Center B cells and T follicular helper cells specific to the context of vaccination against the HIV-1 envelope and the determination of antibodies against the envelope protein in the serum samples by ELISA.

The results obtained demonstrate that the fusion protein GP120C14K forms oligomers that are hexameric in structure, soluble and are superior to the monomeric GP120C protein in terms of the capacity to induce humoral and cellular responses against HIV-1. It has been shown that the immunization protocols that are based on the combination of MVA/protein and DNA/MVA/protein largely confer an immunogenic advantage in the case of the fusion antigen GP120C14K over the monomeric antigen GP120C and a model of action against HIV-1 has been proposed for the same.

INDEX

ABBREVIATIONS

Ab	Antibody.
Ag	Antigen.
AIDS	Acquired Immunodeficiency Syndrome.
APC	Antigen Presenting Cell.
bNAb	Broadly Neutralising Antibody.
CCR5	C-C chemokine receptor type 5.
cART	Combination Antiretroviral Therapy.
CEV	Cell-associated Enveloped Virus.
CSP	Circumsporozoite Protein.
CTL	Cytotoxic T Lymphocyte.
CXCR4	C-X-C chemokine receptor type 4.
DAB	Diaminobenzidine tetrahydrochloride.
DMEM	Dulbecco´s Modified Eagle´s medium.
DNA	Deoxyribonucleic Acid.
dsRNA	Double stranded ribonucleic acid.
E.coli	*Escherichia coli*.
EDTA	Ethylene Diamine Tetraacetic Acid.
ELISA	Enzyme Linked Immunosorbent Assay.
ELISPOT	Enzyme Linked Immunosorbent Spot Assay.
Env	Envelope.
EV	Enveloped Virion.
GC	Germinal Center.
GS	Glutamine Synthetase.
HA Locus	Hemagglutinin Locus.
HIV	Human Immunodeficiency Virus.

HRPO	Horseradish Peroxidase.
i.d	Intradermal.
IEV	Intra-cellular Enveloped Virus.
IFN	Interferon.
Ig	Immunoglobulin.
IL	Interleukin.
i.m	Intramuscular.
i.p	Intraperitoneal.
ITR	Inverted Terminal Repeat.
kDa	Kilodalton.
LB	Luria-Bertani.
LPS	Lipopolysaccharide.
mAb	Monoclonal Antibody.
MCS	Multiple Cloning Site.
MEM	Minimum Essential Medium.
mg	milligrams.
MHC	Major Histocompatibility Complex.
min	Minute.
mM	Milli Molar.
MOI	Multiplicity Of Infection.
MV	Mature Virion.
MVA	Modified Virus Ankara.
NYVAC	New York Vaccinia Virus.
ng	Nanograms.
OD	Optical Density.
ORF	Open Reading Frame.

PBS	Phosphate Buffer Saline.
PFU	Plaque Forming Units.
RNA	Ribonucleic Acid.
rpm	Revolutions per minute.
RT	Reverse Transcriptase.
SDS-PAGE	Sodium Dodecyl Sulfate Polyacrylamide Gel Electrophoresis.
TCA	Trichloroacetic Acid.
TK locus	Thymidine Kinase locus.
TLR	Toll Like Receptor.
TNFα	Tumor Necrosis Factor-α.
VACV	Vaccinia.
VLP	Virus-like particles.
wt	Wild-type.
µg	Micrograms.
µl	Microlitres.
µM	Micromolar.

1. INTRODUCTION

1.1 The AIDS pandemic and HIV diversity

The Acquired Immunodeficiency Syndrome or AIDS is one of the most devastating human disease pandemics challenging global health currently, with more than 35 million deaths worldwide attributed to it so far (Global Health Observatory data, World Health Organisation, 2018 - http://www.who.int/gho/hiv/en/). Ever since the isolation of the Human Immunodeficiency Virus (HIV) as the causative agent behind AIDS in 1983 (Barré-Sinoussi et al., 1983, Gallo et al., 1983), widespread research on a global scale is being carried out in order to understand the virus and its mechanism of action, paving the way for encouraging treatment options and throwing clues for possible prophylactic and therapeutic agents.

HIV is a lentivirus that belong to Retroviridae – an unique family of viruses that uses a reverse transcriptase (RT) enzyme to produce DNA from the negative single strand RNA genome that they carry within (Frankel and Young, 1998). HIV is classified into two groups – HIV-1, which is responsible for the majority of the widespread AIDS pandemic, and HIV-2, which is the mild or less virulent version confined to specific regions of West Africa.

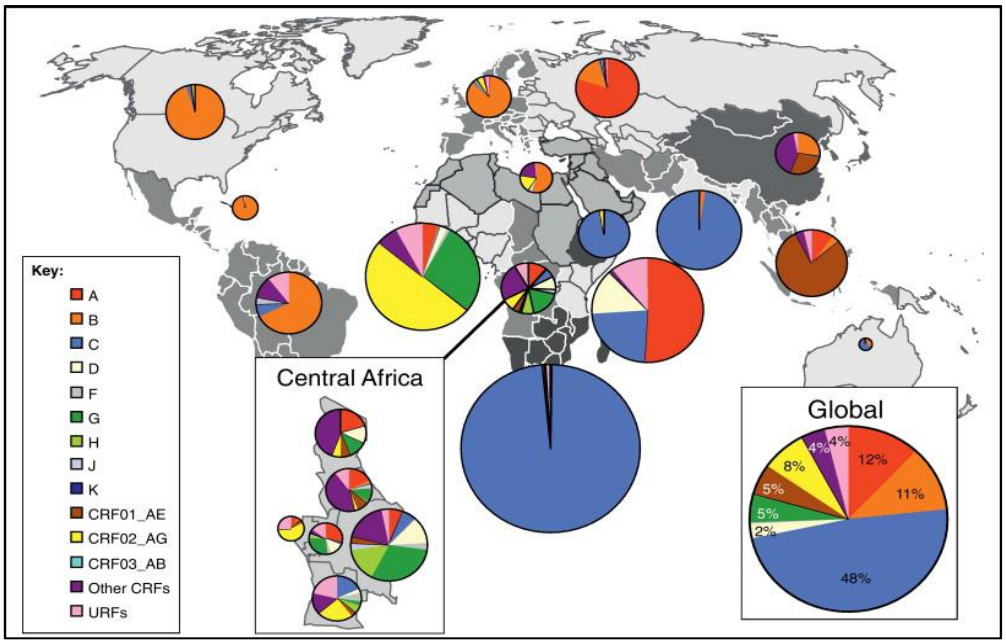

Fig. 1. Global distribution of major HIV-1 subtypes and recombinants. The surface area of the pie charts corresponds to the relative number of people living with the disease in that particular region. Clade C represents almost half (48%) of all the HIV-1 infections. Figure adapted from (Hemelaar, 2012).

The HIV-1 virus shows high genetic diversity owing largely to the error-prone reverse transcriptase enzyme, the selective immune pressure from the host and the replication process (including recombination events and the high turnover rate of the virus) (Buonaguro et al., 2007). In general, HIV-1 is grouped into three phylogenetic forms: main or "M" (which is responsible for the majority of the infections), outlier or "O" and non-M/O or "N". The M group is further classified into ten subtypes or clades (A, B, C, D, E, F, G, H, I, J and K) (Hemelaar, 2012, Sharp and Hahn, 2011). The global distribution of the HIV-1 subtypes is represented in Fig 1. Of particular interest to this work is the clade C, which accounts for almost half of the total HIV-1 infections worldwide and is highly prevalent in developing countries like India and South Africa, where eradication efforts are further complicated by economic and cultural challenges.

1.2 The HIV replication cycle

The predominant targets of HIV-1 virus are the activated CD4 T lymphocytes to which the virus attaches through interactions between the envelope spike and the CD4 molecule present on the target surface, aided by the chemokine co-receptors CCR5 and CXCR4 (Chan and Kim, 1998). Resting CD4 T cells and other cell types that contain the CD4 and chemokine receptors such as macrophages and dendritic cells are also known to be infected by the virus (Steinman et al., 2003, Koppensteiner et al., 2012). Following attachment, the viral and target cell membranes undergo fusion through the conformational change of the HIV-1 envelope protein (Fig. 2), thereby allowing the viral core including the reverse transcriptase, integrase and other viral proteins to enter the cytosol (Sanders and Moore, 2014). The error-prone reverse transcriptase enzyme from the virus then converts the viral RNA to double stranded DNA, introducing approximately 1.1 mutations per viral genome, thereby contributing to the wide sequence diversity of the HIV-1 (Gao et al., 2004).

The viral genome thus produced is transported to the nucleus, where it is eventually integrated into the target genome, resulting in the "provirus" state, which is followed by transcription through cellular machinery and the production of infectious viruses which are released from the cell to infect new target cells (Craigie and Bushman, 2012). The provirus is also known to exist in a latent state where it is not recognized by the host immune system (such as the cytotoxic CD8 T cells) and therefore might become active at a later stage and infect CD4 T cells again (Palmer et al., 2011). Eventually, this repeated infected cycle might lead to an immune system that is seriously compromised,

giving rise to several complications that are characteristic of AIDS. The HIV replication cycle is depicted in Fig. 2.

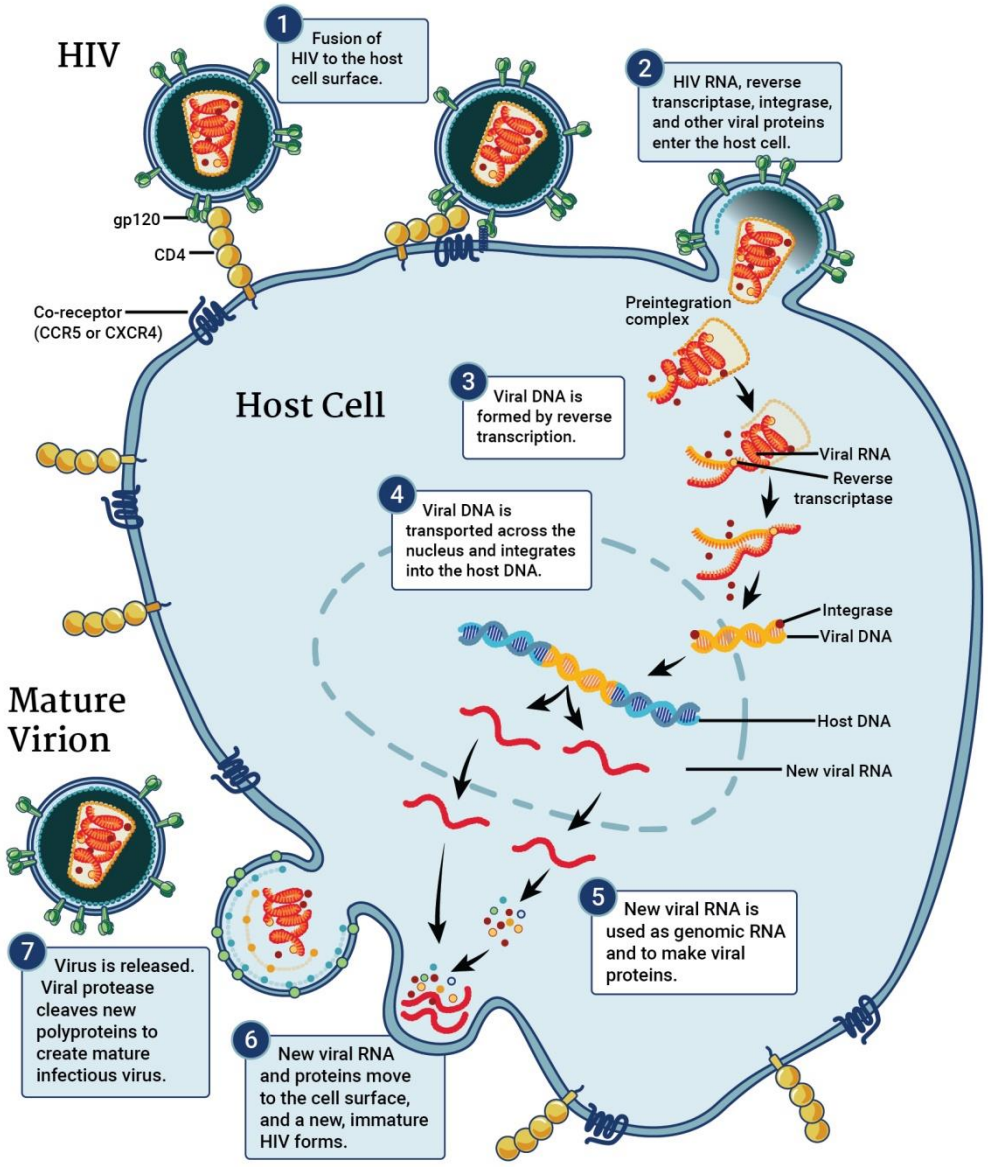

Fig. 2. HIV replication cycle showing the steps involved from host cell attachment to mature virion release. Image adapted from the National Institute of Allergy and Infectious Diseases (NIAID) webpage on the HIV replication cycle (https://www.niaid.nih.gov/diseases-conditions/hiv-replication-cycle).

1.3 The Envelope protein

The GP120, present as a heavily glycosylated trimeric structure on the surface of the HIV-1 particle, represents the most exposed antigenic form of the viral protein products. The GP120 protein consists of five heavily conserved regions, named sequentially as C1

to C5, and five heavily variable regions, named V1 to V5 (Starcich et al., 1986). Each of the GP120 protein present in the trimer is non-covalently bound to the corresponding GP41 molecule, present as a transmembrane trimeric complex. Each GP41 molecule consists of a cytosolic C terminal region, a transmembrane region and an external domain with two heptad repeat regions. Synthesis of the GP120 and GP41 starts with the common *Env* gene translational product GP160 (Fig. 3). This precursor protein contains numerous sites for N-linked glycosylation and therefore, is co-translationally glycosylated in the endoplasmic reticulum. Further glycan processing occurs during the protein transport through the Golgi apparatus and the protein is also subjected to cleavage by furin proteases. The final product is a heavily glycosylated envelope trimer containing three GP120 and three GP41 molecules (Checkley et al., 2011). During HIV replication, the trimeric envelope protein facilitates the infection process by binding to the CD4 receptor, following which the protein undergoes a conformational change and thereby exposes the residues necessary for the CCR5 and CXCR4 binding (Fig. 3). Due to its antigenic nature and immune exposure in the virion and cell surface, the envelope protein of HIV-1 is of high importance in the design and development of vaccine strategies.

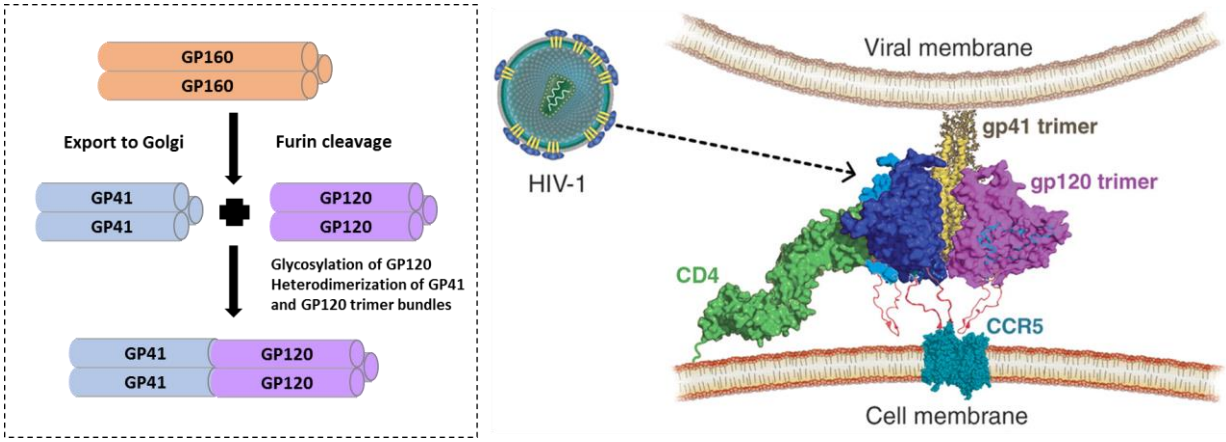

Fig. 3. The HIV-1 envelope protein. Left panel: Processing of the GP160 polyprotein to yield the (GP120 + GP41) trimeric structure, adapted from original image by Ian Perrone (https://microbewiki.kenyon.edu/index.php/HIV_Envelope_and_Cell_Fusion). Right panel: Structure and organisation of the envelope trimer on the surface of the HIV-1 virus and its interaction with CD4 on the host membrane, adapted from (Walker and Burton, 2008).

1.4 An elusive HIV vaccine

The advent of combination antiretroviral therapy (cART) and the current availability of more than 30 antiretroviral drugs that affect different stages of the viral replication cycle, have led to drastic reductions in HIV-associated deaths, increase in patient survival and prevention of further transmission (Cihlar and Fordyce, 2016). However, with 36.7 million people living with HIV at the end of 2016, including 1.8 million new infections and 1 million deaths attributed to AIDS in that year alone (Global Health Observatory data, World Health Organisation, 2018 - http://www.who.int/gho/hiv/en/), the need for an eradication strategy for the virus and the disease is at an all-time high, with a major focus on prevention through vaccination.

1.4.1 Obstacles and Challenges

The fact that more than three decades of intensive and widespread research has yet to yield an effective vaccine against HIV-1 can broadly be attributed to three main factors:

1. Characteristics of HIV-1 infection: the narrow window of clearance opportunity that the virus presents to the immune system between the initial infection and the integration of HIV genome and the subsequent establishment of latent infections.
2. High genetic diversity and mutations that allow the virus to escape detection and clearance by the immune system.
3. Features of the envelope protein that make it an extremely hard target for vaccine design, summarised in Table 1.

Characteristic	Implication for Vaccine Design
Genetic variability of the virus.	The sparsely available conserved epitopes such as the CD4 binding site are rendered structurally inaccessible for antibodies (by variable loops, etc.) (Kwong et al., 2002).

Heavy glycosylation of the protein.	Only about 3% of the protein is available for antibody interaction, effectively shielding important binding sites and conformations (Pancera et al., 2014).
"Breathing" of the envelope between different conformational states.	Reduction in the possibilities of low-affinity naïve B cell receptor binding (Munro et al., 2014).
Limited numbers of only about 8 to 12 Env spikes are typically present on the virion surface.	Reduction in avidity-based binding and the cross linking of B cell receptors (Klein and Bjorkman, 2010).
GP120 shedding by some virions owing to the weak GP120-GP41 interactions (Moore et al., 2006).	Elimination of quaternary epitopes on the trimeric structure and the exposure of non-neutralizing epitopes, inviting non-neutralizing antibody development (Burton and Mascola, 2015).

Table 1. Features of the HIV-1 envelope protein showing the complexity in using it as a target for vaccine design.

1.4.2 Efficacy trials and lessons learnt

Four different vaccine strategies have thus far been tested in human clinical efficacy trials, in-line with the shift in focus of the vaccine community between antibody-based and cytotoxic T cell (CTL) based approaches. Although three of these strategies failed to provide any evidence of protection against the virus and only one of them showed a moderate protection, these studies provide a basis for a better in-depth understanding of the different components used in a HIV-1 vaccine system and how they can work in a real-world scenario:

a. The first Phase III efficacy trials, termed VAX003 and VAX004, were conducted to evaluate the ability of a bivalent purified envelope GP120 protein based vaccine to confer antibody-based protection against HIV-1 (Pitisuttithum et al., 2006). After no vaccine related efficacy was observed in spite of high antibody levels (Gilbert et al., 2005), the focus shifted to CTL strategies for HIV-1 prevention.

b. An adenovirus type 5 (Ad5) based vaccine deemed to induce strong CTL response against HIV-1 was evaluated in two Phase II b trials (Buchbinder et al., 2008, Gray et al., 2011). After observing a transient increase in the incidence of the HIV infection among some vaccine recipients, both the studies were terminated early. However, later

analysis of the study samples revealed that the specific T cell responses mounted by the virus was able to exert some immune pressure on the viruses that encoded the same epitopes (Rolland et al., 2011), providing some proof of efficacy for the CTL based vaccine concept.

c. A multi-clade DNA prime + recombinant Ad5 boost approach (Churchyard et al., 2011), was tested in a Phase II b efficacy trial called HVTN505 that effectively excluded risk groups previously identified by the earlier Ad5 trials. The trial was halted after no protective efficacy (prevention of HIV infection or set-point viral load reductions) were observed among the groups receiving the vaccine (Hammer et al., 2013).

d. The RV144 trial conducted in Thailand in 2009 is the only HIV-1 Phase III efficacy trial that showed some degree of protection (31.2%) against the virus. The study included a combination of approaches: a Canarypox vector prime (ALVAC-HIV) designed to elicit CTL responses and a GP120 protein boost (AIDSVAX B/E) aimed at inducing antibody based protection (Rerks-Ngarm et al., 2009). Although criticised initially for its inability to induce strong neutralizing antibody or CTL responses (Burton et al., 2004), the combination of the two approaches has proven to be effective to at least a moderate degree, when compared with the disappointing results obtained in the other studies, pointing to the fact that protection is possible from HIV-1 acquisition through vaccination.

Following the strategy employed in the RV144 trial, an effective vaccine for HIV should, therefore, aim to equip both the cellular and humoral responses against the virus i.e., it should be able to induce both cytotoxic T lymphocytes and broadly neutralizing antibodies specific to HIV-1. While the search is on for an ideal protein immunogen that can attract neutralizing antibodies against HIV-1, the use of poxvirus based vectors towards equipping the cell-based anti-HIV immunity is of special importance to this work.

1.5 Poxvirus based vaccine vectors

The *Poxviridae* family consists of two subfamilies: *Chordopoxvirinae* (that infects vertebrates and is further classified into 8 genera - *Orthopoxvirus, Parapoxvirus, Avipoxvirus, Capripoxvirus, Leporipoxvirus, Suipoxvirus, Molluscipoxvirus* and *Yatapoxvirus)* and *Entomopoxvirinae* (that infects insects and is further classified into 3

genera - *Alphaentomopoxvirus, Betaentomopoxvirus* and *Gammaentomopoxvirus)* (Mercer et al., 2007). Poxviruses share the following characteristics: a covalently linked double-stranded DNA, a relatively large genome (130 to 360 Kbps), an evolutionary origin that is distinct to those of the other DNA viruses and a highly conserved cytoplasmic replicative cycle (McFadden, 2005, Hughes et al., 2010).

Poxviruses are widely popular due to the most (in)famous member, Variola – the causative agent of smallpox, one of the most devastating diseases that have affected humankind. Smallpox is the first and the unique human infectious disease to have been declared as completely eradicated by the World Health Organization in 1980 (Smith, 1990, Artenstein and Grabenstein, 2008). The other most popular virus that belongs to the *Poxviridae* family is perhaps the Vaccinia virus (subfamily: *Chordopoxvirinae*, genus: *Orthopoxvirus*). To its credit, Vaccinia virus (VACV) was one of the principal active constituents of a smallpox vaccine that was used extensively towards the eradication of the terrible disease caused by its notorious cousin, Variola virus. VACV is the most studied member of the *Poxviridae* family. It was the first animal virus to have been visualized under electron microscopy, grown successfully in cell culture and physically purified while having been subjected to extensive biochemical and molecular analysis (Moss et al., 2007), not surprising given the plethora of vaccine opportunities it presents through its attenuated strains.

The fact that poxvirus based vectors have been tested extensively in pre-clinical and clinical trials vouches for their safety and utility in the vaccine field. There are, in fact, several poxvirus based vaccines approved for use in veterinary medicine (Bhanuprakash et al., 2012). Several factors make poxviruses an excellent platform for the development of new and effective vaccines (Pastoret and Vanderplasschen, 2003):

a. The ability to incorporate large amounts of foreign DNA – this is particularly important considering that specific antigens of different models may require the expression of one or several large gene fragments.

b. The ease of generation of stable recombinant vectors and the relatively high levels of foreign antigen expression by such recombinants.

c. Ease of manufacture – scaling and economic barriers are relatively easily crossed while using poxviruses as vaccines. The viruses can be easily

manufactured using cell culture systems and purified for commercial or large-scale use.

d. High degree of stability of the vaccine in freeze-dried conditions and the ease of administration.

1.6 Vaccinia Virus

1.6.1 Virion Structure

Vaccinia virus particles are observed as brick-shaped virus particles with dimensions of 360 x 270 x 250 nm, as shown in Fig 1.4. Infective vaccinia virus exists in two forms – the Mature Virion (MV) and the Enveloped Virion (EV) – that differ on the number of outer membranes and the type of viral and glycoproteins present on their surface (McFadden, 2005, Smith et al., 2002), as seen in Fig 4. The MVs are enveloped by an 8 nm outer layer and an inner lipid membrane of about 5 nm thickness, while the EV has an additional outer envelope containing viral and cellular proteins (absent in MV). Inside the virions, the genomic DNA, structural proteins and transcriptional enzymes are present in the nucleus, covered by a 18 nm thick core wall (Cyrklaff et al., 2005). During the replication cycle, two more intracellular forms are produced: the intracellular enveloped virus (IEV) that is formed through the wrapping of an assembled mature virus by a Golgi-derived lipid membrane and the cell-associated enveloped virus (CEV) that is formed when IEV fuses to the cell membrane prior to release.

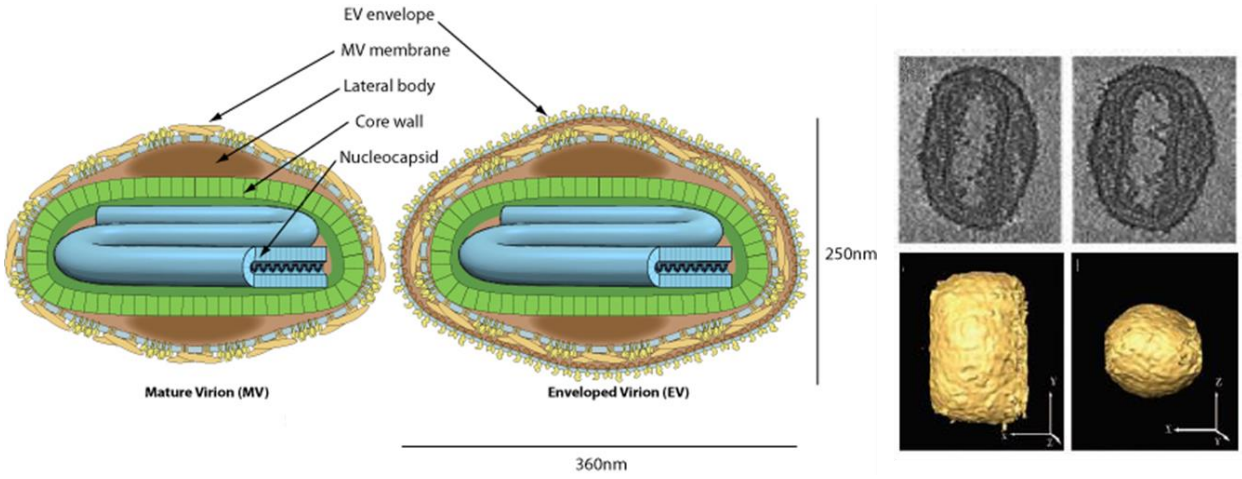

Fig. 4. Structure of the infective Poxvirus particles. Left Panel: Mature Virion (MV) and Enveloped Virus (EV), figure adapted from "© ViralZone 2016, Swiss Institute of Bioinformatics (https://viralzone.expasy.org/174). Right Panel: Cryo-electron

microscopy sections (top) and volumetric representation (bottom) of an MV using tomographic reconstruction, adapted from (Cyrklaff et al., 2005).

1.6.2 Genome Organisation

Vaccinia virus has a linear double-stranded DNA of about 200 Kbp and a size of about 62.3 microns that is Adenine-Thymine rich and has relatively low inter-gene spacing and non-coding regions (Esteban et al., 1977). The ends of the DNA molecule contain hairpin-shaped loop structures formed by ITRs or Inverted Terminal Repeat regions (Fig 5), which play an important role in the replication of the viral DNA (Moss, 2013). Open reading frames within the genome are named based on Hind III enzyme restriction site distribution in the central genome, i.e., each read is assigned with the letter of the DNA fragment in which it is found following digestion with Hind III enzyme (letters arranged from left to right), a number corresponding to the read within the fragment and finally, a letter "L" (for left) or "R" (for right) to denote the direction of transcription (Moss et al., 2007). The conserved central region of the genome contains the genes responsible for essential functions such as replication and assembly, while the variable terminal regions contain non-essential genes such as those related to host-virus interactions and immune evasion.

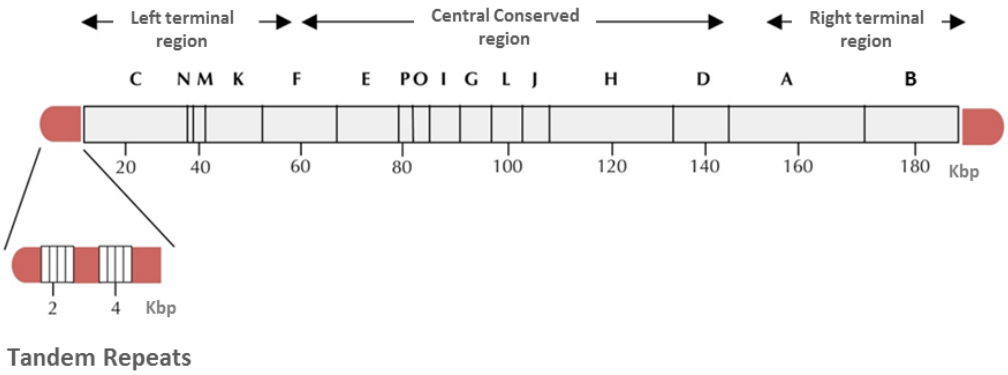

Fig. 5. Structure and organisation of the VACV genome.

1.6.3 Infection Cycle

Vaccinia virus infects a wide variety of tissues and its replication cycle takes place in the cytoplasm of the infected cell. As illustrated in Fig 6, the viral infection cycle takes

place in four steps: entry, uncoating, gene expression and DNA replication, and morphogenesis and release.

Entry: Virion entry is either by direct fusion assisted by a complex of 11 to 12 viral proteins to the plasma membrane or through macropinocytosis into acidified endosomes. In the case of EV, the additional membrane is disrupted before entry using a non-fusogenic mechanism that is dependent on cellular and viral surface proteins (Moss, 2012).

Uncoating: Following entry, the virions are transported through microtubules towards the viral factories where uncoating takes place (Carter et al., 2003). This process is characterized by the loss of viral lipids and a greater exposure of the viral genome to the action of DNA exonucleases (Sarov and Joklik, 1972).

Gene expression and DNA replication: Viral genome transcription is highly regulated and takes place in three stages: early, intermediate and late (Esteban and Metz, 1973, Moss et al., 2007). Within 20 minutes after entry, viral proteins are produced (Metz and Esteban, 1972), the enzymes and transcription factors packaged into the core of the virions come together to carry out early transcription of about half of the viral genome. The mRNAs thus produced encode proteins that are involved in host antiviral response modulation, DNA replication and intermediate gene transcription (Mercer et al., 2007). Intermediate transcription occurs simultaneously with DNA replication and encodes factors necessary for late transcription (Vos and Stunnenberg, 1988). Finally, late transcription of genes encoding structural proteins, virulence factors and other enzymes is carried out. Viral factories are the hotspots of viral DNA replication within the cytoplasm and are established early during the infection (Esteban et al., 1977, Esteban et al., 1979). About 50% of the replicated DNA is packaged into new virions (Joklik and Becker, 1964).

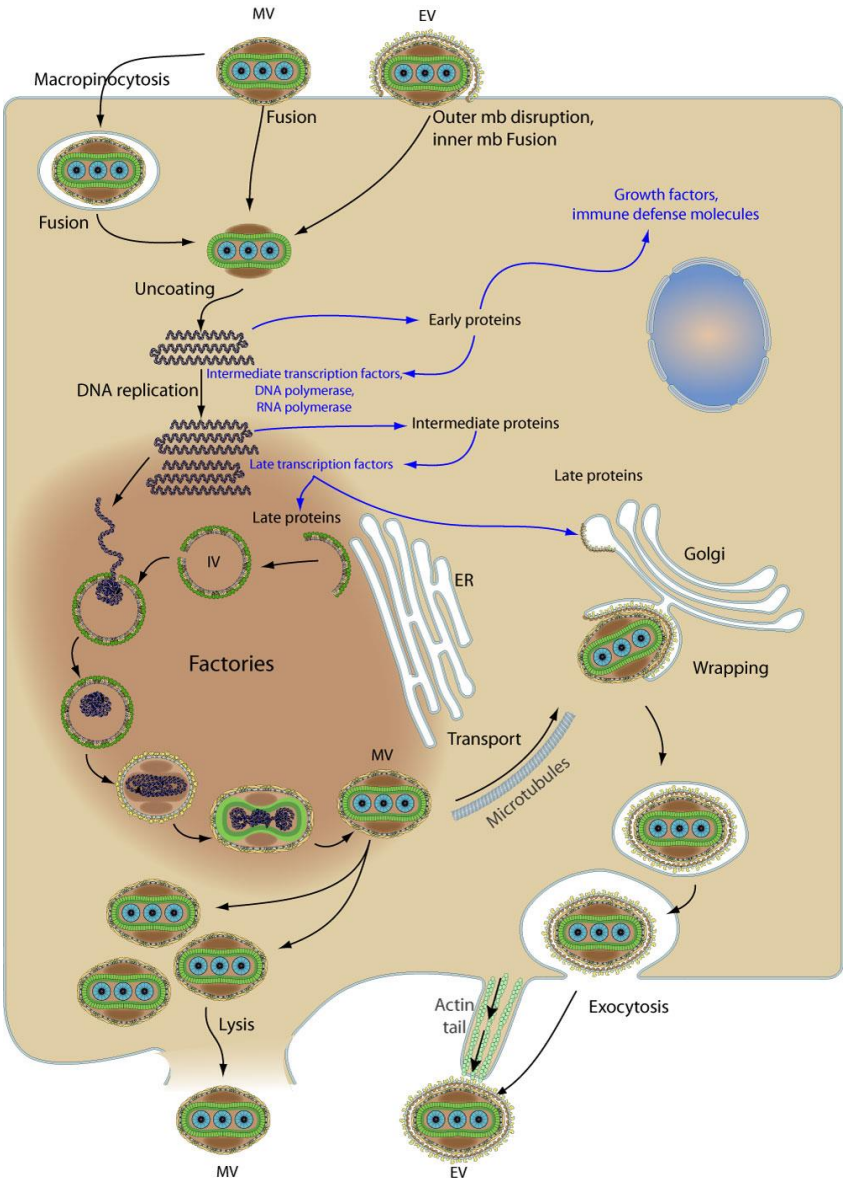

Fig. 6. VACV infection cycle: Scheme representing the VACV infection process, including entry, uncoating, gene expression and DNA replication, morphogenesis and release. Figure adapted from figure adapted from "© ViralZone 2016, Swiss Institute of Bioinformatics (https://viralzone.expasy.org/4399).

Morphogenesis and release: Newly formed virions undergo various changes until they reach the final EV or MV forms. Spherical immature viruses are first formed in the viral factories which mature into MV after the proteolytic processing of some of the viral proteins and core condensation (Rodriguez et al., 1997). Most MVs stay in the cytoplasm until they are released following cell lysis, while a small fraction are transported through the Golgi, where they acquire a second membrane to form the IEV. The IEVs are transported again by microtubules to the plasma membrane and released

as EV by membrane fusion or projected to adjacent cells through actin tails (Blasco and Moss, 1991, Mercer et al., 2007).

1.6.4 Vaccinia based vaccine vectors

Apart from the eradication of smallpox, vaccines based on VACV have also been developed through recombinant DNA technology against other pathogens by the insertion of other heterologous antigens (Paoletti, 1996, Moss, 1996. Also, attenuated strains of vaccinia virus such as the Modified Vaccinia Virus Ankara (MVA) {Mayr, 1978 #174) and the New York Vaccinia Virus (NYVAC) (Tartaglia et al., 1992) have been developed by the repeated passage of the virus in CEF cells (MVA) or the targeted deletion of ORFs (NYVAC) (Pantaleo et al., 2010). The present work is focused on the optimization of the MVA vector as a HIV vaccine candidate in combination with the improvement of the envelope antigen.

1.7 Modified Vaccinia Virus Ankara (MVA)

MVA was developed by the attenuation of the Turkish smallpox vaccine Chorioallontois vaccinia virus Ankara (CVA) after more than 570 serial passages in chicken embryo fibroblast (CEF) cells (Mayr et al., 1978). The process involved the loss of about 30 Kb of genetic components mainly from the ends of the genome, involving genes non-essential for replication, for example, those responsible for host immune modulations (Wyatt et al., 1998). The resulting virus MVA has limited replication ability in mammalian cell types, i.e., the virus can replicate but is not able to form infectious particles and therefore cannot infect surrounding cells and propagate, unless they are grown in permissive cell lines such as CEF and BHK-21 (Elena Gómez et al., 2012). The safety of MVA as a vaccine vector was first established when used for smallpox vaccination by the Bavarian State Vaccine Institute from 1968 through 1985, where the absence of any serious adverse events was recorded in large field trials in Germany (Stickl et al., 1974).

1.7.1 MVA based vaccine candidates for HIV vaccination

Several candidates based on the MVA platform for HIV vaccines are currently in various stages of clinical development and testing. These candidates include:

MVA-HIVA: One of the first MVA-based HIV vaccine candidate to enter clinical trials in humans, the MVA-HIVA vaccine was designed to carry the *Gag* gene from the Clade A HIV-1 and different CD8 T cell epitopes. Vaccination using this vector (which included a DNA priming step) only showed modest immune responses against HIV-1 antigens among the vaccinees (Peters et al., 2007).

MVA-CMDR: MVA-Chiang Mai Double Recombinant or MVA-CMDR expressing the envelope protein from clade E and the Gag-Pol from clade A, when used in clinical trials that included a DNA (expressing Env from HIV-1 clades A, B and C, Gag from clades A and B, and RT and Rev of clade B) priming step, resulted in the induction of strong HIV-1 Env-specific T cell immunity among 90-100% of the healthy immunized volunteers (Gudmundsdotter et al., 2009, Currier et al., 2010).

MVA-B: MVA vector that expresses the envelope protein as a released product and Gag-Pol-Nef as an intracellular fused polyprotein from clade B was developed in our laboratory and has been tested in phase I clinical trials, where three doses of MVA-B were able to induce HIV-1 specific broad and polyfunctional CD4 and CD8 responses among most of the healthy volunteers. Particularly, about 95% of the volunteers showed HIV-1 envelope specific effector memory T cells. The immunization regimen was also able to induce antibodies against the envelope in 95% of the vaccinees and HIV-1 neutralizing antibodies in 33% of them (García et al., 2011, Gómez et al., 2011). An MVA-B booster given 4 years after the first vaccination elicited high T cell and antibody responses against HIV antigens (Guardo et al., 2017). MVA-B was also tested in another phase I therapeutic clinical trial with HIV-infected individuals under ART, providing activation of CD4+ T cell responses and some delay in viral rebound after ART removal (Mothe et al., 2015, Gómez et al., 2015).

1.7.2 Strategies for improving MVA based vaccination

Several strategies have been developed with a view to improving the immunogenicity of poxvirus based vectors. These strategies can be grouped under two main categories:

a. Modifications of the MVA vector backbone:

Deletion of immunomodulatory genes in the MVA genome: In order to improve the host immune responses to vaccination, one of the strategies is the directed deletion of

poxvirus genes that are known to be involved in the modulation of host immunity. Examples include MVA vectors destined for vaccination for HIV-1 with single deletions of genes encoding inhibitors of type I IFN signalling pathway (*C6L*) (García-Arriaza et al., 2011), IL-18 binding protein (*C12L*) (Falivene et al., 2012), apoptosis (*F1L*) (Perdiguero et al., 2012) and inhibitor of IRF-3 (*N2L*) (García-Arriaza et al., 2014), all of which showed an improvement in HIV-1 specific T cell responses. More than one deletion in the same MVA vector have also been shown to aid in the improvement of MVA-induced immunogenicity against HIV, such as the MVA vector lacking the A41L + B16R genes (García-Arriaza et al., 2010), and C6L + K7 R genes (García-Arriaza and Esteban, 2014). However, multiple deletions to the NYVAC vector did not further improve the immune responses to HIV antigens (Gómez et al., 2017).

Insertion of co-stimulatory molecules: The inclusion of the simultaneous expression and delivery of co-stimulatory molecules, such as cytokines and chemokines, is a strategy that aims to improve the MVA induced immune responses towards the heterologous antigen of interest. Examples of this strategy include the insertion of genes coding for the co-stimulatory molecules such as interleukin (IL) 12 (Abaitua et al., 2006), Interferon (IFN) –γ (Abaitua et al., 2006), IL-2 (Bertley et al., 2004), IL-15 (Kolibab et al., 2010), OX40/OX40L (Goulding et al., 2011) and GM-CSF (Rodríguez et al., 2012) into the MVA genome.

b. Optimization of the MVA based vaccination protocol:

The use of prime – boost protocols: One of the most commonplace methods of immunization designed to improve the immune responses generated by MVA based vaccines is to follow a multiple dose prime-boost strategy. The agents used in successive vaccinations can be homologous (MVA prime, MVA boost) or heterologous (eg. DNA prime, MVA boost), given that the use of certain priming agents such as DNA, protein and VLP´s followed by a poxvirus boost are shown to improve long-lasting immune responses (García-Arriaza and Esteban, 2014).

Adjuvant-based improvements in immunity: Although the MVA vectors are highly immunogenic *per se*, the use of appropriate adjuvant molecules has been reported to contribute to the improvement of MVA-based vectors in various studies. These include the use of soluble CD40 ligand (Gómez et al., 2009), GLA adjuvant (McKay et al., 2014) and MF59 (Fouda et al., 2013) among others.

Of particular interest for this study, the use of the vaccinia virus protein 14K as a fusion agent provides an adjuvant like effect to the vaccination protocol involving MVA based vectors, discussed further in this section.

1.7.3 Choosing the correct antigen - the balancing act of arming both T cell and B cell immune responses to HIV

Given that poxvirus based platforms show significant promise towards arming the T cell based vaccines, the focus needs to be on an ideal immunogen design that should fulfil the following features:

a. When provided as a protein vaccine, is able to induce potent broadly neutralizing antibodies against HIV-1

b. When expressed through MVA based vaccine vectors, is stable and is able to mount a strong and specific cytotoxic T cell response against HIV-1

The majority of efforts towards finding an ideal HIV immunogen that can improve vaccine efforts are focussed on the envelope protein of HIV. The requirement for any improvement to a MVA based vaccination effort, in order to improve both the cellular and humoral responses against HIV must, therefore, aim to improve the envelope protein so to enhance those characteristics that make it an ideal antigen, while being compatible and tailor-made for the MVA based platform.

1.8 The use of vaccinia virus 14K molecule as fusion agent for improvement of poxvirus based vaccination

Among the various methods towards improving the immunogenicity of MVA based vaccines, the use of the vaccinia virus 14K protein as a fusion agent in the HIV-1 vaccine models is of particular interest to this work.

1.8.1 The VACV 14K protein

The VACV 14K protein is encoded by the A27L gene (Rodriguez et al., 1987). This protein has multiple functions in the VACV biology and life cycle. For example, it has been implicated in:

a. Virus attachment to cells by mediating virus interaction with cell surface heparan sulfate (Chung et al., 1998).

b. Fusion of the intra and extra cellular membranes of the virions to the cell membrane (Doms et al., 1990).

c. Cell fusion at acidic pH mediated by the N terminus of the 14K protein (Gong et al., 1990).

d. Determination of the plaque size phenotype of the virus (Dallo et al., 1987).

e. Formation of enveloped virions (Rodriguez and Smith, 1990).

f. Microtubule dependant transport of MV (Sanderson et al., 2000).

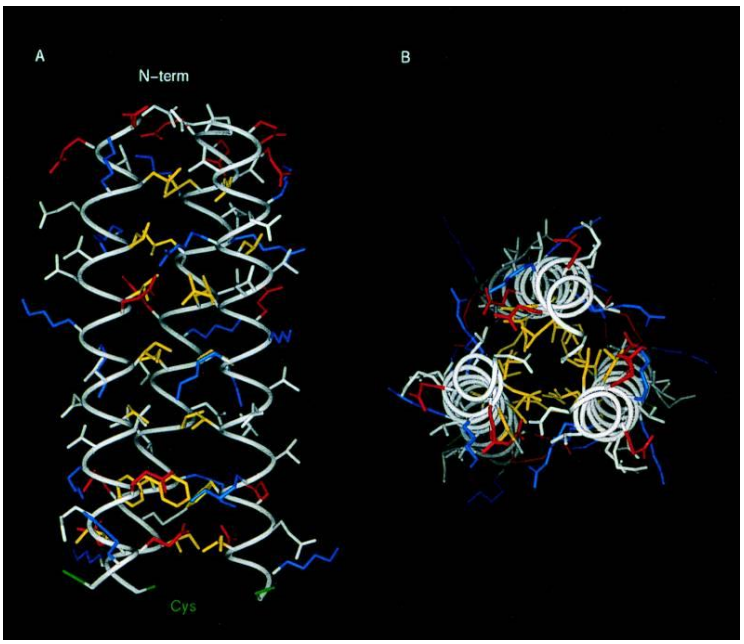

Fig. 7. Three dimensional model of the triple coiled-coil region of the VACV 14K protein in the longitudinal (A) and transversal (B) views. Figure adapted from Vázquez et al., 1998.

1.8.1.1 Structure

Among the various structural genes encoded within the vaccinia virus genome, the A27L gene and its product, the 14K protein are well characterized through previous

work in the Esteban laboratory, where the gene was first described (Rodriguez and Esteban, 1987). The 14K protein is made up of 110 amino acids, composed of a 28 amino-acid region that is devoid of any structural significance but is responsible for the production of neutralizing antibodies (Vázquez et al., 1998). Apart from this component, there is a helical region within the 29 to 37 amino acid region, a triple coiled-coil region from residues 44 to 72 and finally a leucine zipper motif at the C terminal end (Fig 1.7) (Vázquez and Esteban, 1999). It has been reported that the region marked by the amino acids 21 to 32 plays an important role in the binding of the 14K protein to the cell surface through reaction with heparin sulphates, supported by the oligomeric coiled coil portion of the protein (Ho et al., 2005). Crystallization studies of a truncated form of the 14K protein containing the amino acids 21-84 has revealed further structural insights into the protein (Chang et al., 2013): a trimeric base unit composed of two parallel α-helices and an antiparallel α-helix is formed at the N-terminal region interface or NTR while two of these trimers stack with each other to form a hexamer using the C-terminal region interface or CTR. It has been further demonstrated that 14K dimer/trimer formations are impaired in recombinant vaccinia viruses expressing the full-length 14K protein with impaired NTR or CTR interactions, resulting in small plaques that are defective in MV egress (Chang et al., 2013).

1.8.1.2 Use of 14K as a fusion agent

The Esteban laboratory has pioneered the use of 14K protein as a fusion agent i.e. the addition of this protein to antigens of interest in disease models has proven to improve the immunogenicity of the corresponding MVA vectors. In one of the first examples, the HIV-1 Env protein was fused to the C terminal end of the 14K protein. When mice were inoculated with the recombinant vaccinia virus expressing this fusion protein, they were able to generate anti-GP160 antibodies (Rodriguez et al., 1991). It has also been shown that the fusion of the 14K or the 39K proteins and the subsequent expression of the fusion construct from vaccinia virus to the C terminal end of the HIV envelope protein and then expressed through viral vectors, enhances the immunogenicity (measured by both cellular and humoral responses) against Env in a homologous prime-boost vaccination study when compared to using the Env alone (Collado et al., 2000).

Recent work from the Esteban laboratory has shown that the 14K protein contributes through adjuvant like effect to immunogenicity against Malaria using poxvirus based vectors. Priming with a chimeric protein formed by the Circumsporozite (CS) protein fused with the 14k from vaccinia virus, and boosting with MVA expressing the CS from *Plasmodium yoelii*, the magnitude and polyfunctionality of cytokine-secreting CD8 T cells improved while also contributing to sterile protection against liver stage development of the parasite in mice models (Vijayan et al., 2012).

1.9 Scope of this thesis - Improvements to the use of 14K fusion in the HIV vaccine scenario

The scope of this work is to expand on the use of vaccinia virus 14K protein as a fusion protein towards improving the immunity, both humoral and cellular offered against the HIV-1 Env region. Having established through experimental evidence that the fusion of the 14K molecule to the GP120 from HIV, improves the immunogenic potential of the same through oligomerization, we wanted to evaluate this new antigenic form GP120C14K as the basis for developing different vehicles for vaccination – protein, MVA and DNA – and examining the improvements, if any, that these agents bring to the cellular and humoral response when compared to using the monomeric GP120C molecule in the vaccination protocol.

2. OBJECTIVES

The objectives of the present work can be summarized as follows:

1. Generation of the GP120C14K protein by the fusion of the vaccinia virus 14K to the C-terminal end of the HIV-1 envelope protein GP120C.

2. Production, purification and characterization (antigenic and biophysical) of the fusion protein GP120C14K.

3. Generation and characterization of MVA-GP12014K recombinant virus vector.

4. Evaluation in mice of the combined protocol of priming with the MVA-GP120C14K vector and boosting with GP120C14K protein for its ability to generate cellular and humoral responses against HIV-1.

5. Establishment in mice of an optimal protocol to further improve cellular and humoral responses against HIV-1 antigens by the combination of a DNA/MVA/protein immunogens.

3. MATERIALS AND METHODS

3.1 Materials

3.1.1 Cell Lines

The following cell lines have been used in this work:

- CEF: Chicken Embryo Fibroblast cells are primary cells obtained from 11 day incubated embryos of chicken (*Gallus gallus*).
- HeLa: Immortalized human epithelial cells derived from cervical adenocarcinoma.
- DF-1: Immortalized chicken embryo fibroblast cells.
- CHO-K1: Immortalized Chinese Hamster Ovary cells.
- HEK-293T: Immortalized human embryonic kidney cells.

3.1.2 Culture Media

All cell lines except CHO-K1 were grown in Dulbecco´s Modified Eagle Medium or DMEM (Sigma) supplemented with non-essential amino acids (Sigma), 2mM of L-Glutamine (Merck), 100 µg/ml of streptomycin (Sigma), 100 U/ml of penicillin (Sigma), 0.5 µg/ml of fungizone (Gibco), 0.05 µg/ml of gentamycin (Sigma) and 10% of heat inactivated foetal calf serum (Gibco). Stably transfected CHO-K1 cells were grown in Minimum Essential Medium or MEM (Gibco) in the presence of 25 µM of L-methionine sulfoximine (Sigma) and 10% of heat inactivated foetal calf serum. Cells were maintained at 37^0C (39^0C for DF-1) with 5% CO_2 and 95% humidity. The medium was changed two times a week (unless specified otherwise) and passaged with trypsin-EDTA (Gibco).

3.1.3 Bacteria

Escherichia coli bacterial strain DH5α has been used for bacterial transformations, generation of clones during the construction of recombinant plasmid DNA. In all these cases, the media used for growing the bacteria was Luria-Bertani or LB containing 1% bacto-tryptone (BD Biosciences), 1% NaCl (Sigma) and 0.5% yeast extract (BD Biosciences) at pH7 (Green & Sambrook, 2012), usually in the presence of 100 µg/ml of the selection antibiotic ampicillin (Boehringer Mannhein).

3.1.4 Viruses

The various viruses used in this work are based on the parental MVA strain of vaccinia virus and are detailed as follows:

- MVA-wt: the parental strain used for the construction of recombinant MVA vectors, obtained from the Ankara strain of vaccinia virus after 586 serial passages in CEF cells, provided kindly by G. Sutter, Germany.
- MVA-GP120C: MVA with the GP120C antigen inserted into the TK locus had been generated earlier in the Esteban laboratory using standard protocols.
- MVA-GP120C14K: MVA with the GP120C14K fusion antigen inserted into the TK locus, described as part of this work.
- MVA-C: MVA containing the GP120 antigen from clade CN54 and the Gag-Pol-Nef polyprotein from the same clade inserted into the TK locus (Gómez et al., 2007b)

3.1.5 Plasmids

The various plasmid DNA molecules used in this work are as follows:

- pCDNA3.0(+) (Invitrogen): Mammalian expression vector used as such for vaccination and also for the insertion of other antigens described below. The plasmid contains a multiple cloning site or MCS under the cytomegalovirus (CMV) promoter and an ampicillin resistance gene for selection.
- pCDNA-GP120C: pCDNA3.0(+) plasmid with the GP120C antigen inserted into the multiple cloning site (between the EcoR1 and Xba1 restriction sites), used for vaccination and transient transfections.
- pCDNA-GP120C14K: pCDNA3.0(+) plasmid with the GP120C antigen inserted along with the A27L gene into the multiple cloning site (between the EcoR1 and Xba1 restriction sites), used for vaccination and transient transfections.
- pBJ5-GS-GP120C: pBJ5-GS plasmid (Gastinel et al., 1992) containing the insert GP120C (between the BamH1 and Not1 restriction sites), used for stable transfection of CHOK1 cells. The Glutamine synthetase (GS) minigene present in the plasmid allowed for selection of clones positive for the insertion in a

media free from glutamine and containing the selective agent selective agent L-methionine sulfoximine (Sigma-Aldrich).

- pBJ5-GS-GP120C14K: pBJ5-GS plasmid containing the insert GP120C14K (between the BamH1 and Not1 restriction sites), used for stable transfection of CHOK1 cells.
- pCyA20-GP120C14K: Transfer vector derived from the pCyA20 vector backbone used for the insertion of a gene of interest into the MVA genome (Gómez et al., 2013), containing the fusion gene GP120C-14K inserted between the Thymidine Kinase or TK flanks (TK-L and TK-R). This plasmid was used for the infection-transfection protocol aimed at producing recombinant MVA vector expressing the antigen GP120C14K.

3.1.6 Antibodies

The various antibodies used in this work are described in the table below:

Antibody	Characteristics	Source
Primary Antibodies		
Rabbit α GP120	Polyclonal, generated against the GP120 protein of HIV-1	CNB
Rabbit α 14K	Polyclonal, generated against the vaccinia virus 14K protein	CNB
Rabbit α WR	Polyclonal; generated against proteins from the vaccinia virus WR strain	CNB
Goat α -mouse IgG	Polyclonal, human adsorbed	Southern Biotechnology
Goat α -mouse IgG1	Polyclonal, human adsorbed	Southern Biotechnology
Secondary Antibodies		
Goat α Rabbit HRP	Polyclonal antibodies against rabbit IgG, conjugated with horseradish peroxidase	Sigma

Broadly neutralizing human monoclonal antibodies against HIV-1 envelope		
PGT145	Human monoclonal antibody to quaternary structural epitope (V1/V2) of HIV-1 GP120	R.W.Sanders, AMC, The Netherlands
PGT151	Human monoclonal antibody to quaternary structural epitope (GP120-GP41 interface) of HIV-1 GP120	R.W.Sanders, AMC, The Netherlands
PG9	Human monoclonal antibody to structural epitope of HIV-1 GP120	Centre for AIDS Reagents, NIBSC, UK
PG16	Human monoclonal antibody to structural epitope of HIV-1 GP120	Centre for AIDS Reagents, NIBSC, UK
B12	Recombinant human monoclonal antibody to HIV-1 GP120 blocking binding to CD4	Centre for AIDS Reagents, NIBSC, UK
2G12	Recombinant human monoclonal antibody to HIV-1 GP120	Centre for AIDS Reagents, NIBSC, UK
PGT121	Recombinant human monoclonal antibody to N332 glycan–V3 loop of GP120	Centre for AIDS Reagents, NIBSC, UK
257-D IV	Recombinant human monoclonal antibody to V3 loop of HIV-1 GP120	Centre for AIDS Reagents, NIBSC, UK
10-1074	Recombinant human monoclonal antibody to base of the V3 loop of HIV-1 GP120	Centre for AIDS Reagents, NIBSC, UK
Conjugated Antibodies (ELISpot)		
Streptavidin HRP	Peroxidase conjugated with streptavidin for reaction with biotinylated proteins	BD Biosciences
Conjugated Antibodies (Flow Cytometry)		
Rat α Mouse CD8a -	Monoclonal antibody against mouse CD8a	BD Biosciences

PE	conjugated with PE, Clone 53-6.7	
Hamster α Mouse CD3e - PE-CF594	Monoclonal antibody against mouse CD3e conjugated with PE-CF594, Clone 145-2C11	BD Biosciences
Rat α Mouse CD127 - PerCPCy5.5	Monoclonal antibody against mouse CD127 conjugated with PerCPCyanine5.5, Clone A7R34	eBioscience
Rat α Mouse CD4 - PECy7	Monoclonal antibody against mouse CD4 conjugated with PECy7, Clone RM4-5	BD Biosciences
Hamster α Mouse CD3e-APC	Monoclonal antibody against mouse CD3 conjugated with APC, Clone 145-2C11	BD Biosciences
Rat α Mouse CD62L-Alexa700	Monoclonal antibody against mouse CD62L conjugated with Alexa Fluor 700, Clone MEL-14	BD Biosciences
Rat α Mouse CD4-APC-Cy7	Monoclonal antibody against mouse CD4, conjugated with APC-Cy7, Clone GK1.5	BD Biosciences
Rat α Mouse CD8a-V500	Monoclonal antibody against mouse CD8a, conjugated with V500, Clone 53-6.7	BD Biosciences
Rat α Mouse IL2-APC	Monoclonal antibody against mouse IL-2, conjugated with APC, Clone JES6-5H4	BD Biosciences
Rat α Mouse IFNγ-PECy7	Monoclonal antibody against mouse IFNγ, conjugated with PECy7, Clone XMG1.2	BD Biosciences
Rat α Mouse TNFα-PE	Monoclonal antibody against mouse TNFα, conjugated with PE, Clone MP6-XT22	eBioscience
Armenian Hamster α Mouse ICOS - BB515	Monoclonal antibody against mouse ICOS (CD278), conjugated with BB515, Clone C398.4A	BD Biosciences
Rat α Mouse CD134 - PE	Monoclonal antibody against mouse CD134 (OX40),conjugated with PE, Clone OX-86	eBioscience
Rat α Mouse CD3-PerCPCy5.5	Monoclonal antibody against mouse CD3, conjugated with PerCPCy5.5, Clone 17A2	BD Biosciences
Rat α Mouse CD25-PECy7	Monoclonal antibody against mouse CD25, conjugated with PECy7, Clone PC61	BD Biosciences

Rat α Mouse CD4-Alexa700	Monoclonal antibody against mouse CD25, conjugated with Alexa Fluor700, Clone RM4-5	BD Biosciences
Armenian Hamster α Mouse PD1(CD279)-APC-eFluor780	Monoclonal antibody against mouse CD279 (PD1), conjugated with APC-eFluor780, Clone J43	eBioscience
Rat α Mouse CD8a-eFluor450	Monoclonal antibody against mouse CD8a, conjugated with eFluor450, Clone 53-6.7	eBioscience
Rat α Mouse CD19-FITC	Monoclonal antibody against mouse CD19, conjugated with FITC, Clone 1D3	eBioscience
Armenian Hamster α Mouse CD95-PE	Monoclonal antibody against mouse CD95, conjugated with PE, Clone Jo2	BD Biosciences
Rat α Mouse CD38-PerCP-Cy5.5	Monoclonal antibody against mouse CD38, conjugated with PerCP-Cy5.5, Clone 90	BD Biosciences
Rat α Mouse CD45R-PECy7	Monoclonal antibody against mouse CD45R/B220, conjugated with PECy7, Clone RA3-6B2	BD Biosciences
Rat α Mouse T and B cell activation antigen – Alexa Fluor 647	Monoclonal antibody against mouse T and B cell activation antigen, conjugated with Alexa Fluor 647, Clone GL7	BD Biosciences
Rat α Mouse CD138-APC-R700	Monoclonal antibody against mouse CD138, conjugated with APC-R700, Clone 281-2	BD Biosciences
Rat α Mouse IgD-APC-H7	Monoclonal antibody against mouse IgD, conjugated with APC-H7, Clone 11-26c.2a	BD Biosciences
Rat α Mouse IgG1-BV421	Monoclonal antibody against mouse IgG1, conjugated with BV421, Clone A85-1	BD Biosciences

Table 2. Antibodies used in the present work.

3.1.7 Other Proteins / Peptides

Env-1 peptide: HIV-1 peptides Env-1 (sequence: PADPNPQEM) is a H-2^d-Restricted CTL epitope as previously described (Perdiguero et al., 2012).

PfCS: Plasmodium Falciparum Circumsporozite protein, purified in the laboratory as described previously (Vijayan et al., 2017).

GP120C14K: The aminoacid sequence of the fusion protein is given as follows (the under-lined portion represents the 14K section of the protein):

MDRAKLLLLLLLLLLPQAQAVGNLWVTVYYGVPVWKGATTTLFCASDAKAY
DTEVHNVWATHACVPADPNPQEMVLENVTENFNMWKNEMVNQMQEDVISL
WDQSLKPCVKLTPLCVTLECRNVSSNSNDTYHETYHESMKEMKNCSFNATTV
VRDRKQTVYALFYRLDIPLTKKNYSENSSEYYRLINCNTSAITQACPKVTFDPIPI
HYCTPAGYAILKCNDKIFNGTGPCHNVSTVQCTHGIKPVVSTQLLLNGSLAEGE
IIIRSENLTNNVKTIIVHLNQSVEIVCTRPGNNTRKSIRIGPGQTFYATGDIIGDIRQ
AHCNISEDKWNETLQRVSKKLAEHFQNKTIKFASSSGGDLEVTTHSFNCRGEFF
YCNTSGLFNGAYTPNGTKSNSSSIITIPCRIKQIINMWQEVGRAMYAPPIKGNITC
KSNITGLLLVRDGGTEPNDTETFRPGGGDMRNNWRSELYKYKVVEIKPLGVAP
TTTKRRVVEREKRSRGREAKREAIVKADEDDNEETLKQRLTNLEKKITNVTTKF
EQIEKCCKRNDEVLFRLENHAETLRAAMISLAKKIDVQTGRRPYE.

3.1.8 Buffers

The following buffers have been used in the present work:

- PBS: NaCl 137 mM, KCl 2.7 mM, Na_2PO_4 8 mM and KH_2PO_4 1.5 mM.
- PBS Staining: PBS 1x, 0,5% BSA, 1% FCS, 0,065% sodium azide and 2 mM EDTA.
- Loading Buffer (Laemmli): Tris-HCl 50 mM pH 6.8, SDS 2%, β-mercaptoethanol 5%, glycerol 10% and bromophenol blue 0.012%.
- Loading Buffer (DNA): Xylene-cyanol 0.25%, glycerol 30% and bromophenol blue 0.25%.
- Electrophoresis buffer SDS-PAGE (Tris-glycine SDS): Tris 25 mM, glycine 192 mM and SDS 0.1%.
- Proteinase K Buffer: Tris-HCl 50 mM pH 8.0, EDTA 100 mM, NaCl 100 mM and SDS 1%.
- Transfer Buffer: Tris 25 mM, glycine 192 mM and methanol 20%, pH 8.3.
- TBE: Tris-Borate pH 8.3 90 mM and EDTA 2 mM.
- TBS: 0.5M Tris Base, 9% NaCl, pH 8.4.

3.1.9 Oligonucleotides

The following oligonucleotides have been used in the following work:

Oligonucleotide	Sequence (5´- 3´)	Template
TK1	AACGGCGGACATATTC AG	TK Left: MVA
TK2	ATGAGTCGATGTAACA CT	TK Right: MVA
Myc A	GGCGAATGGGTGAGTAACA CG	Mycoplasma genome
Myc B	CGGATAACGCTGCGACCTA TG	Mycoplasma genome
GP120C_Fwd_ECoR 1	GCGAATTCATGGACAGGGCCA AGCTG	Left Flank of GP120C
GP120C_Xba1_Rvs_ Stop	GCTCTAGATATCACCTCTTCTC CCTCTCCACC	Right Flank of GP120C
GP120C_Asc1_Rvs	TTGGCGCGCCAACCTCTTCTCC CTCTCCA	Right Flank of GP120C
A27L_Asc1_Fwd	TTGGCGCGCCAAGAGGCTAAA CGCGAAGC	Left Flank of A27L (VACV)
A27L_Xba1_rev_stop	GCTCTAGACCCTCGAGTGGGTT ACTCATATGG	Right Flank of A27L (VACV)
GP120C-Fwd-Sa1	ACGCGTCGACATGGACAGGGC CAAGCTG	Left Flank of GP120C (for pBJ5-GS cloning)
GP120C-RvsStop-BamH1	CGGGATCCACGCGGAACCAGT CACCTCTTCTCCCTCTC	Right Flank of GP120C (for pBJ5-GS cloning)
A27L-RvsStop-BamH1	CGGGATCCACGCGGAACCAGT TACTCATATGGACGCC	Right Flank of GP120C14K (for pBJ5-GS cloning)
PCYA20-GP120C-GF-XhoSite	ATATAAATAGCTAGCATGGAC AGGGCCAAGCTGCTGCTG	Left Flank of GP120C14K (for Gibson assembly into pCyA20)
PCYA20-A27L-GR-XhoSite	CTCTGCAGTTTAAACTTACTCA TATGGACGCCGTCCAGT	Right Flank of GP120C14K (for Gibson assembly into pCyA20)

GF3.120CRRRRR-14K-F	GTGCAGCGCCGCCGCCGCCGC GAGGCTAAACGCGAAGCAATT	Left Flank of GP120Crrrrr14K (Gibson assembly)
GR3.14K-GP120CRRRRR-R	AATTGCTTCGCGTTTAGCCTCG CGGCGGCGGCGGCGCTGCAC	Right Flank of GP120Crrrrr14K (Gibson Assembly)
GF4.120CREKS-14K-F	GTGGTGGAGAGGGAGAAGAGC GAGGCTAAACGCGAAGCAATT	Left Flank of GP120Creks14K (Gibson assembly)
GR4.14K-GP120CREKS-R	AATTGCTTCGCGTTTAGCCTCG CTCTTCTCCCTCTCCACCAC	Right Flank of GP120Creks14K (Gibson Assembly)

Table 3. Oligonucleotides used in the present work.

3.2 Methods

3.2.1 DNA

3.2.1.1 Cloning of inserts into a plasmid DNA vector

Cloning of inserts into plasmid vectors was carried out using standard molecular cloning procedures outlined in "Molecular Cloning: a laboratory manual" (Green and Sambrook, 2012) in the case of pCDNA and the pBJ5-GS plasmid constructions for the GP120C and GP120C14K genes. Gibson Assembly Master Mix (New England Biolabs) protocol was used for the rest of the plasmid constructions according to manufacturer´s instructions.

3.2.1.2 DNA purification

- Purification of DNA fragments amplified using PCR or extracted from agarose gels was carried out using the Wizard genomic DNA purification kit (Promega) following manufacturer´s instructions.

- Purification of plasmid DNA

Plasmid DNA was extracted from 3 ml cultures of positive bacterial clones during the molecular cloning process using the standard alkaline lysis protocols (Green and Sambrook, 2012). Larger quantities of purified plasmid DNA (for use in transfections and generation of other plasmid vectors through molecular cloning) were obtained using the Plasmid Maxi Kit (Qiagen) following manufacturer´s protocol. Plasmid DNA destined for use for in vivo experiments and for the large scale protein purification in

HEK293-T cells through transient transfections were purified using the Endofree Plasmid Mega Kit (Qiagen) following manufacturer´s instructions.

- Purification of genomic DNA from infected cells

When infected cells exhibit extensive cytopathic effect, the monolayer was recovered and centrifuged (2000 rpm for 2 minutes) and the pellet was stored at -20^{0}C until use. For DNA extraction, the pellet was thawed, resuspended in 50 mM Tris-HCl pH 8.0 and 200 µg/ml of Proteinase K (Roche) was added in its corresponding buffer, followed by 1 to 2 hour incubation at 55^{0}C. Next, 40 µg/ml of RNAse A (PanReac AppliChem) was added and incubated at 37^{0}C for 30 minutes following which saturated NaCl was added and mixed carefully. This mixture is then centrifuged (10000 rpm for 10 minutes at 4^{0}C) and the supernatant was mixed with isopropanol (1:0.7 v/v ratio) and centrifuged (10000 rpm for 10 minutes at room temperature). The precipitated DNA was allowed to dry and was then resuspended in 30 µl of sterile distilled H_2O. The concentration of the purified DNA was measured using NanoDrop (Thermo Scientific, USA). The DNA thus obtained was used to check for the correct insertion of the gene of interest using PCR and sequencing.

3.2.1.3 Polymerase Chain Reaction (PCR)

DNA amplification using PCR was carried out for the molecular cloning of genes of interest into a plasmid backbone (using the DNA polymerase Platinum *Pfx* – Invitrogen) and to check for the correct insertion of genes of interest into the recombinant virus generated (using the DNA polymerase *Taq* – Invitrogen). In all cases, about 100-200 ng of template DNA was used along with 0.4 mM of each oligonucleotide, 1 – 2.5 units of the polymerase with its corresponding buffer, 0.2 mM of each of the four deoxyribose nucleoside triphosphates or dNTPs and 1.5 mM $MgSO_4$ or $MgCl_2$ (depending on the polymerase used). Annealing temperature, extension time and temperatures varied depending on the reaction conditions (melting temperature of the oligonucleotides and length of the target fragment). The reactions were carried out in a Veriti^{TM} 96-well thermocycler (Applied Biosystems).

3.2.2 Proteins

3.2.2.1 Generation of stably transfected CHO-K1 cell lines expressing GP120C14K and GP120C

In order to generate CHO-K1 cells that express the antigen of interest (GP120C14K or GP120C) in a stable fashion (Casasnovas & Springer 1995), the cells were transfected with the corresponding plasmid pBJ5-GS containing the gene that codes for the protein of interest. This process was carried out in collaboration with the Centro Nacional de Biotecnología´s X-Ray Crystallography service. Following transfection, the clones expressing the protein were selected and scaled up. The cells were grown in roller flasks (1450 square cm, BD Falcon) at 37^0C while on a slow and constant rotation at about 0.5 to 1 rpm with MEM medium lacking glutamine in the presence of 25 μM of the negative selective agent L-methionine sulfoximine (Sigma-Aldrich). The media containing the secreted protein were collected every 3 to 4 days depending on the nature and confluence of the cells.

3.2.2.2 Transient transfection of HEK293T cells for the production of other proteins

Transient transfection by calcium phosphate method (Green and Sambrook, 2012) was mostly used to produce other proteins used in this study. HEK293T cells grown to 50-60% confluency in 150 mm plates (NUNC) were transfected with a 50 μg of the plasmid vector pCDNA3.0 containing the insert of interest in a mixture of 1M calcium chloride and HBS2X buffer pre-incubated for 20 minutes at room temperature. The transfection mix was removed after 8 hours and the cells were washed with PBS twice before adding DMEM media containing 2% FCS. The supernatant containing the protein of interest was harvested 72 hours post-transfection.

3.2.2.3 Protein Purification

Purification of HIV-1 envelope proteins was performed using Lectin columns following standard protocols. Briefly, supernatants containing the protein of interest were centrifuged (4000 rpm for 30 minutes at 4^0C), supplemented with 0.05% sodium azide (Sigma) and frozen until used. Prior to purification, the supernatants were thawed and filtered using 0.4 micron filters (Millipore). One litre of clarified supernatant was passed through Agarose bound - *Galanthus nivalis* lectin columns (Vector Labs) at a

rate of roughly 0.2 ml/min using gravity flow. The column was then washed with 15 ml of cold PBS and the elution was carried out with 25 ml of 0.5 M methyl-α-D-manno-pyrannoside (Sigma) at a rate of 0.2 ml/min. Positive fractions were collected and concentrated/buffer changed to 10 mM Tris 150 mM NaCl using 100 kDa centrifugal concentrators (Millipore), and separated through a Superdex-200 10/300 GL and Superdex -200 analytical Size Exclusion Chromatograms (SEC) according to manufacturer´s instructions (GE Healthcare) in collaboration with the Centro Nacional de Biotecnología´s X-ray Crystallography service. The proteins were stored in aliquots at -20^0C or -80^0C depending on the period of storage, after quantification using NanoDrop (Thermo Scientific, Wilmington, USA). Those aliquots destined for *in vivo* experiments were subjected to LPS determination using the Limulus Amebocyte Lysate (LAL) kit (QCL-1000, Lonza) according to manufacturer´s instructions, in order to make sure that the LPS content falls within the limits recommended by the EU regulations (Malyala and Singh, 2008).

3.2.2.4 Electrophoresis and Western Blotting

Protein samples (purified samples or cell extracts) were analysed using one dimensional electrophoresis on polyacrylamide gels in the presence of SDS according to the standard protocols described previously (Green and Sambrook, 2012). The percentage of acrylamide in the gels varied according to the molecular weight of the proteins of interest. The samples were prepared with loading buffers and denatured at 95^0C for 10 minutes prior to loading.

Gradient gels for the separation of larger molecular weight proteins under native conditions were carried out in standard 4-15% Mini-PROTEAN TGX gels (Biorad). The samples were prepared using the Native Page sample buffer (Invitrogen) prior to separation. Staining was done using standard Coomassie Brilliant Blue protocols (Green & Sambrook 2012) or colloidal silver using the PlusOne Silver staining kit (GE Healthcare) according to manufacturer´s instructions.

The manufacturer´s protocol from Mini Trans-Blot® Cell (Bio-Rad) was followed for the transfer of protein samples from the electrophoretic gels to nitrocellulose membranes. The gels after electrophoresis, the nitrocellulose membrane (GE Healthcare) and filter papers (Whattman-3MM®) were moistened in transfer buffer and mounted in the transfer system. The transfer was carried out at 200-400 mA during 50

minutes. The successful transfer was verified using Ponceau staining (0.2% Ponceau in 3% TCA; Sigma).

The nitrocellulose membrane was blocked in a 5% Bovine Serum Albumin (BSA, Sigma) solution prepared in TBST-T (0.01% Tween20 v/v, Sigma) at room temperature for an hour with subtle agitation. The primary antibodies prepared in various dilutions in the blocking buffer were used for overnight incubation of the membrane at 4^0C. Following three washed with TBST-T (0.01% Tween20 v/v, Sigma), the membrane was incubated with secondary antibody (appropriate dilutions prepared in the same buffer) for 60 minutes at room temperature and later washed thrice as described earlier. The bands corresponding to the proteins of interest were detected using the ECL western blotting detection reagent (Amhersham) according to the manufacturer´s instructions, developed on 13 x 18 cm Carestream BioMax XAR films (Kodak).

3.2.2.5 Enzyme Linked Immunosorbent Assay (ELISA) for analysing the reactivity of proteins to standard broadly neutralizing antibodies (bNAbs)

In order to analyse the reactivity of the protein candidates to standard broadly neutralizing antibodies against HIV-1 envelope, 96 well plates (NUNC Maxisorp) were coated with 2 µg/ml of the purified protein of interest in PBS and incubated at 4^0C overnight. The next day, the plates were blocked with 5% skimmed milk prepared in PBS-T (0.01% Tween20 v/v, Sigma). Serial dilutions of the bNAb of interest were prepared and added to the protein coated plates which had been washed thrice with PBS-T following blocking. After 90 minutes of incubation at room temperature, the plates were washed thrice again with PBS-T and 1 : 1000 dilution of secondary antibody (mouse α human HRPO – Sigma) was added to the wells and incubated for an hour. Finally, after another washing step, the plates were developed by adding 100 µl of TMB substrate (3,3',5,5' Tetramethylbenzidine; Sigma) and before reading the absorbance at 450 nm, the reaction was stopped by adding 50 µl of 1 M H_2SO_4.

3.2.2.6 GraFix of GP120C14K for negative-staining EM

GraFix stabilization for GP12014K samples carried out in collaboration with Ms. María del Mar Pérez Ruíz of Prof. Carrascosa´s group (CNB-CSIC) by the following method: the protein samples were purified and stabilized by Gradient Fixation (GraFix) (Stark, 2010). During this process, the macromolecular complex was separated in a 10%-40%

(v/v) glycerol gradient (50 mM HEPES pH 7.5, 150 mM NaCl, 10% glycerol, 40% glycerol and 0.15% glutaraldehyde) by ultracentrifugation 16h at 32000 rpm using a SW55Ti rotor (Beckman). The glycerol gradient was prepared in a Gradient Master, (Biocomp, Fredericton, NB, Canada) and after centrifugation the fractions were collected and the cross-linking reaction were stopped with 80 mM glycine.

3.2.2.7 Electron microscopy and image processing

Electron microscopy of negatively stained samples was performed in collaboration with Ms. María del Mar Pérez Ruíz of Prof. Carrascosa´s group (CNB-CSIC) as described (Vijayan et al., 2015). Briefly, GP120C14K molecules were applied onto carbon-coated copper grids and stained with 2% uranyl acetate. Micrographs were taken under lose dose conditions in a JEOL JEM1010 microscope operated at 80 kV, at 50000x magnification and acquired in a 4kx4k digital TemCam_F416 camera (TVIPS) with a pixel size of 2.53 A/pix. Particles were automatically selected using XMIPP3.1 (Scheres et al., 2008) (Abrishami et al., 2013) (De la Rosa-Trevín et al., 2013), and homogeneous image populations was obtained after 2D classification with RELION (Scheres, 2012b, Scheres, 2012a). A 25 A resolution final model was obtained from 16600 selected particles applying C3 symmetry using a RANSAC result as initial volume (Vargas et al., 2014).

3.3.2.8 Biotinilation of proteins

Biotin-XX Microscale Protein Labeling kit (Thermo Fisher) was used according to the manufacturer´s protocol for the biotinilation of primary amines of the GP120C, GP120C14K and PfCS proteins.

3.3.2.9 Stability and oligomerization state analysis of proteins

Protein stability measurements and oligomerization state analysis were undertaken as part of an iNEXT structural audit at the protein facility of the Netherlands Cancer Institute (NKI), Amsterdam. Briefly, the protein samples were resuspended in various buffer conditions (Table 4) and the Tm was measured using a Thermofluor assay based on previously described methods (Boivin et al., 2013). The propensity for aggregate formation was measured under the same buffer conditions using a Prometheus instrument (Nanotempertech) according to manufacturer´s instructions. The oligomerization state of proteins was analysed using a size exclusion coupled multi

angle light scattering (SEC - MALLS) assay according to previously described protocols (Van Dijk and Smit, 2000).

3.2.3 Virus

3.2.3.1 Generation of recombinant virus MVA-GP120C14K

In order to generate the recombinant viral vector MVA-GP120C14K, DF-1 cells grown to 70-80% confluency in a p60 (Nunc) plate were infected with 0.01 pfu/cell of the wild type virus MVA-wt. After an hour of adsorption, the inoculum was removed; the cells were washed thrice with 4 ml of OPTIMEM media (Gibco) and transfected with the DNA-liposome mixture made up by mixing 8 µg of the plasmid pCyA20-GP120C14K and 24 µl of lipofectamine reagent (Invitrogen) in OPTIMEM media during 20 minutes at room temperature. The mix was removed 5 hours post-transfection and the cells were washed twice with 4 ml of OPTIMEM media following which complete DMEM medium with 2% FCS was added and incubated at 37^0C with 5% CO_2. The cells were harvested when extensive cytopathic effect was observed, centrifuged (1800 rpm for 5 min), resuspended in 1 ml of DMEM and lysed using three freeze-thaw cycles. The extract thus obtained was sonicated before use (three cycles of 10 second sonication with a 10 second pause using the MISONIX INCORPORATED, S3000-010 sonicator). DF1 cells grown in M6 plates (Nunc) were infected using serial dilutions of this extract and after the inoculum was removed, 3 ml of 1:1 agar (1.9%) and DMEM 2X with 2% FCS was added and incubated at 37^0C with 5%CO_2. Following the observation of lysis plaques (about 48 hours later), X-Gal (0.03%) in 1 ml of agar (1.9%) and DMEM 2X (1:1) (Chakrabarti et al., 1985, Carroll and Moss, 1995)was added.

Those plaques that developed blue colour corresponding to the recombinant viruses were picked, resuspended in 0.5 ml DMEM and used as inoculum for further rounds of infection in DF-1 cells. This process of blue plaque selection was repeated thrice followed by two more rounds where white plaques (corresponding to those viruses that have lost the selection marker gene) were picked. The isolated recombinant virus thus obtained was used to generate the first intermediate stock (referred to as "P1 stock") for successive scaling up and generation of working stocks (referred to as "P2 stock"). The correct insertion of the antigen and the purity of the isolated recombinant virus was checked using PCR, while the correct expression of the GP120C14K antigen was

confirmed using Western Blotting. The viral DNA isolated was also sequence confirmed for the presence of the antigen of interest.

3.2.3.2 Virus Purification

Purification of virus through sucrose gradient was carried out using previously described methods (Joklik, 1962) (Esteban, 1984). Briefly, Chicken Embryo Fibroblast (CEF) cells were infected at 0.01 pfu/cell. When cytopathic effects were achieved, the cells were harvested, centrifuged (2000 rpm for 10 minutes at 4^0C) and the precipitate was washed once with PBS and resuspended in Tris-HCl 10 mM pH 9.0. This was followed by two cycles of sonication/centrifugation (three 10 second pulses/ 1800 rpm for 5 minutes). The supernatant from each cycle was centrifuged (20000 rpm for 60 minutes at 4^0C, in SW28 rotor (Beckman) over a 36% sucrose cushion in 10 mM Tris-HCl (pH 9.0). The pellet obtained was recovered and centrifuged over another sucrose cushion under the same conditions. The purified virus was resuspended in 10 mM Tris-HCl and was titrated and checked for contamination (bacteria in LB agar plate, fungi in blood agar plate and mycoplasma through PCR), while stored in small aliquots at -80^0C until further use.

3.2.3.3 Virus Titration

Titrations have been carried out according to standard protocols previously described (Ramírez et al., 2000). Briefly, DF-1 cells were infected with serial dilutions of the virus. 48 hours post infection, the medium was removed and the cells were fixed using 1:1 methanol acetone mixture and the titer was determined using immunostaining assay with rabbit anti-vaccinia polyclonal antibody and developed using 39,39-diaminobenzidine tetrahydrochloride (DAB; Sigma).

3.2.3.4 Growth Curve

The replication capacity of the viruses was determined through a growth curve experiment performed in DF-1 cells. Cells were infected at 0.01 pfu/cell with the virus for one hour at 37^0C, following which the inoculum was removed and DMEM with 2% FCS was added. At various time points post-infection (0, 24, 48, 72 and 96 hpi), the

infected cells were recovered and lysed through three free-thaw cycles and sonication. The infectious virus was determined using titration techniques described above (section 3.2.3.3).

3.2.3.5 Detergent treatment of purified virus particles for fractionation of viral proteins into different compartments

Sequential disruption of virus membranes was carried out using various detergents as previously described (Gomez and Esteban, 2001). Briefly, purified virions were resuspended through sonication in 0.2 ml of Tris/buffer (50 mM Tris-HCl pH 8.5, 10 mM $MgCl_2$) containing the non-ionic detergent NP-40 (1%). This and the following treatments were carried out at 37^0C for 30 minutes. The E1 fraction or the soluble lipid envelopes were removed by centrifugation while the pellet was re-suspended in 0.2 ml of Tris-buffer – 1% NP40 with 50 mM DTT. The E2 fraction or the soluble protein matrix-like membrane was separated by centrifugation and the pellet was re-suspended in 0.2 ml of the previous buffer with the addition of 0.5% DOC and 0.1% SDS. The E3 fraction or the soluble core proteins were removed by centrifugation and the pellet containing the remaining core (Core) were re-suspended in 0.2 ml of lysis SDS-buffer. All the fractions collected were run on SDS-PAGE under reducing conditions and the recombinant protein was identified using Western blotting.

3.2.4 Immunizations and Immunological methods

3.2.4.1 Animal Immunizations

The animal procedures detailed in this thesis were granted prior approval by the Ethical Committee of Animal Experimentation of Centro Nacional de Biotecnología (CEEA-CNB). All experiments were carried out in female BALB/c mice (H-2^d), 6-8 weeks old, obtained from Harlan Laboratories.

The different immunization protocols carried out within this work in order to assay the immunogenicity of the fusion construct GP120C14K compared with its controls involved the injection of

- 100 μg of DNA per mouse given via intra-muscular route

- 2 x 10^7 PFU of recombinant or wild-type MVA virus per mouse given via intra-muscular route
- 20 μg of protein per mouse given via intra-dermal route

All inoculum preparations were made in endotoxin-free PBS (Gibco). In the case of proteins, the final inoculum contained 10 μg ODN 1826 (Invivogen), 2% Alhydrogel (Invivogen) and equal parts Sigma adjuvant Oil (Sigma-Aldrich).

At the end of each immunization study, the corresponding animals were sacrificed using carbon dioxide (CO_2). The following samples were extracted from the animals:

- Blood
- Spleen
- Draining Lymph Nodes (Popliteal, Inguinal, Iliac and Sacral)

3.2.4.2 Intracellular Cytokine Staining or ICS

- Analysis of CD8 T cells

HIV-1 specific CD8 T cell responses were analysed by flow cytometry and intracellular cytokine staining (ICS) using previously described protocols (Vijayan et al., 2015). Briefly, cells were harvested from the spleen and the lymph node from vaccinated animals. 4×10^6 splenocytes and 10^6 cells from the lymph node were stimulated with 5 μg/ml of HIV-1 Env1 peptide along with 1 μl/ml GolgiPlug (BD Biosciences), anti-CD107a-Alexa 488 (BD Biosciences), and monensin (1X; eBioscience), using RPMI 1640 media (10% FCS) for 6 hours in a 96 well plate. Next, the cells were washed and mixed with anti CD16/CD32 (BD Biosciences) for blocking the Fc receptos, stained for the surface markers, fixed, permeabilized (Cytofix/Cytoperm kit; BD Biosciences), and later, stained intracellularly for cytokines conjugated with the appropriate fluorochromes. Live cells were selected using the violet LIVE/DEAD stain kit (Invitrogen). Cells were stained with different mouse antibodies, such as CD3-PE-CF594, CD4-APC-Cy7, CD8-V500, IFN-γ-PE-Cy7, IL-2-APC and TNF-α-PE and then passed through GALLIOS flow cytometer (Beckman Coulter). Data analysis was carried out using with FlowJo (Tree Star. Inc) and Spice (version 5.0). The response to specific stimuli was obtained after corrections were made with values obtained for control stimulated samples.

- Analysis of Germinal Center B cells or GC B cells

About 10^6 cells from the spleen and the lymph node were centrifuged and the live cells were marked using FVS 520 (BD Biosciences). Next, the cells were washed and mixed with anti CD16/CD32 (BD Biosciences) for blocking the Fc receptors, and then incubated with 0.3 µg of Biot-GP120C for 30 minutes at 4 degree C. After washing, staining of different markers used for the gating process (CD19+, B220+, IgD-, CD95+, CD38+, IgG1+, GL7+) was carried out with different antibodies such as CD19-FITC, B220-PECy7, IgD-APCH7, CD95-PE, CD38-PerCPCy5.5, IgG1-BV421, GL7-Alexa647, Av-PECF594, and the cells were passed through GALLIOS flow cytometer (Beckman Coulter). Data analysis was carried out using with FlowJo (Tree Star. Inc).

- Analysis of Follicular T Helper Cells or Tfh Cells

For the analysis of Env-specific Tfh cells, 4×10^6 splenocytes and 10^6 cells from the lymph node were stimulated with 10 µg/ml of Env-1 peptide and 0.5 µg/ml of GP120C protein. After 18-20 hours of incubation, live cells were marked using FVS 520 (BD Biosciences), and then stained for the markers corresponding to the gating strategy (CD3+, CD4+, CD8-, ICOS+, CXCR5+, PD1+), conjugated with the appropriate fluorophores such as CD3-PerCPCy5.5, CD4-Alexa700, CD8-eFluor450, PD1-APCeFluor780, CXCR5-PECF594, CD134-PE and CD25-PECy7. Cells were then passed through GALLIOS flow cytometer (Beckman Coulter). Data analysis was carried out using with FlowJo (Tree Star. Inc).

3.2.4.3 ELISPOT assay to analyse the IgG/IgG1 specific B cells

96-well Multiscreen® filter plates (Millipore) were incubated overnight with 10 µg/mL of unlabelled IgG or IgG1 antibody. One million splenocytes, previously stimulated with 0.5 µg/ml R848 Resiquimod (Invivogen) and 0.03 U/ml IL2 (BD Pharmingen) for 5 days, were added to the wells after prior blocking with RPMI-10% FCS. Cells were stimulated with 0.1 µg/ml of the respective labelled proteins (Biot-GP120C or Biot-PFCS) for 20 hours and the spots were developed after washing with PBS-T and using 1:800 streptavidin conjugated with horseradish peroxidase (BD Biosciences) and 1 µg/ml of DAB substrate (Sigma) resuspended in 50 mM Tris-HCl ph 7.5 and 0.015% H_2O_2. The spots were counted after extensive washing the plates with distilled water in

"ELISpot reader system – ELR02" (Autoimmun Diagnostika GmBh, Germany) using the software AID ELISpot reader system (Vitro).

3.2.4.4 ELISA analysis to determine the antibodies present in the serum of the immunized animals

To analyse the antibodies present in the serum of immunized animals, enzyme linked immunosorbent assays were performed. Following extraction, blood samples were incubated at 37^0C for one hour, left overnight at 4^0C and then centrifuged at 3600 rpm for 20 minutes at 4^0C to obtain the serum. To perform the ELISA, 96 well plates (NUNC Maxisorp) were coated with 2 μg/ml of the purified protein of interest in PBS and incubated at 4^0C overnight. The next day, the plates were blocked with 5% skimmed milk prepared in PBS-T (0.01% Tween20 v/v, Sigma). Serial dilutions of the serum were prepared and added to the protein coated plates which had been washed thrice with PBS-T following blocking. After 2 hours of incubation at room temperature, the plates were washed thrice again with PBS-T and the appropriate IgG antibody conjugated with horse radish peroxidase prepared in PBS-T was added to the wells and incubated for 90 minutes at room temperature. Finally, after another washing step, the plates were developed by adding 100 μl of TMB substrate (3,3',5,5' Tetramethylbenzidine; Sigma) and before reading the absorbance at 450 nm, the reaction was stopped by adding 50 μl of 1 M H_2SO_4. The endpoint dilution for each serum was calculated as the dilution which gave an absorbance value greater than thrice the value of the absorbance given by the corresponding dilution of the naïve serum.

3.3.4.7 Statistical methods

Statistical analysis for the ICS data for the analysis of CD8 T cells, GC B cells and Tfh cells were carried out by Dr. Carlos Oscar Sorzano (CNB, CSIC) based on previously defined methods published in the lab (García-Arriaza et al., 2010). The measurements were corrected for the unstimulated RPMI control sample prior to calculations of confidence intervals and *p* values of hypothesis tests. Only those antigen values significantly higher than the RPMI values are represented and the background for the distinct cytokines in the unstimulated controls were never less than 0.05%. SPICE software version 5.1 (Roederer et al., 2011) was used for the analysis and representation of the polyfunctional CD8 T cell responses.

4. RESULTS

4.1 Production, purification and characterization of protein components based on the HIV-1 clade C envelope region

4.1.1 Production and purification of HIV-1 envelope protein GP120C using stably transfected CHO-K1 cells

As shown in Fig. 8, the monomeric envelope protein GP120C from the HIV-1 CN54 isolate (clade C), was produced from CHO-K1 cells that were stably transfected with the plasmid PBJ5-GS with the GP120C gene sub-cloned within. The CHO-K1 cells were grown in roller flasks and the supernatant containing GP120C protein was purified by exploiting the high affinity between a lectin affinity column (derived from *galanthus nivalis*) and the compound sugars present on the glycosylated protein.

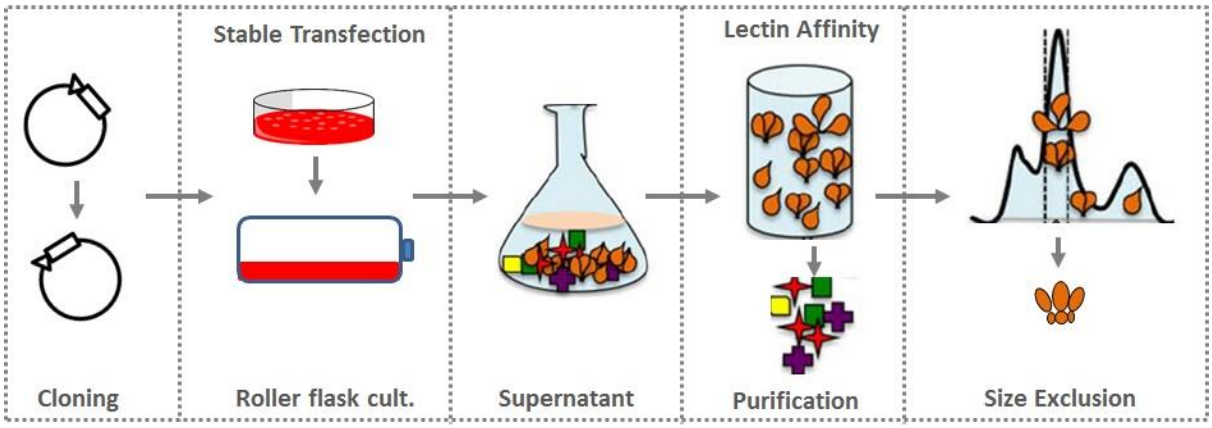

Fig. 8. Overall scheme of recombinant protein production and purification on a mammalian expression platform. Figure adapted from (Guenaga et al., 2015).

Final purification step was carried out using size exclusion chromatography, where the fractions (fraction size = 0.5 ml) containing the protein of interest (shown in Fig. 9) were selected. The typical yield of pure protein from 1 litre of supernatant was about 1.5 mg.

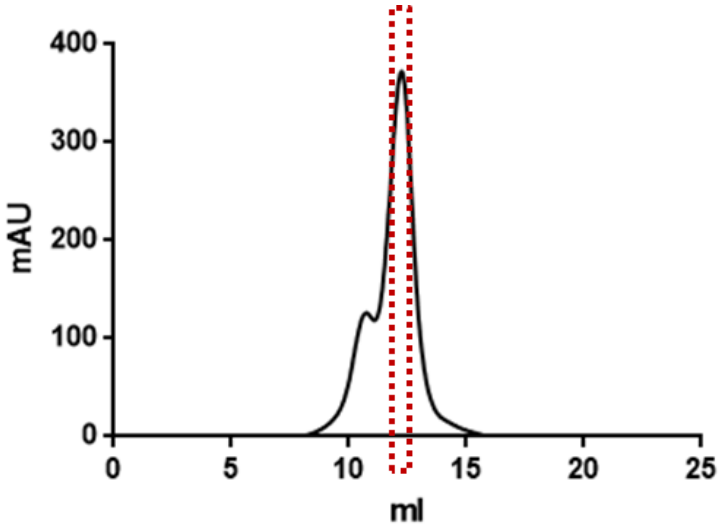

Fig. 9. Size exclusion chromatography profile of the purified GP120C protein. The red dotted area marks the fraction corresponding to the purified monomeric protein.

4.1.2 Production and purification of the oligomeric fusion protein GP120C14K

The fusion protein GP120C14K was produced by first fusing the GP120C gene from HIV-1 CN54 genome to N-terminal truncated VACV *A27L* gene coding for 110 amino acids that contribute to the post-translational formation of a trimeric coiled-coil region. This fusion gene, GP120C14K was then sub-cloned into the pBJ5-GS plasmid and subsequently used in the stable transfection of the CHO-K1 cell line. The protein purification was largely similar to that of the GP120C protein but in this case, the protein peak selected in the size exclusion separation procedure (Fig. 10) corresponded to a higher molecular weight (oligomeric state). The GP120C14K protein was clearly eluted well ahead of the GP120C monomeric protein, with the peak corresponding to the molecular weight range of 700 kDa. The typical yield of pure protein from 1 litre of supernatant was around 1 mg.

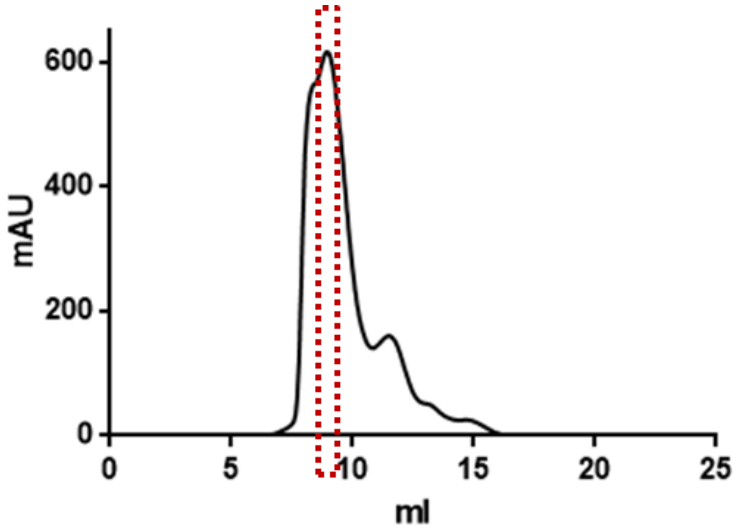

Fig. 10. Size exclusion chromatography profile of the purified GP120C14K protein. The red dotted area marks the fraction corresponding to the purified oligomeric protein.

4.1.3 Analysis of the GP120C and GP120C14K proteins

Following size exclusion, the presence of the purified proteins GP120C and GP120C14K in the selected fractions was analysed in electrophoresis under native/non-reducing conditions and in a Western blot under denaturing/reducing conditions. Under native conditions (Fig. 11-A), the GP120C protein was observed as a monomeric protein in the native gel (130 kDa), with the extra molecular weight attributed to the glycosylation of the molecule, while under reducing conditions (Fig. 11-B), GP120C reacted against a polyclonal antibody against GP120 at around 120 kDa. The fusion protein GP120C14K, however, was present at a higher molecular weight (around 700 kDa) in a native gel (Fig. 11-A) suggesting its existence as an oligomer and as a protein of around 150 kDa under reducing conditions in a Western blot (Fig 11-B).

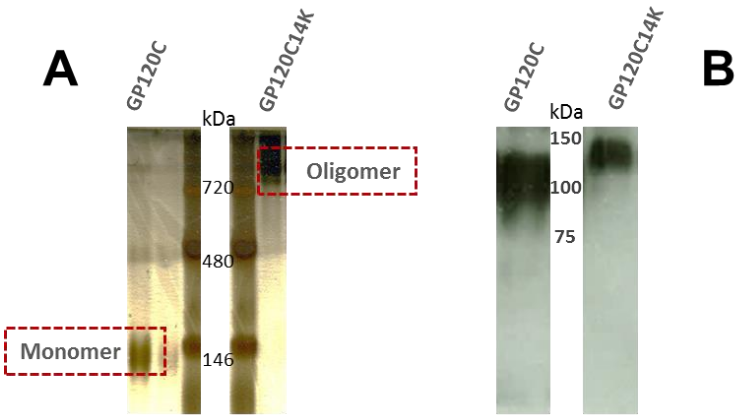

Fig. 11. Electrophoresis of GP120C and GP120C14K proteins under (A) native/non-reducing conditions (4-15% gel, silver stained) and (B) denaturing/reducing conditions in a Western blot (reacted with a rabbit polyclonal antibody against GP120).

Next, the GP120C and the GP120C14K proteins were tested for their reactivity to the monoclonal antibody C3 against the VACV 14K protein in a standard ELISA (Fig. 12). The GP120C14K protein reacted strongly to the C3 antibody at dilutions up to 1 in 10^6, confirming the presence of the 14K region within the oligomeric protein whereas the GP120C showed no reactivity against the C3 antibody as expected.

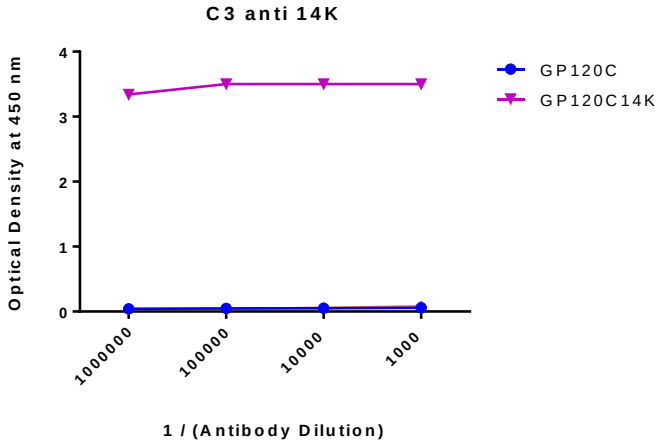

Fig. 12. Reactivity of GP120C and GP120C14K proteins to the C3 monoclonal antibody against the VACV 14K protein measured by ELISA.

4.1.4 Design and purification of mutants of the fusion protein incorporating the furin cleavage sites – GP120Crrrrr14K and GP120Creks14K

Given the importance of the furin cleavage event in the correct proteolytic processing of the HIV-1 envelope glycoprotein and its implied role in the determination of appropriate antigenic properties displayed by the GP120 molecule (Chakrabarti et al., 2011) (Ringe et al., 2013), two different mutants of the GP120C14K protein were constructed by changing the furin cleavage site "REKR" present between the GP120C and the 14K segments, in order to study the effect of furin cleavage on the antigenic characteristics of the fusion protein. These mutants were:

a. GP120Crrrrr14K – where the REKR was replaced by RRRRR to allow enhanced cleavage by endogenous furin.

b. GP120Creks14K – where the REKR was replaced by REKS to prevent any furin cleavage event.

The plasmids encoding these mutant fusion proteins – pCDNA-GP120Crrrrr14K and pCDNA-GP120Creks14K were generated using Gibson Assembly protocols and used for transient transfection of HEK 293T cells from which the proteins were purified using lectin columns and subsequent size exclusion chromatography. As shown in Fig.13, the differential effect of endogenous furin cleavage was observed in the size exclusion profiles. While the furin permissive mutant – GP120Crrrrr14K wass eluted in three distinct peaks suggesting a resolution into oligomer, monomer and cleavage intermediates, the furin non-permissive mutant – GP120Creks14K maintained a single peak corresponding to the un-cleaved oligomeric molecule.

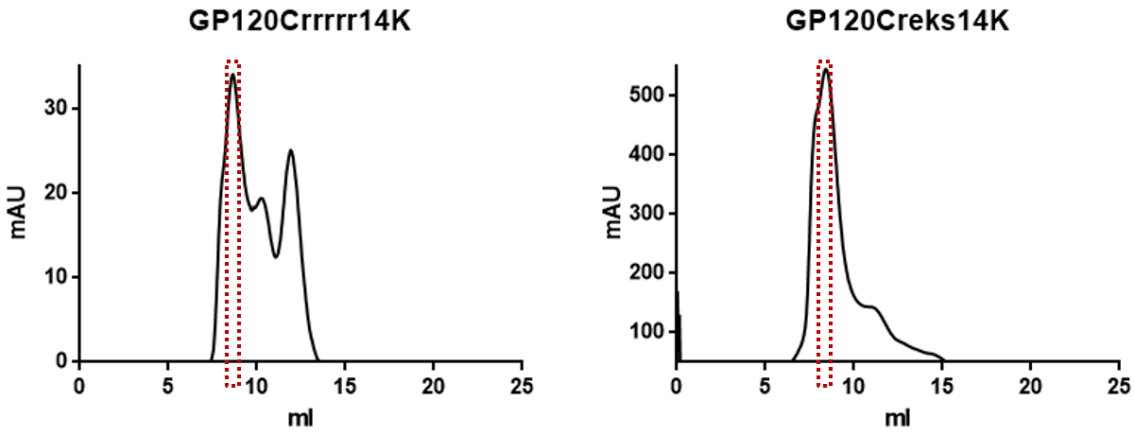

Fig. 13. Size exclusion profiles of the mutant fusion proteins GP120Crrrrr14K (left) and GP120Creks14K (right). GP120Crrrrr14K resolves into three peaks suggesting the resolution of oligomeric, monomeric and intermediate populations while GP120Creks14K maintains the uncleaved oligomeric peak in the size exclusion profile. The red dotted areas mark the fraction corresponding to the purified oligomeric protein.

4.1.5 Binding of the envelope mutants with standard neutralizing antibodies against HIV-1

In order to determine the antigenic characteristics of the fusion protein GP120C14K, we next examined the ability of the protein to bind to standard neutralizing antibodies. Therefore, ELISAs to test binding to such antibodies were performed with the GP120C14K protein, its monomeric control GP120C, the furin cleavage mutants GP120Crrrrr14K and GP120Creks14K, and an HIV-1 BG505.SOSIP (referred to as simply SOSIP from now on) native-like trimeric envelope protein as a positive control.

The binding characteristics of the different proteins under consideration were determined for the quaternary bNAb PGT 151 which is directed to GP120-GP41 interface (Blattner et al., 2014). As expected, the highest binding affinity was observed with the native-like SOSIP trimeric protein which was included as a positive control (Fig. 14-A). Among the other proteins tested, the highest binding affinity was detected with the GP120C14K protein when compared to the rest, suggesting that this oligomeric protein has more chances of exposing this key quaternary epitope implied in antibody-based neutralisation.

Next, the binding characteristics of these proteins were tested with the broadly neutralizing antibody PGT 121 (Julien et al., 2013) which is directed to specific glycans

at the N332 position of the envelope trimer. In this case, strong binding to PGT121 was detected in both the native-like SOSIP trimers and the GP120C14K protein (Fig. 14-B) suggesting that both the proteins might contain and/or better expose the corresponding epitope of this neutralizing antibody. The mutant proteins GP120Crrrrr14K and GP120Creks14K, and the monomeric GP120C showed relatively low binding to PGT 121.

Further, the reactivity of the proteins to neutralizing antibodies directed to the V3 variable region of the HIV-1 envelope spike such as 257-D IV (Gorny et al., 1991) (Gorny et al., 1993) and 10-1074 (targeting a carbohydrate dependant epitope on the V3 loop) (Mouquet et al., 2012, Garces et al., 2014) were determined. The GP120C14K protein showed the highest reactivity to both 257-D IV (Fig. 14-C) and 10-1074 (Fig. 14-D) demonstrating the presence and/or exposure of the corresponding epitopes from the V3 region.

Similar binding assays were performed against other bNAbs described in the literature such as PG9 (McLellan et al., 2011) and PG16 (Pancera et al., 2013) (quaternary bNAbs directed to the V2 and V3 loop region of the HIV-1 envelope), PGT 145 (Lee et al., 2017) (a quaternary bNAb against the V1-V2 region of the GP120 protein) and VRC01 (Li et al., 2011) (directed to the CD4 binding site). Apart from strong binding to the SOSIP native like trimers, these antibodies did not show significant binding to any of the other proteins analysed (data not shown).

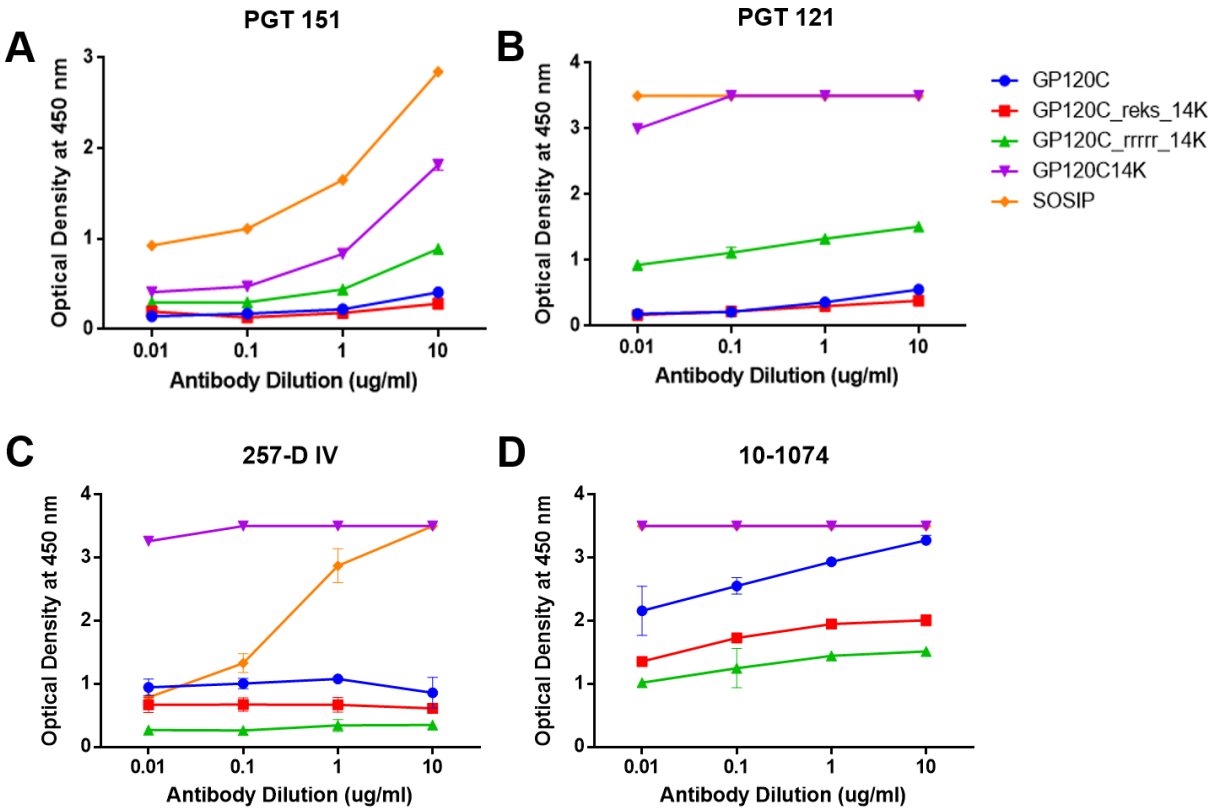

Fig. 14. Reactivity of envelope proteins to (A) quaternary conformational bNAb PGT 151 and broadly neutralizing antibodies (B) PGT 121, (C) 257-D IV and (D) 10-1074. The SOSIP protein was used as positive control.

Given the favourable antigenic characteristics of the GP120C14K fusion protein (with the partial cleavage site REKR) when compared with the furin cleavage mutants GP120Crrrrr14K and GP120Creks14K with respect to their reactivity to standard HIV-1 neutralising antibodies, this protein was selected for further biophysical, structural and immunological evaluation.

4.1.6 Biophysical characterization of the GP120C14K protein

4.1.6.1 Determination of the GP120C14K protein stability

Standard protein stability assays of the GP120C14K protein were performed as a part of the iNEXT Structural Audit grant at the Protein facility of the Netherlands Cancer Institute, Amsterdam. For the stability analysis, 0.2 mg/ml of the protein prepared under different buffer conditions (listed under Table 4) were analysed for their melting

temperatures (Tm) using Thermofluor assay and propensity for aggregation using Prometheus instrument.

Aggregate formation was not detected (as denoted by "ND" or "No Data" in Table 4) by the Prometheus instrument in 28 among 32 conditions tested during the structural audit. The absence of aggregation under a large majority of the conditions suggests that the GP120C14K protein is largely soluble and lacks any strong propensity to form aggregates under most of these buffer conditions.

Analysis of the melting temperatures (Tm) obtained through the Thermofluor assay revealed no major transition (Table 4) throughout the various conditions analysed (ranging between 56-58ºC), suggesting that the GP120C14K protein maintains a reasonable stability profile.

Condition	Description	Aggregation	Thermofluor Tm
1	50 mM MIB, 150 mM NaCl, pH 4.5	ND	58
2	50 mM MIB, 150 mM NaCl, pH 5.5	ND	58
3	50 mM MIB, 150 mM NaCl, pH 6.5	ND	57
4	50 mM MIB, 150 mM NaCl, pH 7.0	ND	57
5	50 mM MIB, 150 mM NaCl, pH 7.5	ND	57
6	50 mM MIB, 150 mM NaCl, pH 8.0	ND	57
7	50 mM MIB, 150 mM NaCl, pH 8.5	ND	57
8	50 mM MIB, 150 mM NaCl, pH 9.5	ND	57
9	50 mM Hepes pH 7.5, 25 mM NaCl	ND	57
10	50 mM Hepes pH 7.5, 100 mM NaCl	ND	57
11	50 mM Hepes pH 7.5, 250 mM NaCl	ND	57
12	50 mM Hepes pH 7.5, 500 mM NaCl	ND	57
13	50 mM Tris pH 7.5, 25 mM NaCl	ND	57
14	50 mM Tris pH 7.5, 100 mM NaCl	ND	57
15	50 mM Tris pH 7.5, 250 mM NaCl	ND	57
16	50 mM Tris pH 7.5, 500 mM NaCl	ND	58
17	100 mM NaPO4 pH 6.5	ND	58
18	100 mM NaPO4 pH 7.5	ND	57
19	100 mM NaPO4 pH 8.5	ND	56
20	50 mM Hepes pH 7.5, 150mM NaCl, 10% glycerol	ND	57
21	50 mM Hepes pH 7.5, 150mM NaCl, 20% glycerol	ND	57
22	50 mM Hepes pH 7.5, 150mM NaCl, 0.05% Tween	78.6	ND
23	50 mM Hepes pH 7.5, 150mM NaCl, 10 mM TCEP	57.9	58
24	50 mM Hepes pH 7.5, 150mM NaCl, 200 mM NDSB201	ND	57
25	50 mM Hepes pH 7.5, 150mM NaCl, 5 mM EDTA	ND	57
26	50 mM Hepes pH 7.5, 150mM NaCl, 20mM MgSO4	85.6	57
27	50 mM Hepes pH 7.5, 150mM NaCl, 2.5 mM ZnCl2	ND	56.5
28	50 mM Hepes pH 7.5, 150mM NaCl, 10 mM MnCl	ND	56
29	50 mM Hepes pH 7.5, 150mM NaCl, 20 mM LiCl	57.4	56.5
30	50 mM Hepes pH 7.5, 150mM NaCl, 20 mM CaCl	ND	56.5
31	50 mM Hepes pH 7.5, 150mM NaCl, 200 mM Glu/Arg	ND	57.5
32	50 mM Hepes pH 7.5, 150mM NaCl, 50 mM NaSCn	ND	58

Table 4. Stability analysis of the GP120C14K protein. The different buffer conditions under which the stability of the protein was analysed through Prometheus (measurement of aggregation events) and Thermofluor assay (measurement of Tm) are indicated. "ND" indicates No Data. All temperatures indicated are in degree Celsius.

4.1.6.2 Determination of the molecular weight of the GP120C14K protein using Size Exclusion Chromatography coupled Multi Angle Light Scattering (SEC - MALLS) assay

Further structural audit of the GP120C14K protein included the molecular weight and oligomerization state analysis using multi angle light scattering coupled to size exclusion chromatography. The elution curve indicating the scattering profile of the GP120C14K protein obtained using this technique is represented in Fig. 15.

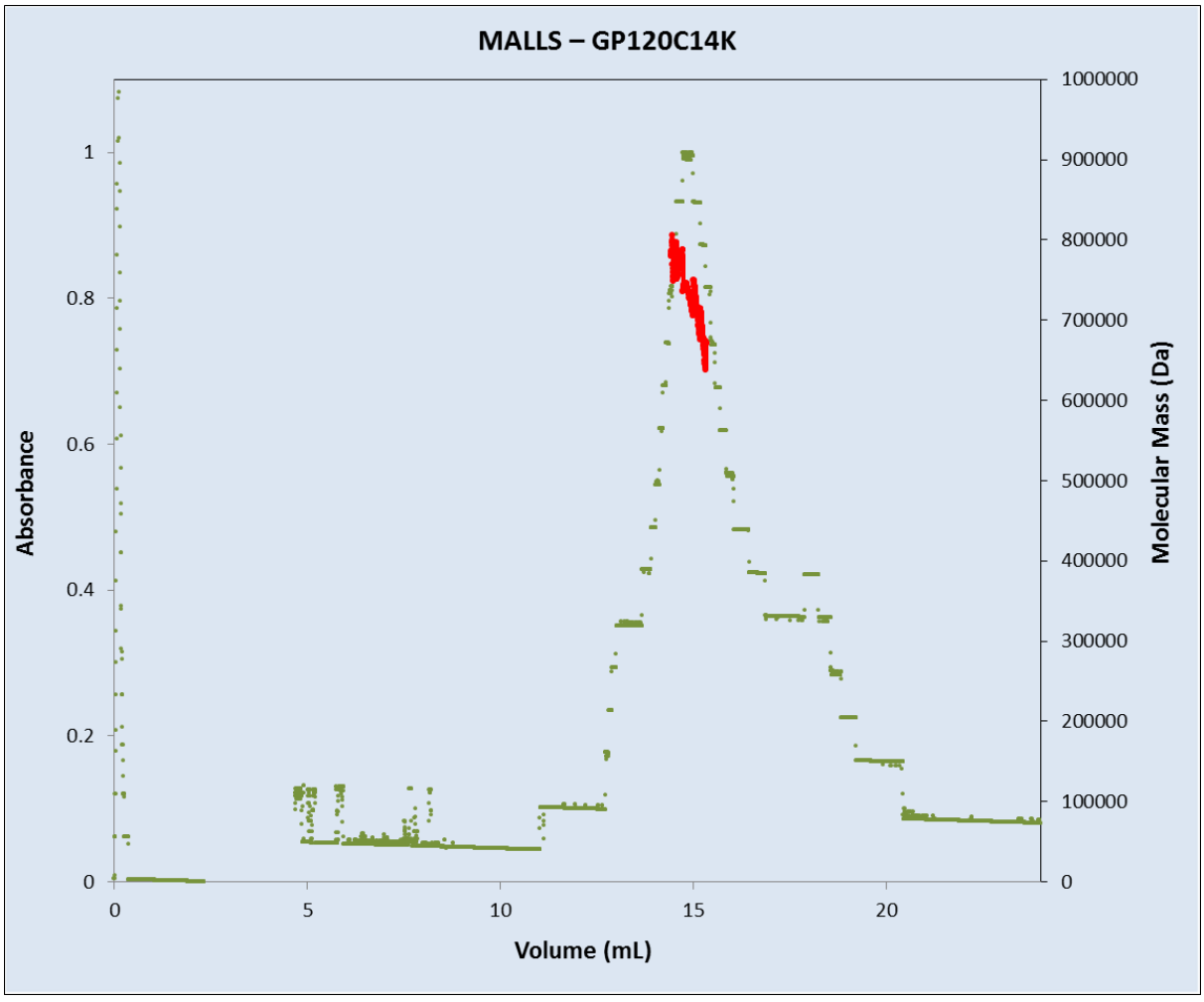

Fig. 15. Elution profile (elution volume against absorbance) of GP120C14K obtained through Size Exclusion Chromatography coupled Multi Angle Light Scattering (SEC-

MALLS) technique. The molecular mass corresponding to the protein peak obtained (indicated in red) is above 700 kDa.

The scatter-plot obtained for the GP120C14K protein represented on the size-exclusion elution profile (elution volume against absorbance) appears above 700 kDa, suggesting that the GP120C14K protein exhibits a molecular weight around this value (Fig. 15). Further, this observation is in concordance with the resolution of the purified protein around 700 kDa when analysed under native conditions (Fig. 11-A). Taken together, these observations suggest that the oligomeric GP120C14K molecule might exist as a hexamer.

4.1.6.3 Electron Microscopy (EM) analysis of the GP120C14K protein

Through a collaboration with Prof. Carrascosa´s group at the CNB, negative-stain electron microscopy (EM) analysis was performed to obtain structural insights into GP120C14K. The protein was prepared using the Gradient Fixation (GraFix) method. The three-dimensional representation of the GP120C14K protein was generated after the analysis of the image obtained from negative-stain EM (represented in Fig. 16). A closer look at the frontal and lateral views of the model suggests that the protein may exist as a hexamer. The arrangement of the molecule appears to be such that one trimeric unit of the GP120C14K molecule is superimposed on another to form the hexameric structure. This model is in concordance with the relatively high molecular weight of the protein (>700 kDa) observed in both native gels (Fig. 11-A) and size exclusion coupled MALLS graph (Fig. 15).

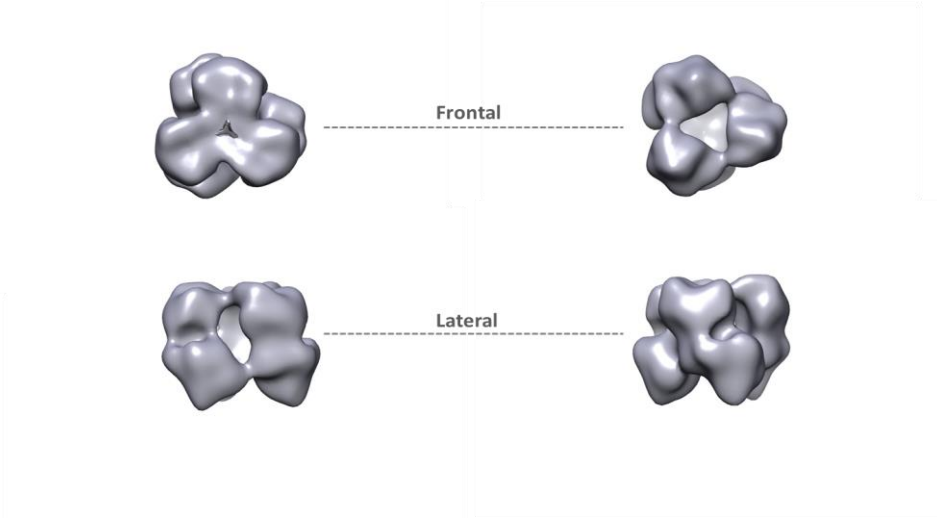

Fig. 16. Three dimensional image reconstruction of the GP120C14K protein based on negative stain electron microscopy data including the frontal (top) and the lateral (bottom) views of a 25 Å model of the GP120C14K protein obtained from multiple selected particles.

4.2 Generation and *in vitro* characterization of recombinant MVA vector expressing the fusion antigen GP120C14K (MVA-GP120C14K)

In order to express the homologous antigenic form of the oligomeric HIV-1 GP120C protein fused with the coiled coil region of the vaccinia virus 14K antigen from a vaccinia virus-based vector, a recombinant MVA virus expressing the fusion protein GP120C14K was constructed as described under Materials and Methods (Section 3.2.3.1) (Fig. 17).

4.2.1. PCR amplification to confirm the presence of the insert GP120C14K gene in the recombinant virus MVA-GP120C14K

Following the successful generation of the virus MVA-GP120C14K, the correct insertion of the gene of interest (GP120C14K) into the TK locus of the MVA parental genome was checked by PCR amplification using primers that cover the flanking regions of the TK locus. As observed in Fig. 17-B, the larger fragments obtained while amplifying the DNA of MVA-GP120C14K or pCyA20-GP120C14K (plasmid transfer vector used for the generation of MVA-GP120C14K) using the TK locus primers (flanking regions) correspond with the expected size of the GP120C14K insert, and no

wild-type contamination is observed. Thus, the presence of GP120C14K insert gene was confirmed using PCR amplification and further verified using DNA sequencing.

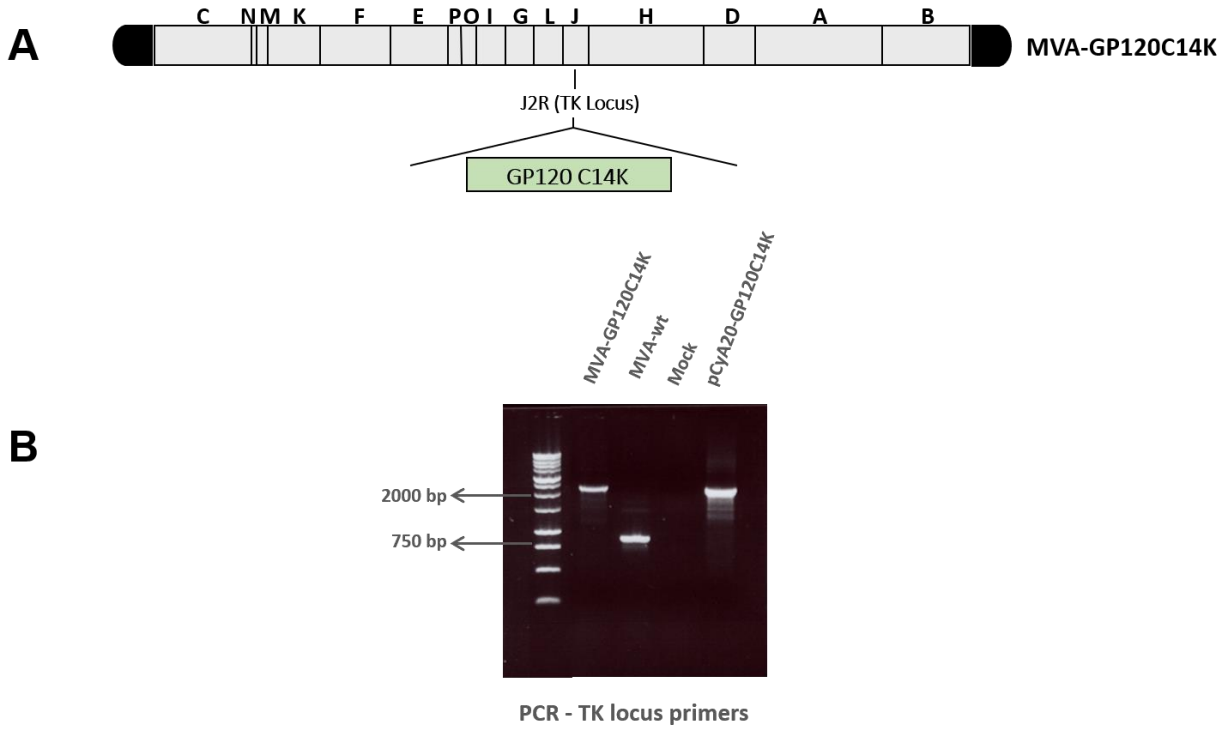

Fig. 17 (A) MVA-GP120C14K virus genome showing the presence of the GP120C14K gene within the TK locus of the parental MVA genome. (B) PCR amplification carried out on the viral DNA extracted from DF1 cells infected with MVA-GP120C14K or MVA-wt viruses using the TK locus primers, showing the difference in size between the amplified segments from both viruses indicating the correct insertion of GP120C14K (2215 bp) in the TK locus of MVA. The plasmid containing the fusion insert was used as a positive control template for the PCR.

4.2.2 Virus growth and replication characteristics

In order to determine whether the insertion of the GP120C14K gene had any effect on the growth and replication characteristics of the MVA virus, a growth curve analysis was carried out in DF-1 cells. The infected cell monolayers were fixed at different time points post-infection and viral titers were determined by immunostaining plaque assay. A sample plate of the immunostaining assay of the GP120C14K-expressing MVA recombinant virus using antibodies against vaccinia virus Western Reserve strain at 40 hours post-infection is represented in Fig. 18 for reference.

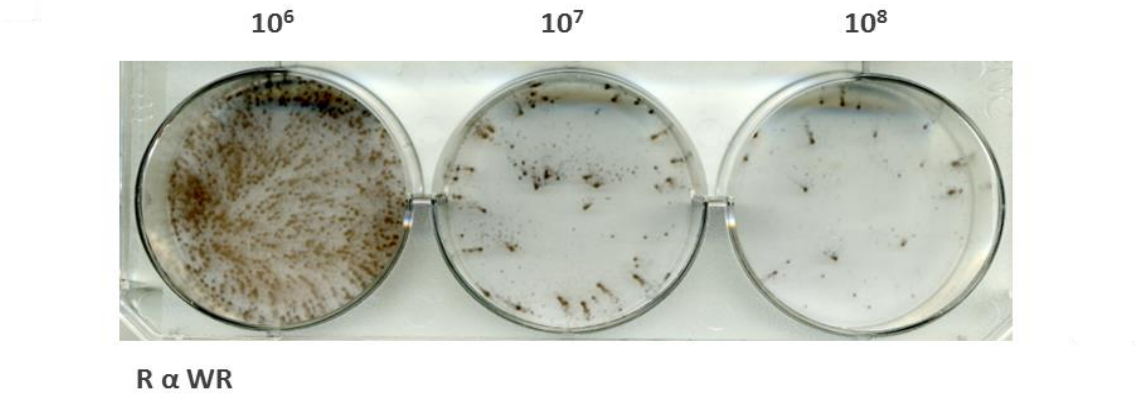

Fig. 18. Immunostaining plaque assay of MVA-GP120C14Kplaques in DF-1 cells infected with serial dilutions of the viral P3 stock. Cells were fixed at 40 hours post-infection and incubated with rabbit polyclonal anti-WR antibody

In a standard growth curve experiment, where the growth kinetics of the virus MVA-GP120C14K was compared with those of its parental MVA-wt virus and the MVA-GP120C virus, it is observed that all the three viruses show a similar growth pattern yielding similar titers across the different times post-infection (Fig. 19). Thus, it is confirmed that the insertion of the gene GP120C14K into the MVA-wt genetic backbone, had no effect on its growth and replication properties *in vitro*.

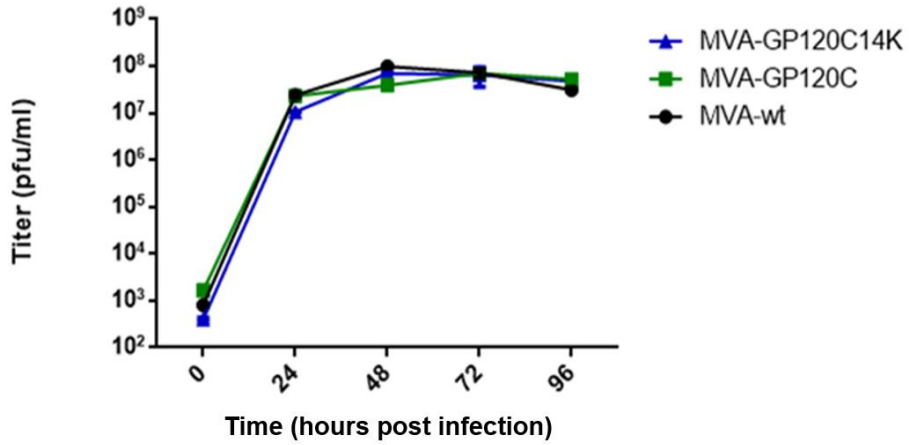

Fig. 19. Growth kinetics of MVA-GP120C14K compared with that of MVA-GP120C and MVA-wt viruses in DF-1 cells (MOI 0.01 pfu/cell).

4.2.3 Western-blot analysis to confirm the correct expression of the fusion protein GP120C14K by the recombinant virus MVA-GP120C14K

In order to verify the correct expression of the fusion protein GP120C14K from the recombinant virus MVA-GP120C14K in a permissive cell line, a standard Western-blot

analysis of cellular pellets and supernatants from DF-1 cells mock-infected or infected with MVA-GP120C14K at 1 pfu/cell for 24 hours was performed. As it is observed in Fig. 20, the presence of a band corresponding in size to the full-length fusion protein GP120C14K both in the supernatant and the cellular pellet of infected cells (when probed with either of antibodies that recognize GP120 or VACV 14K protein) confirmed the correct expression of the fusion protein by the virus MVA-GP120C14K.

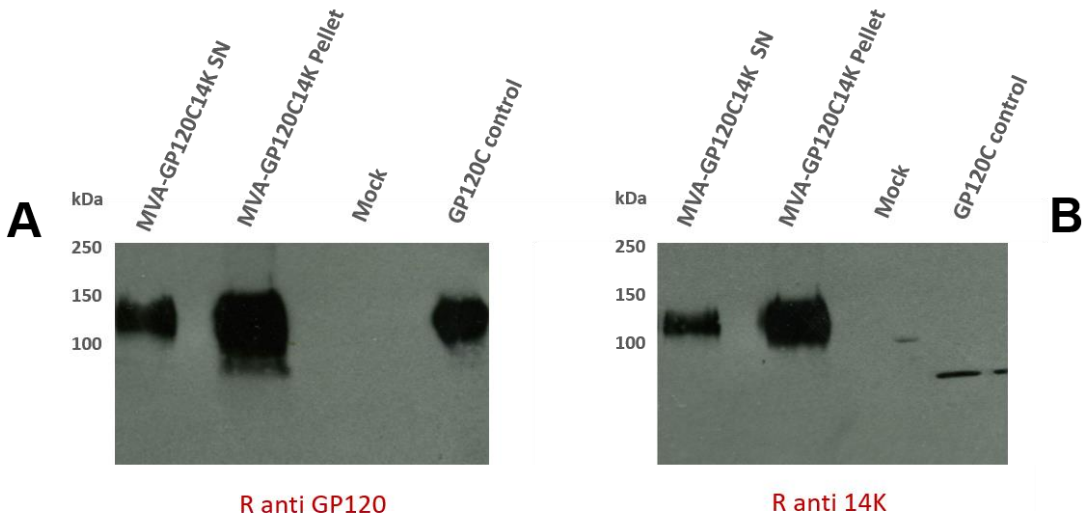

Fig. 20. Analysis of GP120C14K expression by Western-blot. GP120C14K expression was analysed in both supernatant (SN) and cellular pellet of DF-1 cells infected with MVA-GP120C14K virus at a multiplicity of infection or MOI of 1 pfu/cell for 24 hours. 500 ng of purified GP120C protein was used as control. Reactivity against rabbit anti-gp120 (A) and anti-14K (B) proteins are shown.

4.2.4 Time-course expression of GP120C14K antigen by the recombinant virus MVA-GP120C14K

The pattern of antigen expression by the virus MVA-GP120C14K was determined by Western-blot analysis in the cellular pellets (Fig. 21-A) and supernatants (Fig. 21-B) from non-permissive HeLa cells mock-infected or infected with MVA-C, MVA-GP120C or MVA-GP120C14K at 1 pfu/cell and harvested at different times post-infection (0, 4, 8 and 16 hours). The correct expression of the GP120C14K recombinant protein is observed in the cellular pellet from the early time point of 8 hours following infection by the virus MVA-GP120C14K. In the supernatant, the expression of GP120C14K is observed at the later time point (16 hours) post-infection when

compared with that of the GP120C antigen expression by MVA-GP120C (8 hours), which can be explained by the relatively larger size of the fusion protein and the possible formation of oligomeric structures in the cytoplasm of the cells prior to secretion.

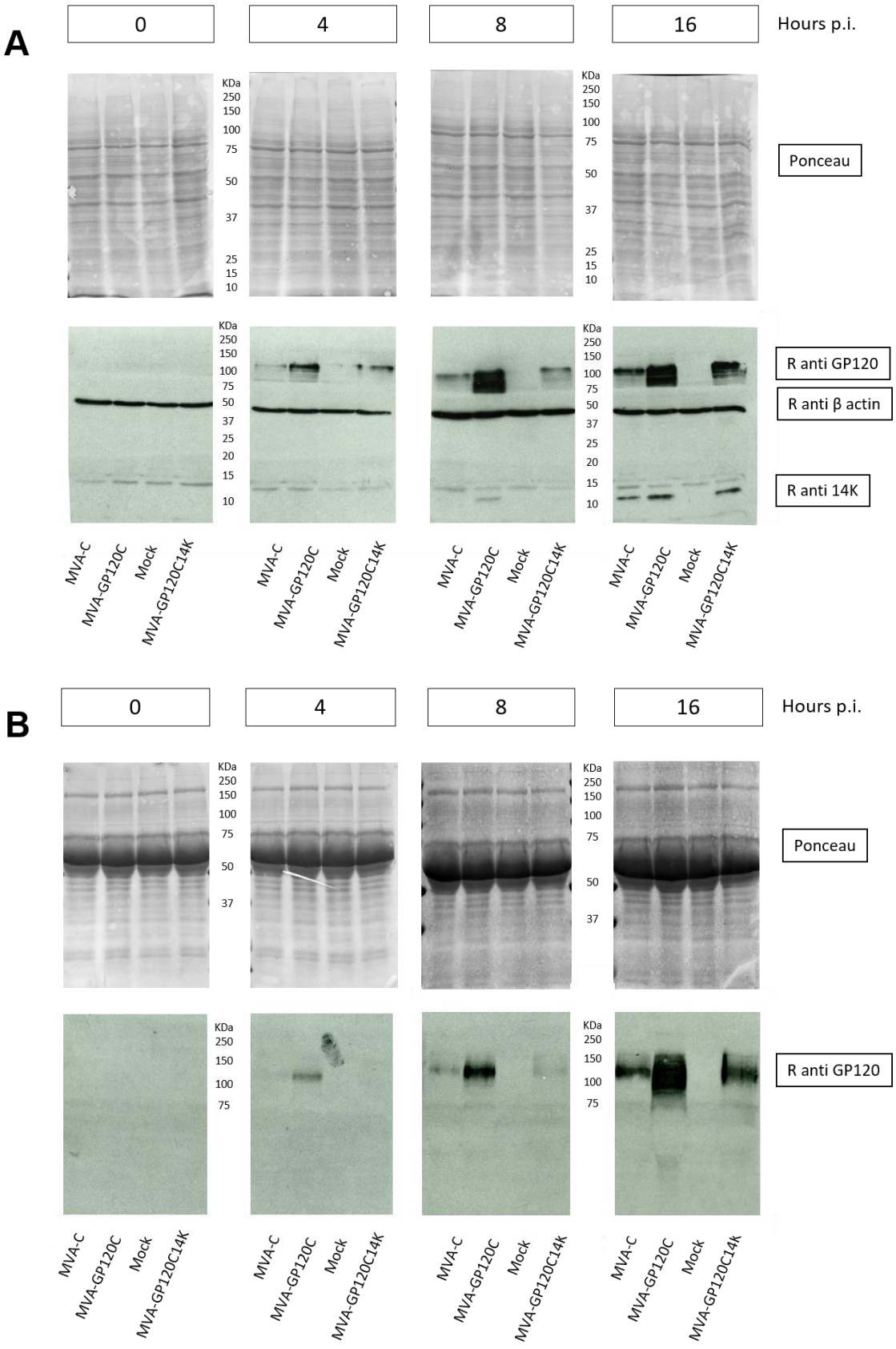

Fig. 21. Time-course expression of GP120C14K antigen by Western-blot analysis. HeLa cells were mock-infected or infected with MVA-C, MVA-GP120C or MVA-GP120C14K viruses at 1 pfu/cell and harvested at different times post-infection (0, 4, 8

and 16 hours). Antigen expression was analysed in (A) cellular pellet (showing reactivity against GP120, β-actin and VACV 14K proteins) and (B) supernatant (showing reactivity against GP120 protein). Top panels of both (A) and (B) show staining of the nitrocellulose membranes with Ponceau reagent.

4.2.5 Stability of antigen expression by the virus MVA-GP120C14K

In order to check the stability of the GP120C14K fusion protein expressed by the recombinant MVA-GP120C14K virus, 32 isolated plaques of the recombinant virus were picked after nine successive passages in DF-1 cells at low multiplicity of virus infection (0.01 pfu/cell) and the ability of these plaques to express the fusion protein was analysed in the cellular pellet of infected cells by Western-blot. As it is observed in Fig. 22, 100% of the individual plaques expressed VACV E3 protein confirming viral infection and 94% of the plaques (30 out of 32 plaques) expressed correctly the antigen GP120C14K. This observation indicates that the virus MVA-GP120C14K is highly stable, maintaining the integration of the transgene in the viral genome and the expression of the fusion protein GP120C14K after long-term passages.

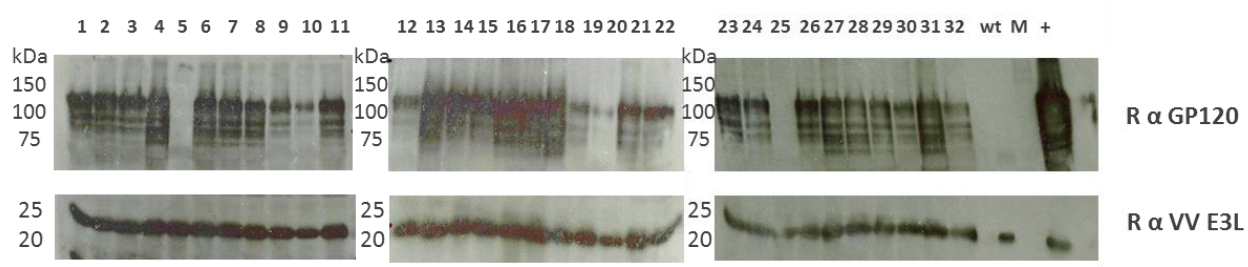

Fig. 22. Stability of MVA-GP120C14K recombinant virus after successive passages in DF-1 cells. Western blot of cell pellets under denaturing conditions following infection by MVA-GP120C14K plaques 32 individual plaques (numbered 1 through 32) isolated after 9 passages of MVA-GP120C14K in DF-1 cells were analysed by Western-blot. wt: MVA-wt; M: mock-infected; (+): MVA-GP120C14K P2 stock. Top panels show the blotting using the primary antibody against GP120 and the bottom panels against the vaccinia virus E3 protein as control of VACV infection.

4.2.6 Virion particle localization of the recombinant protein GP120C14K by step-fractionation of the purified MVA-GP120C14K virus

In order to determine the localization of the recombinant protein GP120C14K within the virion particle, the sucrose-purified MVA-GP120C14K viral preparation (P3 stock) was subjected to sequential disruption using different detergents (Section 3.2.3.5) to

obtain the various fractions E1, E2, E3 and Core. The analysis of these fractions by Western-blot using anti-GP120 and anti-VACV 14K antibodies revealed the presence of GP120C14Kin the total extract (T.E.) and in all the compartments (E1, E2, E3 and Core) of the purified recombinant virus MVA-GP120C14K.(Fig. 23). Interestingly, most of the anti-gp120 reactivity was found in the virus membrane E1 sample, while most of the anti-14K reactivity was in the core-associated fraction (Fig. 23). These findings revealed an association of the GP120C14K with the virion and its differential compartmentalization within in the virus particle.

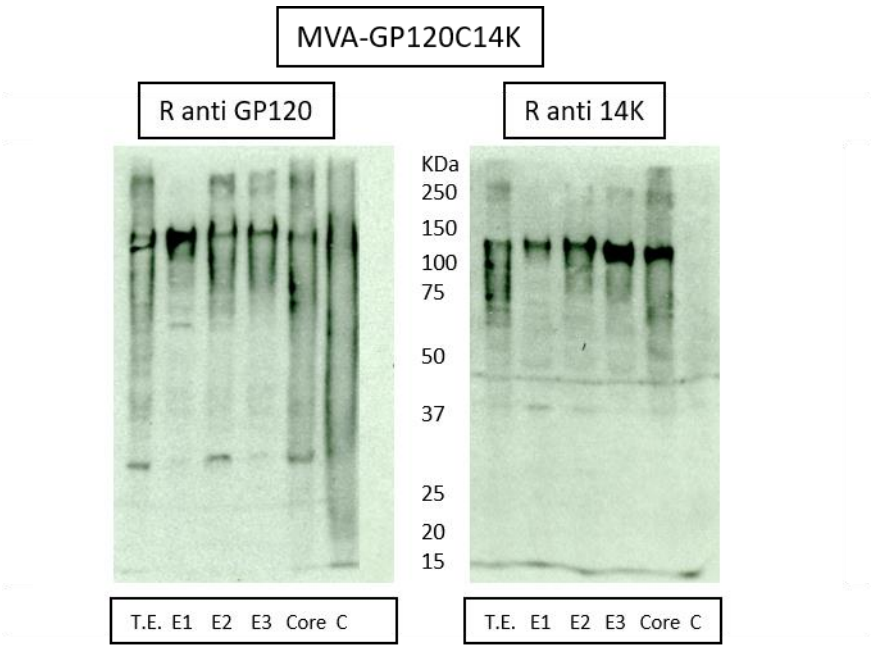

Fig 23. Sub-virion localization of GP120C14K by fractionation of the sucrose-purified MVA-GP120C14K virus. The unfractionated lysate virions (T.E.) and the various fractions (E1, E2, E3 and Core) obtained after sequential disruption by detergents were analysed by Western-blot. Reactivity against GP120 (left) and 14K (right) proteins are shown. “C” denotes unfractionated lysate virions (T.E.) of the MVA-C virus used as a control.

4.3 Immunological evaluation in mice of the purified protein GP120C14K and of the virus MVA-GP120C14K administered in homologous or heterologous combination of vectors

To examine whether the fusion of the 14K molecule and the subsequent oligomerization of the GP120C envelope protein lead to an enhancement of the T cell and/or B cell immune responses against the HIV- envelope, *in vivo* studies using BALB/c mice were performed according to the schedule depicted in Fig. 24. A total of 8 animals per group were immunized (intra-dermally for the proteins and intra-muscularly for the MVA) with the corresponding immunogens: protein prime + protein boost (P+P) or virus (MVA) prime + protein boost (M+P). With a view to optimizing the parameters for the detection of Tfh and GC B cell responses specific to the proposed vaccination regimen, the immune responses were analysed in two stages: early response (10 days post-boost) and late response (20 days post-boost). The purified proteins and their corresponding controls were delivered together with an adjuvant (Section 3.2.4.1).

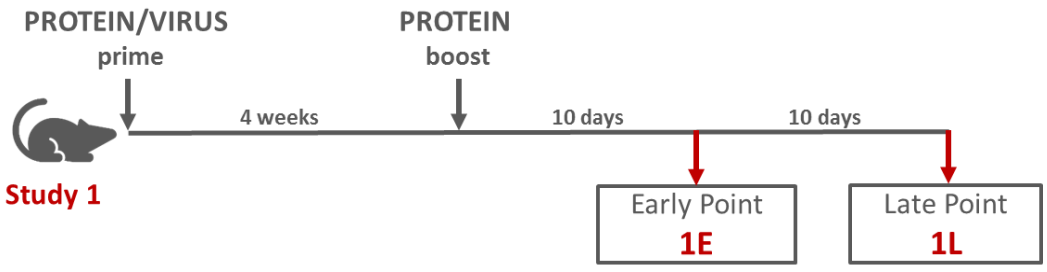

Prime	Boost
GP120C14K + adj.	GP120C14K + adj.
GP120C + adj.	GP120C + adj.
MVA-GP120C14K	GP120C14K + adj.
MVA-GP120C	GP120C + adj.
PBS + adj.	PBS + adj.
MVA-wt	PBS + adj.

Fig. 24. Immunization scheme for the evaluation of the immunogenicity *in vivo* of GP120C14K over GP120C using a protein prime + protein boost (P+P) protocol and an MVA based prime + protein boost (M+P) approach. The groups used for the analysis are listed in the table below with the composition of the prime and boost injections,

where adj. refers to the adjuvant mixture used. 1E and 1L refer to the early (10 days post-boost) and late points (20 days post-boost) respectively of the first *in vivo* study, where 4 mice per group were sacrificed at each time point for further analysis.

4.3.1 Analysis of the HIV-1 Env-specific CD8 T cell responses in spleen and draining lymph nodes by intracellular cytokine staining

To determine the HIV-1 Env-specific CD8 T responses, cells from the spleen and the draining lymph nodes harvested from the vaccinated animals were stimulated with an Env-1 peptide (specific for the GP120 envelope molecule from the clade C CN54 isolate). Following stimulation, the percentage of cells that secrete one or more of the specific cytokines (IFN-γ, IL-2, TNF-α) and/or display CD107a (an indirect marker for cytotoxicity) was analysed and compared between the groups as shown in Fig. 25 for the early point of 10 days post-boost.

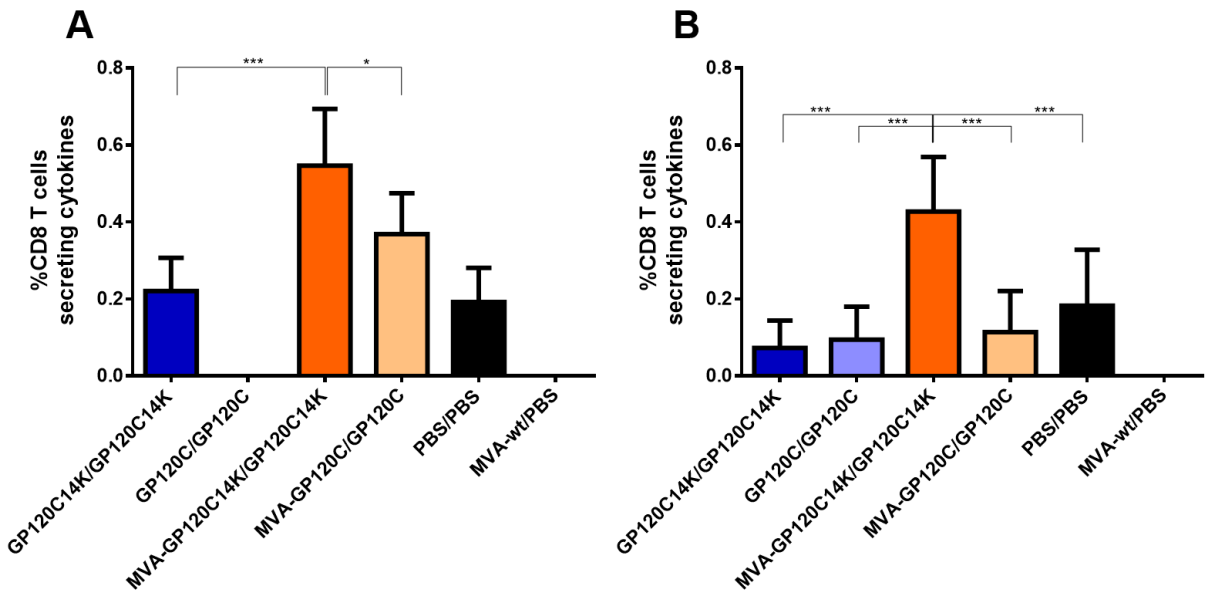

Fig. 25. Env-specific CD8 T cell responses measured at 10 days post-boost (early point) in the spleen (A) and the draining lymph nodes (B), represented as percentage of CD8 T cells secreting cytokines. Values were obtained from analysis of pooled spleen and lymph nodes from 4 animals per group and are represented with their corresponding confidence intervals. * $p<0.05$, *** $p<0.001$.

In general, the groups that had a MVA-primed and protein-boosted groups (M+P) showed higher HIV-1 Env-specific CD8 T cell responses than their corresponding protein-only groups (P+P). Specifically, the highest magnitude of HIV-1 Env-specific CD8 T cell response was observed with the GP120C14K (M+P) group and the response was statistically significant when compared with the rest of the groups analysed in both the spleen and the draining lymph nodes.

The quality of the CD8 T cell response was measured by the analysis of the polyfunctional profile elicited by the different immunization groups (measured by the ability of cells to secrete more than one type of cytokine and/or CD107a). As observed in Fig. 26, the groups containing the fusion antigen induced higher polyfunctional responses compared to their corresponding monomeric counterparts, i.e., higher polyfunctional responses were detected in the animals immunized with GP120C14K (M+P) compared with those immunized with GP120C (M+P) with more than 75% of the HIV-1 Env-specific CD8 T cells exhibiting three or four functions. CD8 T cells producing CD107a+IFN-γ+IL-2+ TNF-α and CD107a+IFN-γ+ TNF-α were among the populations most represented by the heterologous M+P vaccination groups. Similarly, in the draining lymph nodes, higher polyfunctional responses were detected in the animals immunized with GP120C14K (M+P) than the rest of the groups, although the majority of the responses were CD8 T cells producing IFN-γ (data not shown).

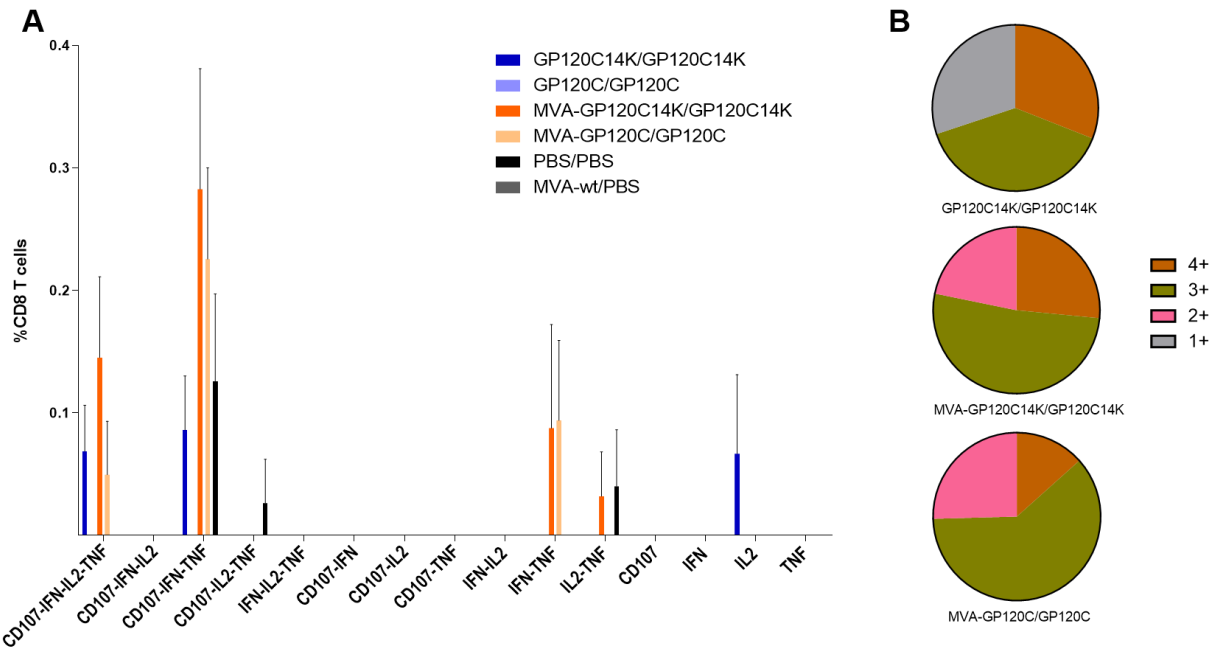

Fig. 26. (A) Polyfunctional profile of the envelope-specific CD8 T cell response obtained at 10 days post-boost in the spleen. Data are represented with their respective confidence intervals for each of the population analyzed. (B) The relative proportions of cell populations that express four (brown), three (green), two (pink) and one (grey) cytokine(s)/ CD107a are represented in the pie charts.

At 20 days post-boost, analysis of CD8 T cell responses from the spleen in Fig. 27-A, paints a picture largely similar to that of the early time point but now providing slightly higher response levels. Here again, the HIV-1 Env-specific CD8 T cell response tended to be higher in the groups primed with MVA-GP120C14K and boosted using the protein (M+P). Nevertheless, this response was not statistically significant compared to that obtained with the GP120C M+P group, although being significantly higher (*** $p<0.001$) than the GP120C14K P+P and the control groups. In the draining lymph nodes (Fig. 27-B), the trend of responses observed point to a higher response among the groups immunized with the fusion protein (P+P and M+P) than their corresponding monomeric counterparts.

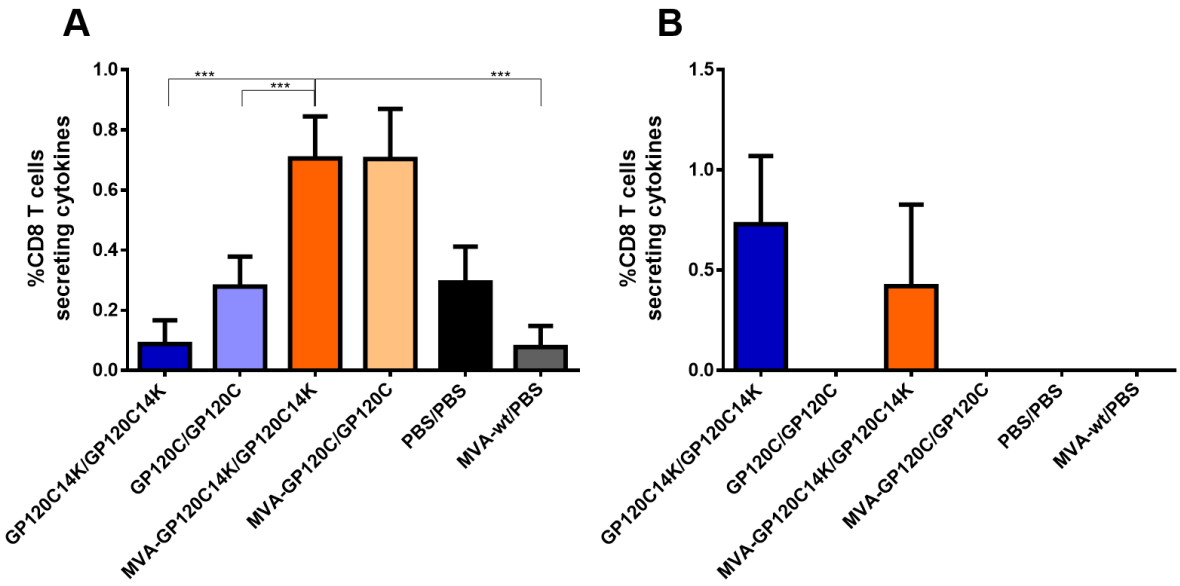

Fig. 27. Env-specific CD8 T cell responses measured 20 days post-boost (late point) in the spleen (A) and the draining lymph nodes (B), represented as the percentage of CD8 T cells secreting cytokines. Values were obtained from the analysis of pooled spleen and draining lymph nodes from 4 animals per group and are represented with their corresponding confidence intervals. *** $p<0.001$.

4.3.2 Analysis of the HIV-1 Env-specific IgG/IgG1 secreting cells (B cells) in spleen and draining lymph node using ELISPOT assay at 10 days post-boost.

In order to detect B cells that are capable of secreting HIV-1 Env-specific IgG or IgG1 among the cells from the spleen and lymph node at the early time point (10 days post-boost) a standard ELISPOT assay was modified and adapted for this experiment (described in the section 3.2.4.3).

In the case of spleen (Fig. 28-A), GP120C-specific IgG secreting cells were only observed with the groups containing the fusion protein. In particular, the GP120C14K protein only group (P+P) showed the highest number of spots and this response was statistically significant compared with the rest of the groups ($p<0.05$) compared with GP120C (P+P) and both the M+P groups, $p<0.005$ compared with the rest). The GP120C14K (M+P) immunization group showed the second highest number of spots and this response was statistically significant ($p<0.05$) compared with all the groups except for the GP120C14K (P+P) group.

A similar analysis to determine GP120C-specific IgG1 secreting cells in the spleen did not yield any significant responses from any of the groups.

When the GP120C-specific IgG1 secreting cells were analysed in the draining lymph nodes (Fig. 28-B), again, the only groups that showed a positive response were the ones containing the fusion protein. Interestingly, the GP120C14K (M+P) group showed the highest response in this case and this response was statistically significant ($p<0.005$) when compared with the rest of the groups. A similar analysis to determine GP120C-specific IgG secreting cells in the draining lymph node did not yield significant responses from any of the groups. Similarly, analysis of GP120C-specific IgG or IgG1 secreting cells at the late point (20 days) did not yield significant responses from the groups in spleens and the draining lymph nodes.

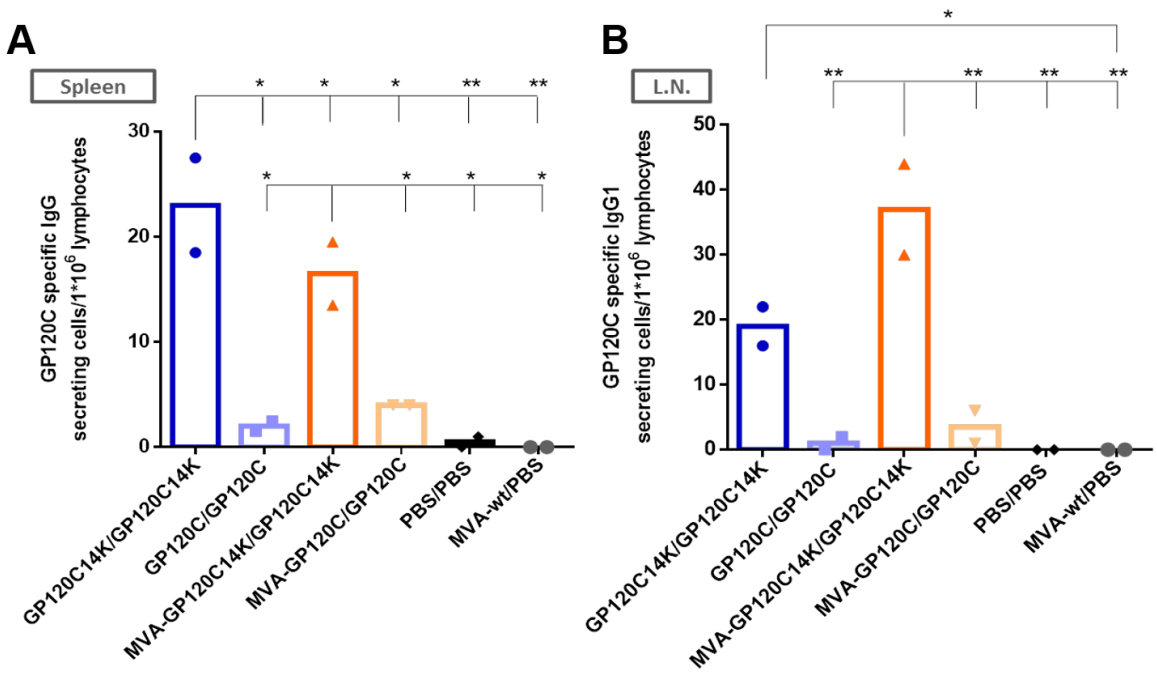

Fig. 28. (A) GP120C-specific IgG secreting cells in the spleen and (B) GP120C-specific IgG1 secreting cells in the draining lymph nodes by ELISPOT assay at 10 days post-boost. The number of spots obtained as duplicates are represented (as the total number of GP120C-specific IgG or IgG1 secreting cells per a million lymphocytes) after subtracting the individual background obtained for each group with the control (RPMI). Values were obtained from analysis of pooled spleens and draining lymph nodes from 4 animals per group. A two-way ANOVA test was performed for obtaining statistical relevance for the data. * $p<0.05$, ** $p<0.005$.

4.3.3 Analysis of HIV-1 Env-specific Germinal Center B cells (GC B cells) in the lymph nodes of immunized mice by flow cytometry

The germinal centre (GC) responses play a central role in the development of humoral immunity following vaccination (Victora and Nussenzweig, 2012). Within the GCs, antigen specific B cells, with the help of the appropriate Tfh cells, undergo rapid proliferation, somatic hypermutation, isotype class switching and affinity maturation, leading to the development of high affinity antibody production and memory B cells (Hamel et al., 2012).

In order to analyse the ability of the vaccine candidates to exploit the germinal centres reactions for the development of humoral responses to HIV-1, the percentage of Env-specific GC B cells elicited in the draining lymph nodes following vaccination was determined through flow cytometry.

In the early point (10 days post-boost), the highest percentage of GC B cells among the total B cell population detected in the lymph nodes was obtained in the mice immunized with the fusion antigen (M+P). This response was significantly higher ($p<0.001$) than those obtained with all the other groups (Fig. 29-A). Within the respective populations of the GC B cells, the highest proportion of HIV-1 Env-specific GC B cells was observed with the GP120C14K fusion protein only group (P+P), which was statistically significant ($p<0.001$) compared to those obtained with the other vaccination groups (Fig. 29-B). Among the other groups, the percentage of Env-specific GC B cells was significantly higher ($p<0.001$) in the group immunized with the MVA-GP120C14K followed by the GP120C14K protein boost (M+P).

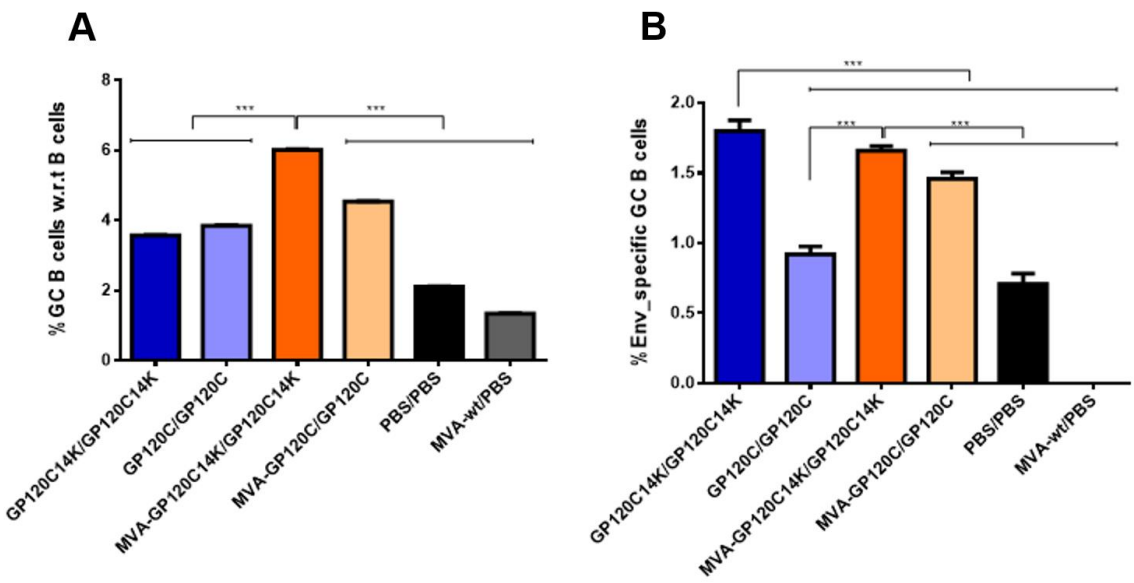

Fig. 29. Percentage of total GC B cells among the B cells detected in draining lymph nodes of immunized animals at the early time point of 10 days (A) and the corresponding percentage of Env-specific GC B cells present among this population (B). Values were obtained from analysis of pooled draining lymph nodes from 4 animals per group and are represented with their corresponding confidence intervals. *** $p<0.001$.

At the late point (20 days post-boost), the draining lymph nodes from the mice immunized with the fusion antigen GP120C14K (M+P) showed the highest percentage of GC B cells among the total population of B cells, when compared with the levels obtained from the other immunization protocols ($p<0.001$) as seen in Fig. 30-A. The proportion of GC B cells observed with the GP120C14K protein only group (P+P), although lower than that observed with the M+P protocol, was significantly higher ($p<0.001$) than the rest of the groups analysed. Within the respective populations of the GC B cells, the highest proportion of HIV-1 Envelope specific GC B cells were observed with the GP120C14K (M+P) group as seen in Fig. 30-B, (which was statistically significant ($p>0.005$) compared to the GP120C14K P+P group and ($p<0.001$) with respect to the GP120C M+P group).

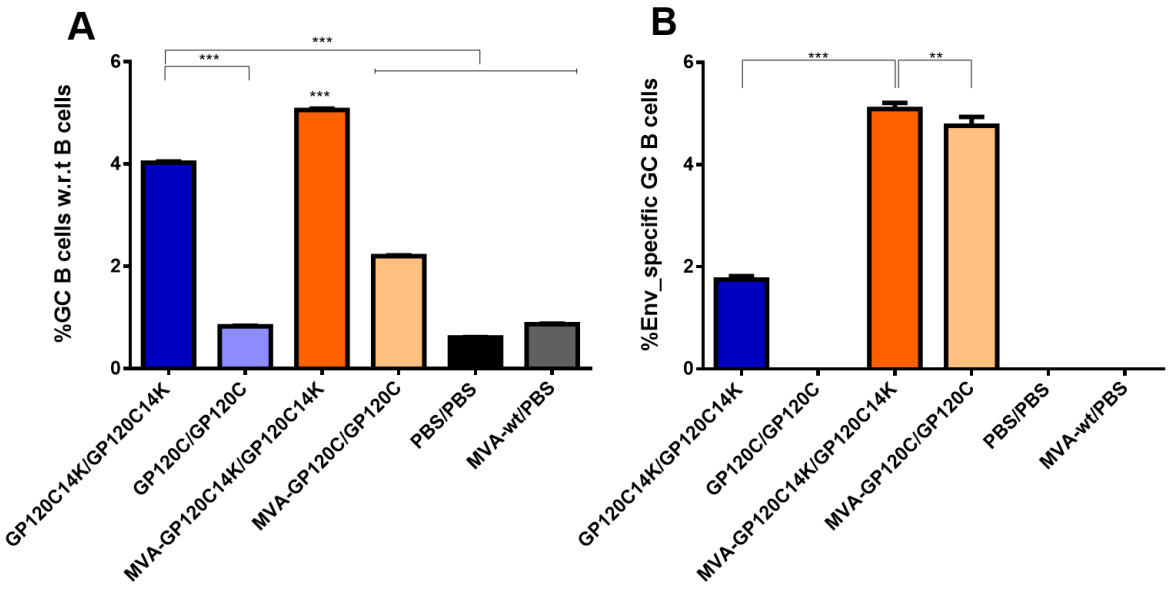

Fig. 30. Percentage of total GC B cells among the B cells detected in draining lymph nodes of immunized animals at the late time point of 20 days (A) and the corresponding percentage of Env-specific GC B cells present among this population (B). Values were obtained from analysis of pooled draining lymph nodes from 4 animals per group and are represented with their corresponding confidence intervals. ** $p<0.005$, *** $p<0.001$.

4.3.4 Analysis of the HIV-1 Env-specific T follicular helper cells (Tfh cells) in the spleen of immunized animals by flow cytometry

T follicular helper cells (Tfh) are an important sub-set of CD4 T cells that are critical for the generation of high-affinity GC B cells and for the promotion of inter-zonal migration of B cells for repeated rounds of somatic hypermutation (Vinuesa et al., 2016). Given the importance of Tfh cells in the development of humoral responses against the HIV-1 envelope in the context of vaccination (Niessl and Kaufmann, 2018), the proportion of Env-specific Tfh cells in the spleen of vaccinated animals was analysed in the early and late time points by flow cytometry.

As observed in the Fig. 31-A, in the early point of 10 days post-boost, the percentages of Tfh cells among the total CD4 cell population detected in the splenocytes obtained from mice immunized with the fusion antigen GP120C14K in either protocols – P+P and M+P, were significantly higher ($p<0.001$) than those observed in the groups immunized with their monomeric GP120C counterparts. Overall, the response obtained by the protein only groups were higher than those in the M + P groups. However, the

highest proportion of total Tfh cells were seen in the control groups (PBS+PBS and MVA-wt+PBS). Within the Tfh population, the highest proportion of HIV-1 Env-specific Tfh cells was observed in the splenocytes from mice immunized with the GP120C14K fusion antigen under the M+P protocol (Fig. 31-B), and this response was significantly higher ($p<0.001$) than those obtained with all the other groups.

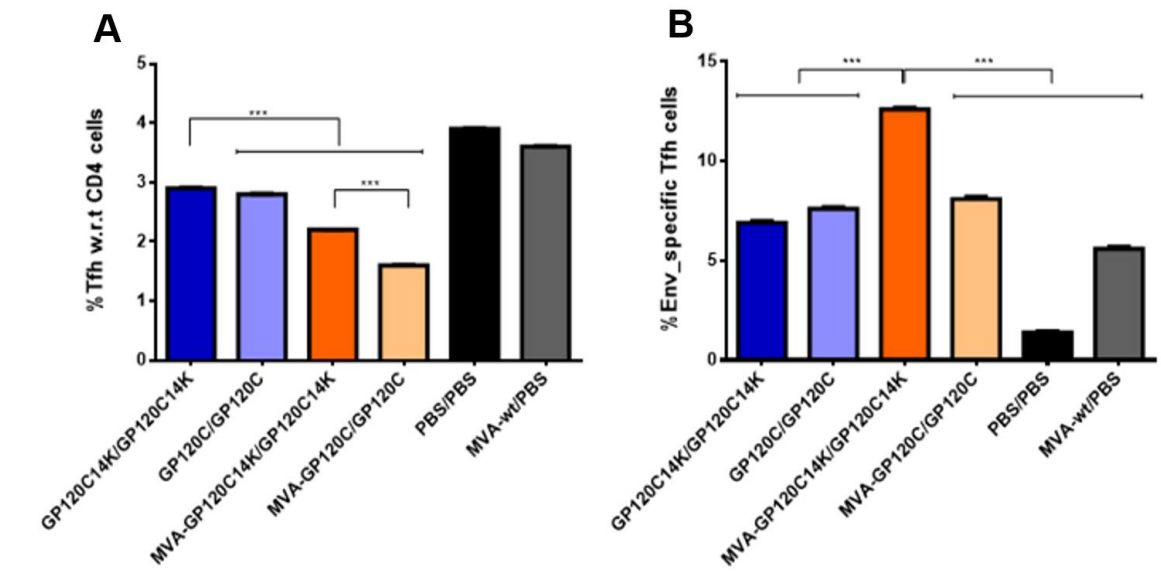

Fig. 31. Percentage of total Tfh among the CD4 T cells detected in the splenocytes of immunized animals at the early time point of 10 days post-boost (A) and the corresponding percentage of Env-specific Tfh cells present among this population (B). Values were obtained from analysis of pooled spleens from 4 animals per group and are represented with their corresponding confidence intervals. *** $p<0.001$.

The percentage of total Tfh cells among the CD4 population obtained in the late point of 20 days post-boost (as seen in Fig. 32-A) indicates similar levels among the groups analysed. However, the profile of percentage of envelope-specific Tfh cells among the groups is maintained with respect to the early time point (Fig. 32-B), where the groups immunized with the M+P protocol show significantly higher values ($p<0.001$) than the rest of the groups.

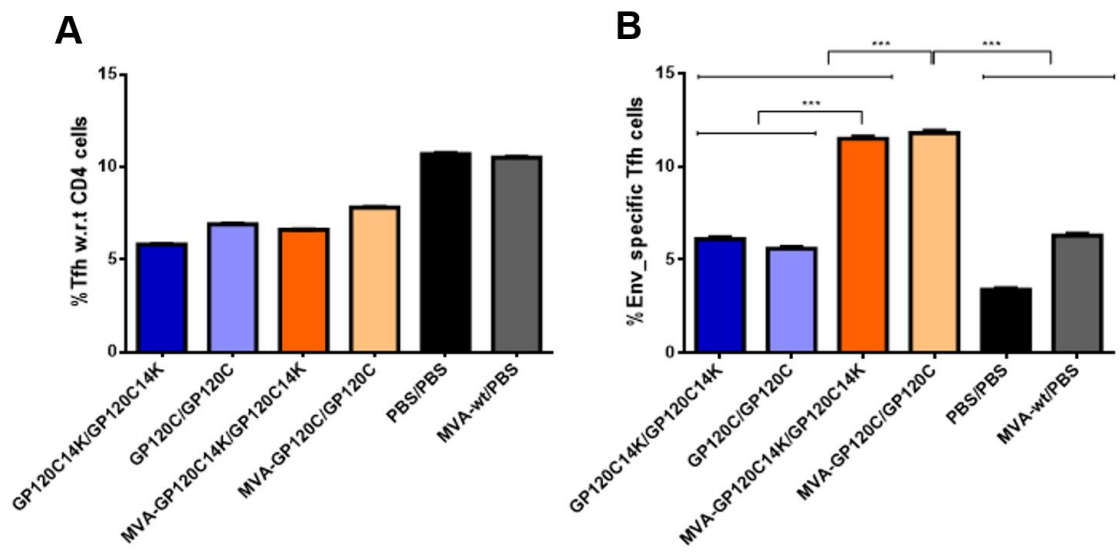

Fig. 32. Percentage of total Tfh cells among the CD4 T cells detected in the splenocytes of immunized animals at the late time point of 20 days post-boost (A) and the corresponding percentage of Env-specific Tfh cells present among this population (B). Values were obtained from analysis of pooled spleens from 4 animals per group and are represented with their corresponding confidence intervals. *** $p<0.001$.

4.3.5 Analysis of anti-GP120C and anti-vaccinia virus antibodies in the serum of immunized mice with the P+P and M+P protocols.

The capacity of the immunization protocol to raise antibodies (total IgG) against the HIV-1 envelope protein GP120C was analysed by ELISA. The end-point titers obtained for the different groups of immunization and the progression of the optical density measured at 450 nm are shown in Fig. 33. Similar levels of very high titers of antibodies against GP120C (1,024,000) were detected in both the groups containing the fusion antigen GP120C14K (P+P and M+P) (Fig. 33-A) with a largely interchangeable optical density progression profile (Fig. 33-B). While the protein only group with the GP120C monomer (P+P), showed a very low response (1000 times lower) in comparison with that elicited by the fusion protein, the GP120C (M+P) group showed improved titers of anti-GP120C antibodies (320,000) on an average.

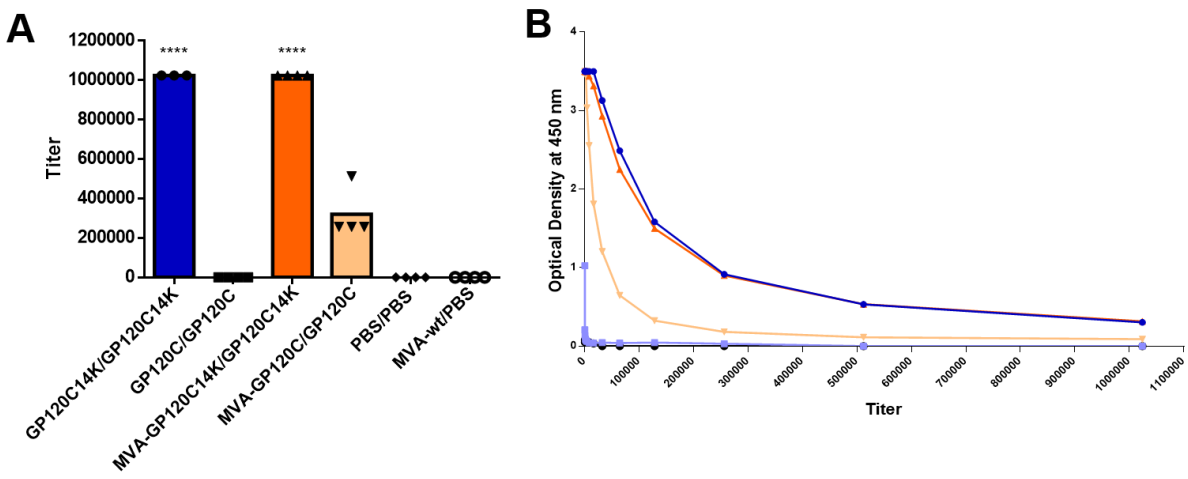

Fig. 33. Anti-GP120C antibody levels (total IgG) in the serum of immunized mice at the early point of 10 days post-boost measured by ELISA. (A) End-point titers of antibody responses obtained for each group (n = 4), calculated as the last dilution that provided an optical density value (at 450 nm) that is more than three times the value obtained at the same dilution by the naïve serum. (B) Optical density (at 450 nm) progression of serum dilutions from the different groups. A two-way ANOVA test was performed for obtaining statistical relevance. **** $p<0.0001$.

At the late point of 20 days post-boost, titers of anti-GP120C antibodies were measured in the serum of immunized animals by ELISA (Fig. 34-A). Similar to the 10-day point, very high titers of antibodies (1,024,000) against the GP120C antigen were obtained in both the groups (P+P and M+P) containing the fusion antigen GP120C14K with a largely interchangeable optical density profile (Fig. 34-B). These higher titers obtained with both the GP120C14K groups were statistically significant ($p<0.0001$) compared with the titer obtained with the GP120C (M + P) group (448,000).

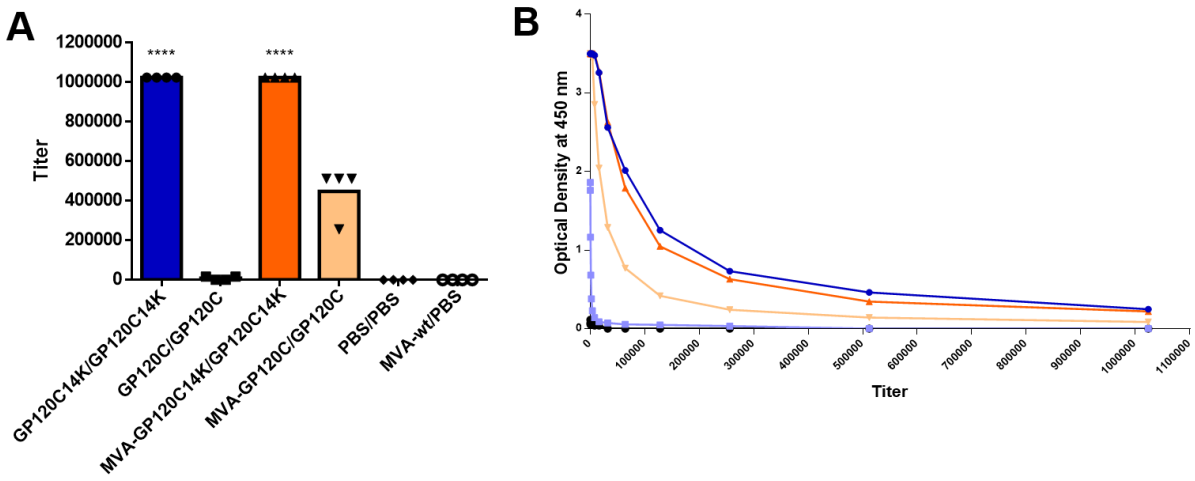

Fig. 34. Anti-GP120C antibody levels (total IgG) in the serum of immunized mice at the late point of 20 days post-boost measured by ELISA. (A) End-point titers of antibody responses obtained for each group (n = 4), calculated as the last dilution that provided an optical density value (at 450 nm) that is more than three times the value obtained at the same dilution by the naïve serum. (B) Optical density (at 450 nm) progression of serum dilutions from the different groups. A two-way ANOVA test was performed for obtaining statistical relevance. **** $p<0.0001$

The presence of antibodies against vaccinia virus (a soluble extract from cells infected with 2 pfu/cell of the WR strain of vaccinia virus for 24 hours) was tested in the serum of immunized animals at both the early (Fig. 35-A) and late points (Fig. 35-B). At both time points, the highest titer of anti-vaccinia antibodies were detected in the GP120C14K (M+P) and the corresponding MVA-wt/PBS control groups, followed by the GP120C (M+P) group. The presence of anti-vaccinia antibodies was also detected in the groups immunized with only the GP120C14K fusion protein at both time points, indicating the ability of the 14K protein *per se* to raise antibodies in the serum of immunized animals.

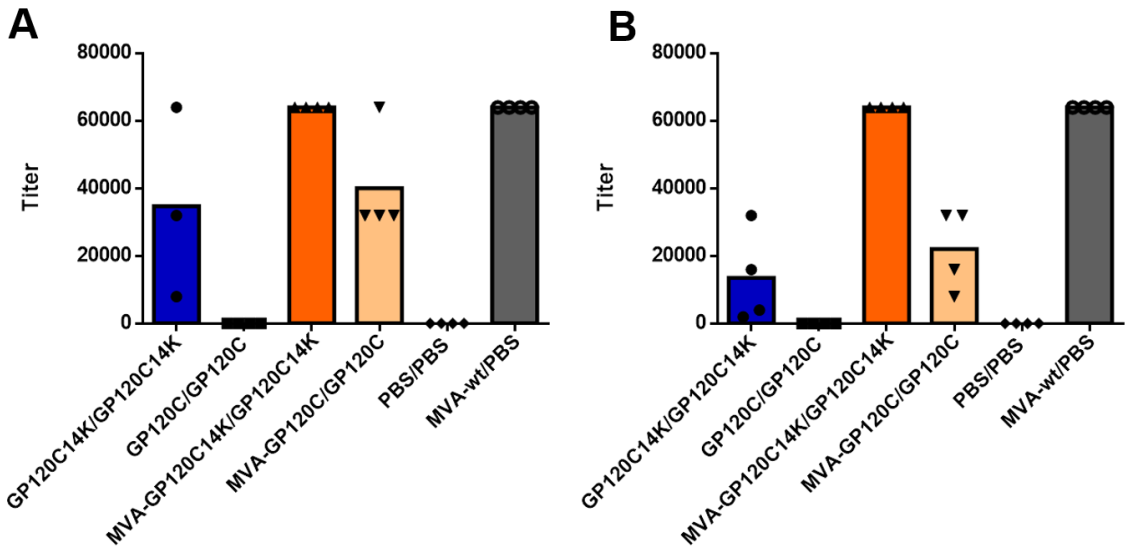

Fig. 35. Anti-VACV antibody levels (total IgG) in serum of immunized animals at the early point of 10 days post-boost (A) and late point of 20 days post-boost (B) against vaccinia virus measured by ELISA. The end-point titers of antibody responses obtained for each group was calculated as the last dilution that provided an optical density value (at 450 nm) that is more than three times the value obtained at the same dilution by the naïve serum.

4.4 Immunological evaluation in mice of the fusion protein GP120C14K expressed from a DNA vector followed by boosting with MVA- GP120C14K and adjuvanted protein GP120C14K (protocol D+M+P).

We have previously described that HIV-1 Env expressed from a DNA vector was a potent priming agent for cellular responses when combined with a poxvirus vector (Gómez et al., 2007b). Thus, next we examined whether the addition of a priming step using a DNA vector expressing the fusion antigen GP120C14K leads to an improvement in the T and B cell immune responses against HIV-1 Env protein when compared with the monomeric GP120C delivery using the same protocol. Hence, we performed an *in vivo* study using BALB/c mice according to the immunization protocol shown in Fig. 36. A total of 8 animals per group were immunized (intra-dermally for the proteins and intra-muscularly for the MVA and the DNA) with the corresponding immunogens.

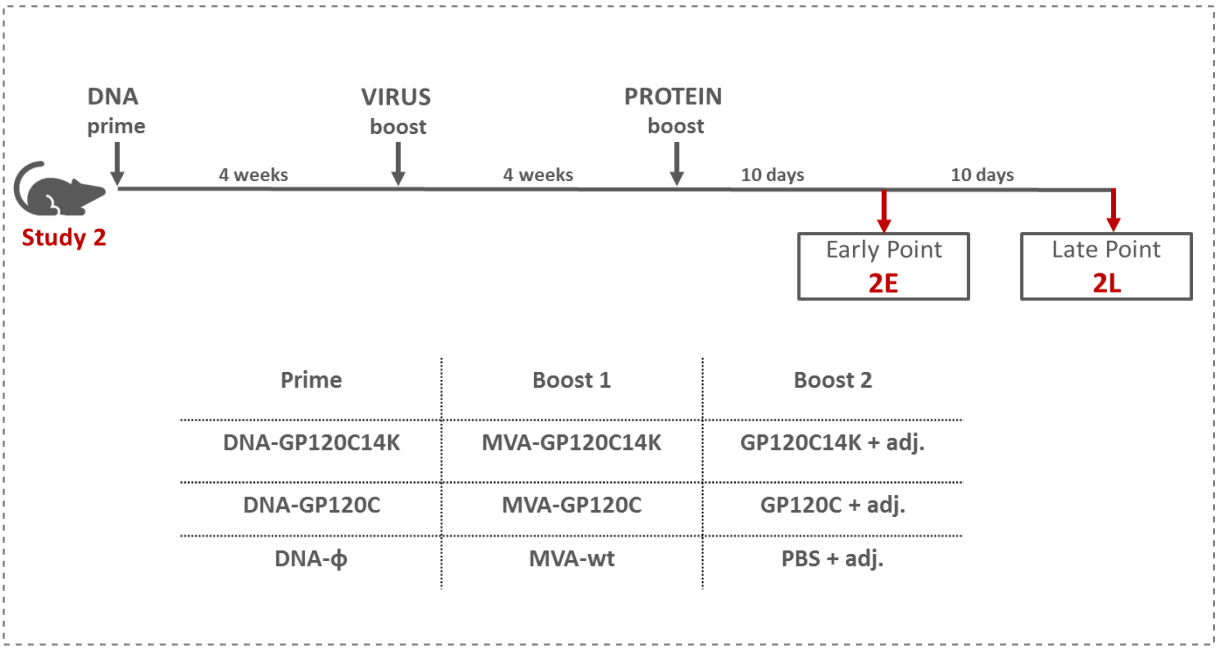

Fig. 36. Immunization and analysis scheme for the evaluation of the immunogenicity in mice of GP120C14K over GP120C using a DNA prime (D) + virus (MVA) boost (M) + protein boost (P) or a D+M+P approach. The mouse groups used for the analysis are listed with the composition of the prime and boost injections where adj. refers to the adjuvant mixture used. 2E and 2L refer to the early (10 days post-protein boost) and late points (20 days post-protein boost) respectively, where 4 mice per group were sacrificed at each time point for further analysis.

4.4.1 Analysis of the HIV-1 Env-specific CD8 T cell responses in spleen and draining lymph nodes in the D+M+P protocol

The percentages of CD8 T cells from spleen and the draining lymph nodes that secrete one or more of the specific cytokines (IFN-γ, IL-2, TNF-α) and/or display CD107a when stimulated with an Env-peptide were analysed and compared between the groups (Fig. 37).

In general, the addition of the DNA priming step lead to a marked improvement in the magnitude of Env-specific CD8 T cell responses in the spleen at 10 days post-protein boost (Fig. 37-A). This combined protocol induced in the spleen over 10-fold higher Env-specific CD8 T cells compared with a similar protocol but lacking the DNA priming component (comparing Fig. 25-A with Fig. 37-A). However, the highest Env-specific CD8 T cell response was obtained in the mice immunized with the monomeric GP120C antigen in the D+M+P protocol, significantly higher ($p<0.001$) than that

obtained with the fusion antigen GP120C14K in the same immunization scheme. In the case of the cells from the draining lymph nodes, the overall response obtained was lower compared to that of the spleen and no significant differences were observed between the groups (Fig. 37-B).

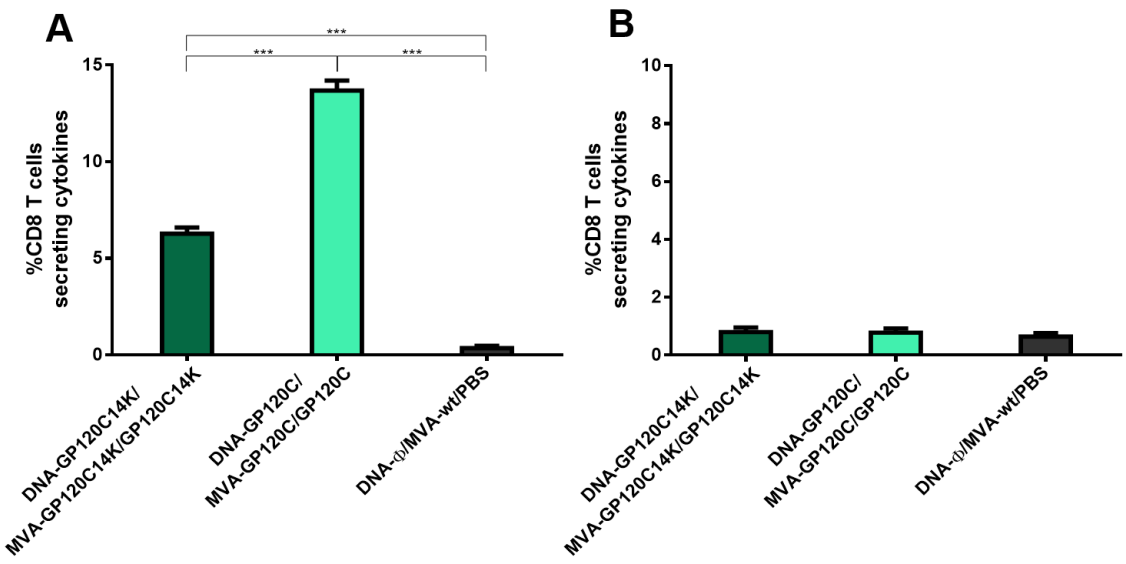

Fig. 37. Env-specific CD8 T cell responses measured 10 days after the final protein boost (early point) in the spleen (A) and the draining lymph nodes (B), represented as the total percentage of CD8 T cells secreting cytokines/CD107a. Values were obtained from analysis of pooled spleens and draining lymph nodes from 4 animals per group and are represented with their corresponding confidence intervals. *** $p<0.001$.

When the polyfunctionality of the HIV-1 Env-specific CD8 T cell response obtained in the spleen was analysed, it was observed that the group immunized with the fusion antigen GP120C14K induced a polyfunctional profile that was largely similar to that obtained with the group immunized with its monomeric counterpart GP120C (Fig. 38). HIV-1 Env-specific CD8 T cells producing CD107a+IFN-γ+IL-2+TNF-α, CD107a+IFN-γ+ TNF-α and CD107a+TNF-α were among the populations most represented by the heterologous D+M+P vaccination groups. In the case of the draining lymph nodes, the polyfunctionality of the CD8 T cell responses were largely similar

among both the groups (GP120C14K and GP120C) with most of the CD8 T cells producing IL2 (data not shown).

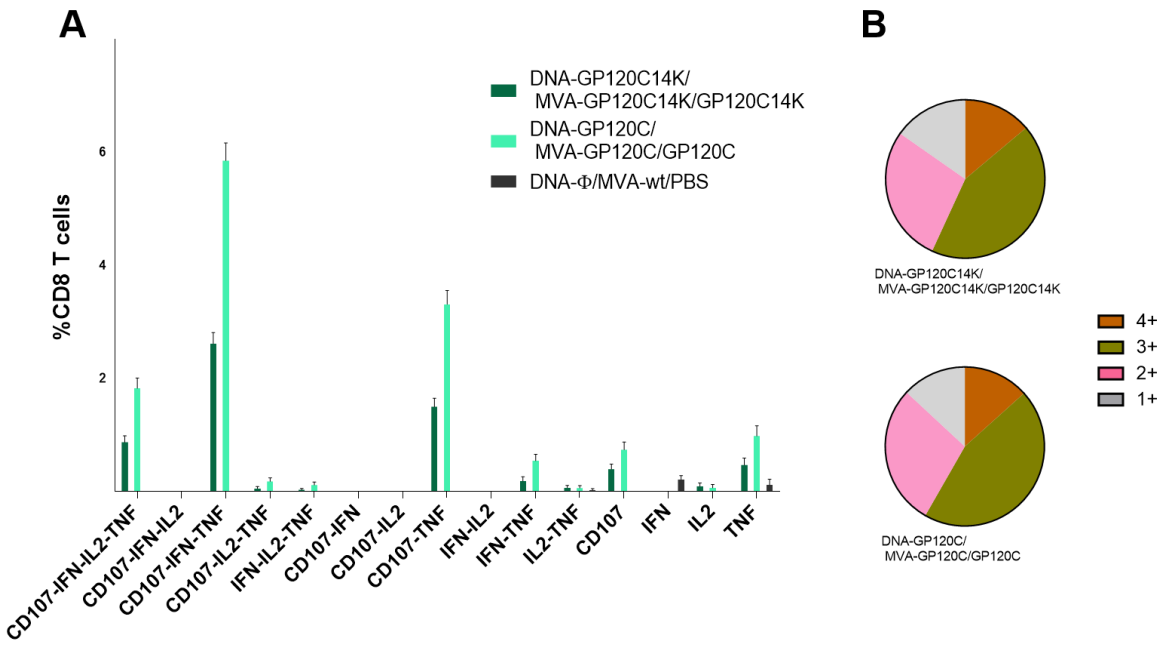

Fig. 38. (A) Polyfunctional profile of the HIV-1 Env-specific CD8 T cell response obtained at 10 days post-protein boost in the spleen by the different immunization protocols under Study 2. Data are represented with their respective confidence intervals for each of the population analyzed. (B) The relative proportions of cell populations that express four (brown), three (green), two (pink) or one (grey) cytokine(s)/ CD107a are represented in the pie charts.

At 20 days after the protein boost, the Env-specific CD8 T cell responses obtained in the spleen (Fig. 39-A), were again over 10-fold higher than when DNA priming was not used (compared with Fig. 27) and largely similar to that obtained in the early time point of 10 days. The group immunized with the monomeric antigen GP120C (D+M+P) induced the highest response ($p<0.001$) compared with the group immunized with the fusion antigen GP120C14K (D+M+P). The polyfunctionality of these responses also maintained a similar profile to that observed in the early point (data not shown).

In the case of the draining lymph nodes (Fig. 39-B), the overall Env-specific CD8 T cell responses were much lower than those observed in the spleen. However, the magnitude of the responses seen in mice immunized with the fusion antigen GP120C14K were

marginally higher ($p<0.05$) than that observed in the mice immunized with the monomeric counterpart GP120C.

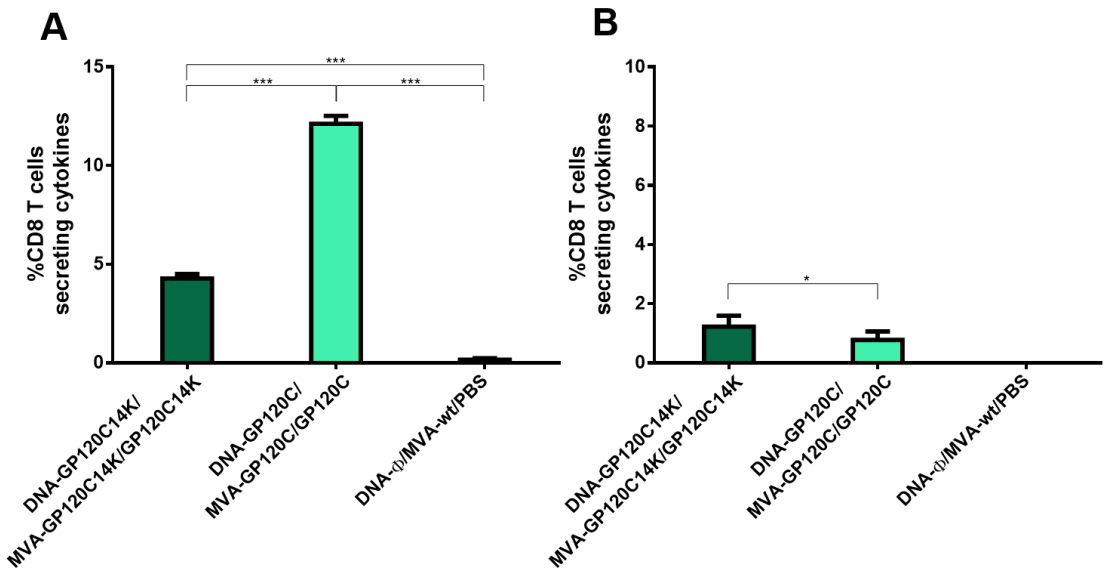

Fig. 39. Env-specific CD8 T cell responses measured 20 days after the final protein boost (late point) in the spleen (A) and the draining lymph nodes (B), represented as the percentage of Env-specific CD8 T cells secreting cytokines/CD107a. Values were obtained from the analysis of pooled spleens and draining lymph nodes from 4 animals per group and are represented with their corresponding confidence intervals. * $p<0.05$, *** $p<0.001$.

4.4.2 Analysis of the HIV-1 Env-specific GC B cells in immunized mice by flow cytometry in the D+M+P protocol.

As in Study 1, the ability of the vaccine candidates to exploit the germinal centres reactions for the development of humoral responses to HIV-1 was analysed as the percentage of Env-specific GC B cells elicited through flow cytometry.

Analysis of the percentages of total GC B cells among the B cells detected during the early point of 10 days, indicated a significantly higher proportion ($p<0.001$) of GC B cells in the draining lymph nodes of mice immunized with the fusion antigen

GP120C14K (D+M+P) than that observed in the other groups (Fig. 40-A). Among the population of the GC B cells, the percentage of cells that are specific to the HIV-1 Env was also significantly higher ($p<0.001$) among the mice immunized with the fusion antigen GP120C14K when compared with the response from mice immunized with the monomeric antigen GP120C (Fig. 40-B).

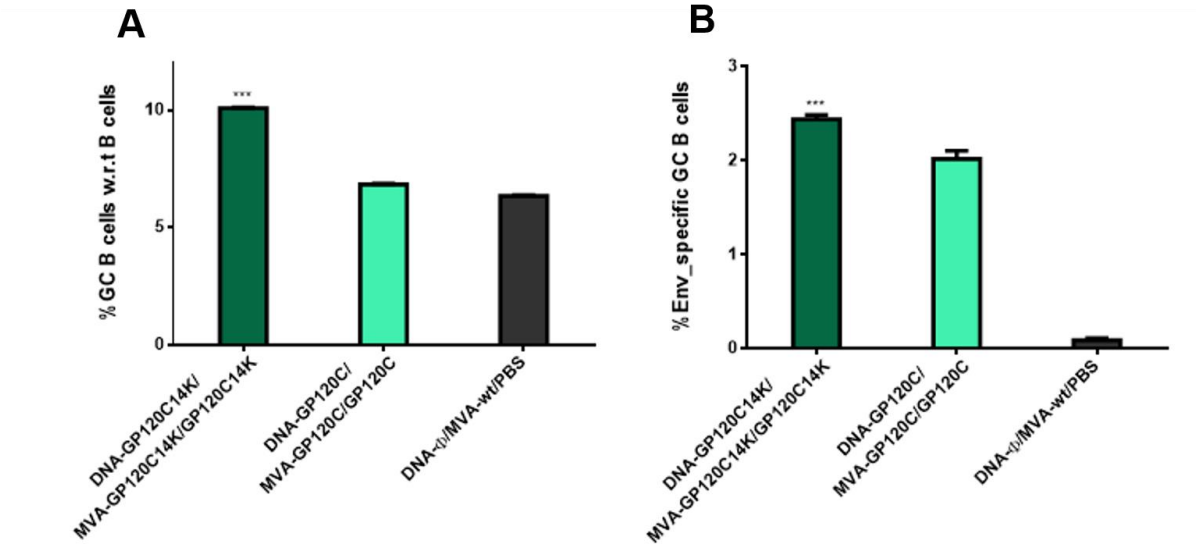

Fig. 40. Percentage of total GC B cells among the B cells detected in the draining lymph nodes of immunized mice at the early time point of 10 days post-protein boost (A) and the corresponding percentage of Env-specific GC B cells present among this population (B). Values were obtained from the analysis of pooled draining lymph nodes from 4 animals per group and are represented with their corresponding confidence intervals. *** $p<0.001$.

At the late point of 20 days, the proportion of total GC B cells among the B cells was slightly higher ($p<0.005$) in the spleen of mice immunized with the monomeric antigen GP120C than that observed in the mice immunized with the fusion antigen GP120C14K (Fig. 41-A). However, within the respective populations of GC B cells, the percentage of HIV-1 Env-specific GC B cells was significantly higher ($p<0.001$) in the mice immunized with the fusion antigen GP120C14K when compared with the response from mice immunized with the monomeric antigen GP120C (Fig. 41-B).

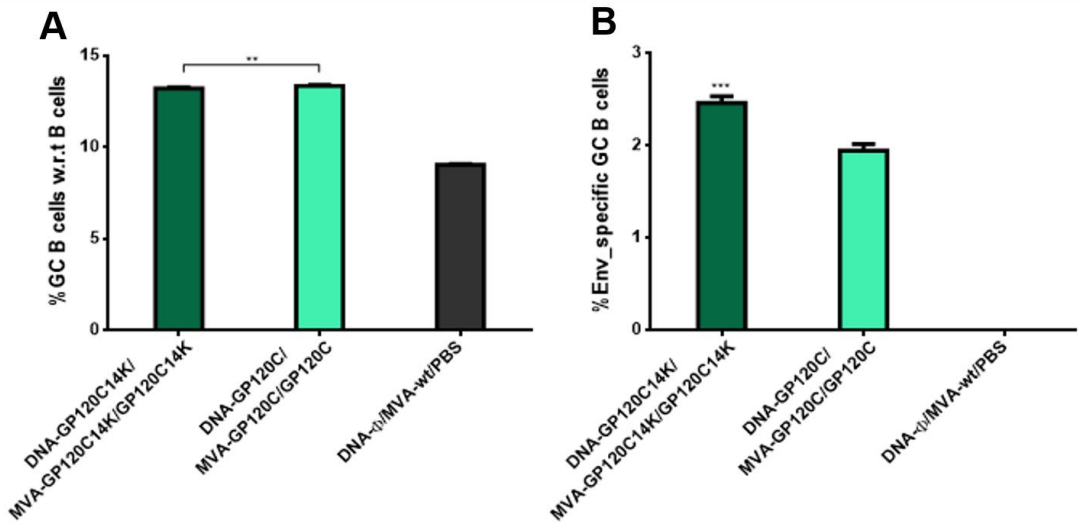

Fig. 41. Percentage of total GC B cells among the B cells detected in the spleen of immunized animals at the late time point of 20 days post-protein boost (A) and the corresponding percentage of Env-specific GC B cells present among this population (B). Values were obtained from analysis of pooled lymph nodes from 4 animals per group and are represented with their corresponding confidence intervals. ** $p<0.005$, *** $p<0.001$.

4.4.3 Analysis of the HIV-1 Env-specific Tfh cells in the spleen of immunized animals in the D+M+P protocol by flow cytometry.

As in Study 1, the proportion of Envelope-specific Tfh cells in the spleen of vaccinated mice was analysed in the early and late time points of 10 and 20 days post-protein boost respectively.

At the early time of 10 days post-protein boost, the percentage of Tfh cells within the total population of the CD4 T cells was significantly higher in the spleen from mice immunized with the monomeric GP120C antigen in a D+M+P protocol when compared with the response obtained from the other groups (Fig. 42-A). However, when the proportion of HIV-1 Env-specific Tfh cells were analysed within this general population of Tfh cells, the GP120C14K group showed significantly higher ($p<0.001$) percentage of Env-positive Tfh cells when compared with the GP120C and the control groups (Fig. 42-B).

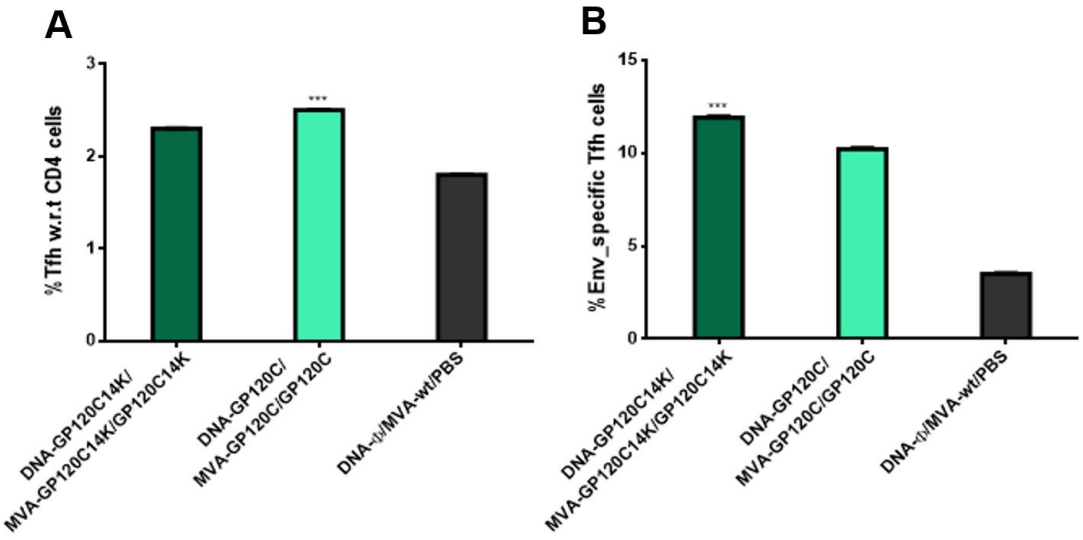

Fig. 42. Percentage of total T follicular helper cells with respect to the CD4 T cells analysed in the splenocytes from immunized animals at the early time point of 10 days post-protein boost (A) and the corresponding percentage of Env-specific Tfh cells present among this population (B). Values were obtained from the analysis of pooled spleens from 4 animals per group and are represented with their corresponding confidence intervals. *** $p<0.001$.

Similar to the pattern observed in the early point, the percentage of Tfh cells among the total CD4 T cell population was significantly higher ($p<0.001$) in the group immunized with the monomeric GP120C antigen compared to the group administered with the fusion GP120C14K antigen (Fig. 43-A). However, the percentage of HIV-1 Env-specific Tfh cells among the general Tfh population was significantly higher ($p<0.001$) in the spleen of mice immunized with the GP120C14K antigen when compared with the rest of the groups (Fig. 43-B).

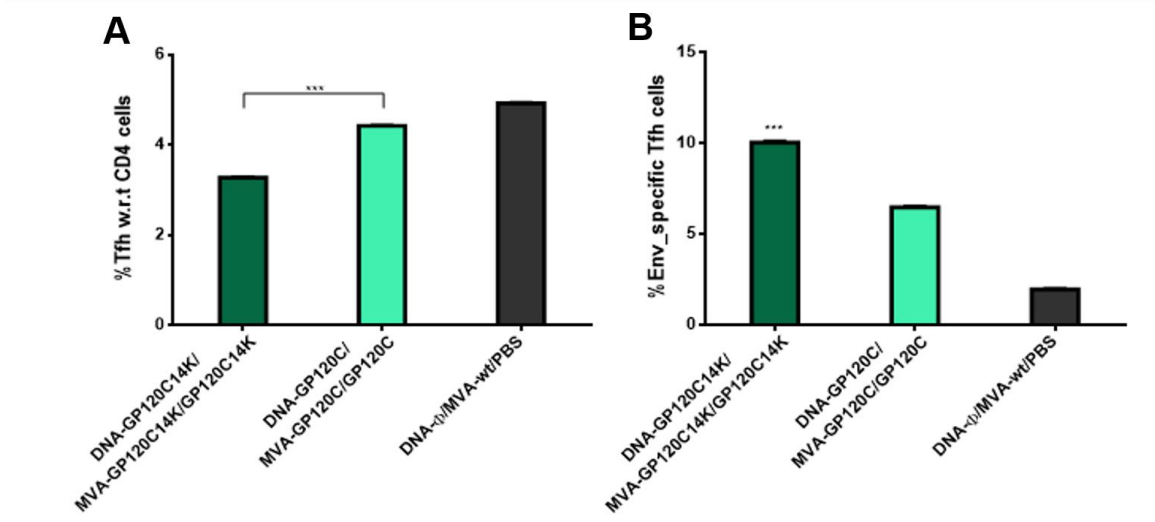

Fig. 43. Percentage of total T follicular helper cells with respect to the CD4 T cells analysed in the splenocytes from immunized animals at the late time point of 20 days (A) and the corresponding percentage of Env-specific Tfh cells present among this population (B). Values were obtained from the analysis of pooled spleens from 4 animals per group and are represented with their corresponding confidence intervals. *** $p<0.001$.

4.4.4 Analysis of anti-GP120C envelope protein antibodies analysed in the serum of immunized mice with the D+M+P protocol.

As can be observed in the Fig. 44-A, high titers (1,024,000) of HIV-1 GP120C specific antibodies (total IgG) were present in the serum of animals immunized with both the fusion antigen GP120C14K and the monomeric GP120C. The progression of optical density was also similar between these two groups (Fig. 44-B).

.

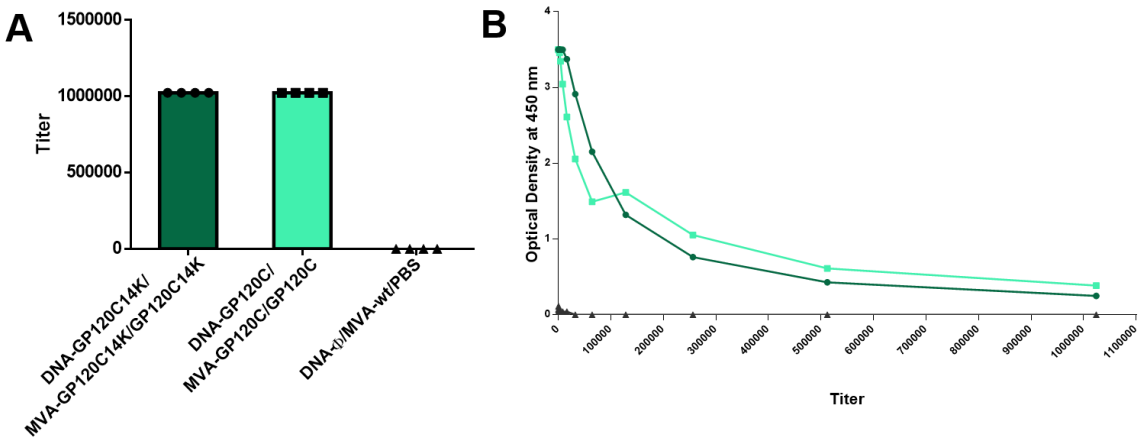

Fig. 44. Anti-GP120C antibody levels (total IgG) in the serum of immunized mice at the early point of 10 days post-protein boost measured by ELISA. (A) End-point titers of antibody responses obtained for each group (n = 4) calculated as the last dilution that provides an optical density value (at 450 nm) that is more than three times the value obtained at the same dilution by the naïve serum. (B) Optical density (at 450 nm) progression of serum dilutions from the different groups

In the late point of 20 days post-protein boost, the anti-Env titers among both groups were lower than those observed at the early point of 10 days post-protein boost. Among them, the average titer of anti-GP120C antibodies obtained from animals immunized with the fusion antigen GP120C14K was slightly higher (768,000) compared with that obtained with the monomeric antigen GP120C (704,000) (Fig. 45-A). The progression of optical density was also similar between these two groups (Fig. 45-B).

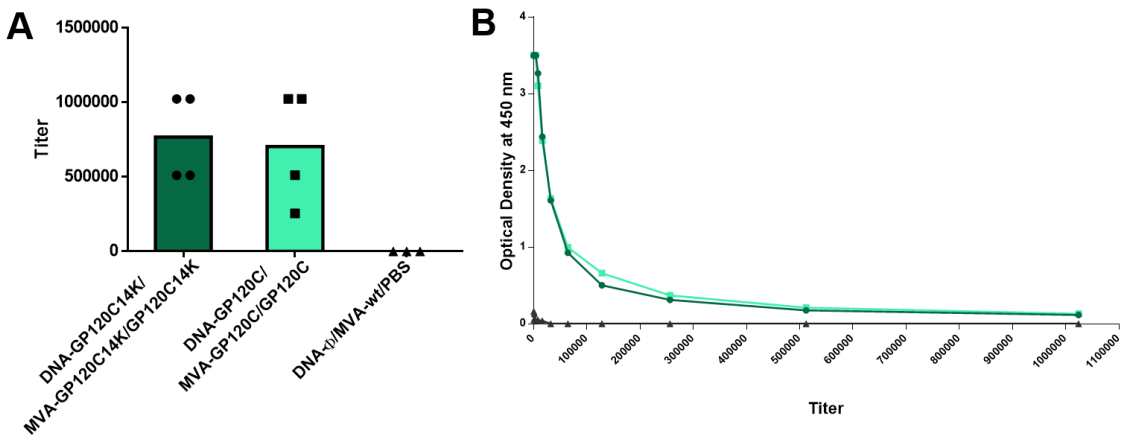

Fig. 45. Anti-GP120C antibody levels (total IgG) in the serum of immunized mice at the late point of 20 days post-protein boost measured by ELISA. (A) End-point titers of antibody responses obtained for each group (n = 4) calculated as the last dilution that provides an optical density value (at 450 nm) that is more than three times the value obtained at the same dilution by the naïve serum. (B) Optical density (at 450 nm) progression of serum dilutions from the different groups

5. DISCUSSION

14K as an oligomeric protein fusion agent for HIV-1 GP120

The development of an effective vaccine against HIV-1 has been hampered by several inherent features of the virus that make it a difficult and tricky target. The scientific search is on for an ideal antigen that can raise the possibilities of invoking the right immunogenic responses against the virus when administered through vaccination, both in quantity and quality.

Thus far, the efforts towards designing and developing such an antigen have largely been driven by the previous vaccination efforts, including the RV144 trial that, for the first time, provided a modest protection of 31.2% against the virus (Rerks-Ngarm et al., 2009).

It is abundantly clear that the conformational integrity of the GP120 protein plays a crucial role in influencing the nature of anti-HIV-1 responses (Kovacs et al., 2012). Therefore, there is a need for the use of modified *Env* antigens capable of displaying several desired immunological characteristics as vaccine candidates.

In this work, we proposed the use of the VACV 14K protein as an oligomer-driven fusion agent for modifying the GP120 from clade C HIV-1 envelope to form the novel antigen GP120C14K, with superior antigenic characteristics better suited for vaccination against HIV-1.

The idea behind the use of the 14K oligomer fusion agent is to make use of the adjuvant like effect that it confers to the vaccination regimen involving poxvirus based vectors. This has been demonstrated in the case of malaria, where the fusion with the 14K molecule to the CS malarial antigen, generated an oligomeric CS14K antigen that markedly improved the poxvirus based vaccination protocol, including the inhibition of the liver-stage development of the malarial parasite leading to sterile protection in mice models (Vijayan et al., 2012).

In the case of HIV-1, previous efforts in the lab have led to the fusion of the 14K molecule to the GP120 segment from the clade B (isolate BX08) to create the oligomeric protein GP120-14K which displayed superior antigenic characteristics and suitability for vaccination. In immunization studies in mice, a prime using the DNA vector expressing the fusion antigen and a boost using the HIV-1 vaccine candidate

MVA-B (Gómez et al., 2007a) showed significant improvements in the HIV-1 specific CD4 and CD8 T cell responses over the use of a DNA priming agent expressing the monomeric GP120 antigen from the same clade (Vijayan et al., 2015).

Encouraged by these improvements that the fusion with the 14K brought out over the HIV-1 antigen GP120, we decided to extend those findings and explore how the fusion antigen GP120C14K:

a. Would form oligomers and serve to improve the immunogenicity of the GP120C molecule by oligomerization of the monomeric protein, providing an adjuvant-like effect when used as a recombinant protein-based vaccine.

b. Is capable of increasing the HIV-1-specific immune responses, both cellular and humoral, when expressed through an MVA-based vector.

c. Would contribute to the further improvement of the immune response against HIV-1 when delivered through a DNA-based vector as a priming step in the immunization process, followed up by the MVA vector and the fusion protein component.

Hence, in this Thesis we have defined by genetic, biochemical, biophysical and immunological properties the generation of vectors, protein production, conformation and nature of the immune cell populations triggered in mice by various vaccination protocols that might be relevant for protection against HIV-1, like Env-specific T cell responses (CD8+) and for induction of neutralizing antibodies (Tfh and GC B cells).

GP120C14K biophysical and antigenic characteristics

As determined in this work, the fusion of the VACV 14K protein to the GP120C antigen results in the oligomerization of the molecule as evident from the distinct size exclusion profile and the separation pattern of the protein under native conditions.

The GP120C14K protein seems to exist predominantly as a hexameric structure, with two trimers positioned together as suggested by the electron microscopy data. This observation is further supported by the conclusions obtained from the SEC-MALLS analysis, where the apparent molecular weight of the protein was calculated to be around 700 kDa. Further analysis of the biophysical data also indicate the relative absence of aggregation events by the protein, suggesting that the oligomeric form is

stable and soluble and by extension, that the GP120C14K protein exists in a homogenous form when provided as a vaccine.

Further experimental examination of the GP120C14K protein is required to shed more light on the finer details of the protein structure and the oligomeric state.

Cryo-EM studies, in this regard, can provide a greater magnification into the oligomeric forms of the molecule and help us deduce details with respect to the relative conformation of the HIV-1 Envelope. This work is part of an ongoing collaboration with Prof. Carrascosa´s group at the CNB-CSIC.

Crystallisation of the GP120C14K protein and subsequent structural elucidation using techniques such as X-ray crystallography can provide valuable information regarding the conformation and epitopes exposed on the surface of the protein. Extended analysis and interpretation of such information can help us design and introduce mutations that can improve the antigenicity of the GP120C14K molecule with regards to its reactivity to bNAbs. In fact, along this thesis, an active collaboration has been established with the Protein Facility at the Netherland´s Cancer Institute (NKI, Amsterdam) through an iNEXT Structural Audit grant with the aim of crystallizing the GP120C14K fusion protein and possibly resolving its structure by X-ray analysis. This work is ongoing and some crystals have been observed in the purified GP120C14K preparation and are yet to be resolved.

Oligomerization of the GP120C can prove a favourable immunological quality considering the possibility of more epitopes being presented to the immune system per molecule when used as a vaccine. However, there are two outstanding concerns with the final antigenic structure of the GP120C14K fusion protein.

The first consideration is the exposure of immunologically relevant epitopes, especially those that are known targets of broadly neutralizing antibodies against HIV-1, given the oligomerization of the envelope protein.

The second consideration is the role of the furin cleavage in the proteolytic processing of the final envelope structure and its subsequent implications in the antigenic structure of the molecule. Despite the claims by certain groups that the furin cleavage event does not affect the immunogenicity of certain envelope structures touted to be HIV-1 vaccination capable (Kovacs et al., 2014, Liu et al., 2017, Sharma et al., 2015),and

given the plethora of evidence to the contrary (Castillo-Menendez et al., 2018, Chakrabarti et al., 2011, Ringe et al., 2013), we decided to construct two different mutants of our fusion protein - a furin cleavage permissive GP120Crrrrr14K and a furin cleavage non-permissive GP120Creks14K proteins in order to evaluate them along with the non-mutated GP120C14K and the monomeric protein GP120C for their reactivity with some standard neutralizing antibodies.

The binding studies with standard bNAbs have shown that the GP120C14K protein (containing the partial furin cleavage sequence "REKR" present in the natural GP160 molecule of the HIV-1), shows a better binding profile to the antibodies tested than the furin-permissive and non-permissive mutants.

The favourable reactivity of the GP120C14K protein to the quaternary antibody PGT151 and broadly neutralizing antibodies PGT 121, 257-D IV and 10-1074 highlights the presence and/or greater exposure of the corresponding epitopes. While suggesting the antigenic superiority of this protein when compared with the monomer and other furin cleavage mutants, these results also hint at the possible conformational changes of the GP120 protein induced by the 14K fusion and the effect that the furin cleavage has on the same. It will be of interest to explore the structural similarities between the 14K protein and the naturally occurring GP41 protein of the HIV, which could explain the behaviour of the fused GP120C14K protein with respect to furin digestion.

To check if limited reactivity to other standard bNAbs might be explained by the conformational changes and epitope masking effects of the standard ELISA technique, further exploration of the binding characteristics of the GP120C14K protein with these standard bNAbs through Surface Plasmon Resonance or SPR technique will be needed. The SPR results can help us obtain a greater understanding of the spatial arrangement of relevant epitopes on the surface of the GP120C14K protein.

Immunizations – study design

Having generated and *in vitro* characterized at the antigenic construct of interest - GP120C14K, we wanted to examine the potential immunological improvements that this construct can confer over the monomeric GP120C in mice when delivered directly as an adjuvanted protein and through a recombinant MVA based vector.

The GP120C14K recombinant protein was produced from the supernatant of stably transfected CHOK1 cell line and purified using standard lectin affinity and size exclusion chromatography techniques, highlighting the ease of large-scale manufacturing. With a view to complementing the adjuvant like effect conferred by the 14K fusion component of the recombinant protein GP120C14K (Vijayan et al., 2012), the final composition of the protein immunogen also consisted of the following mixture of adjuvants: 1) Aluminium hydroxide (commonly referred to as alum), one of the oldest adjuvants currently in use and with a great safety record in humans, is a known promotor of antibody responses (Kool et al., 2012), 2) a stable oil-in-water emulsion base containing immuno-stimulatory components such as MPL (monophosphoryl lipid A) and TDM (trehalose dicorynomycolate) (Gavin et al., 2006) and 3) Class B CpG oligonucleotides that are recognised by Toll-like receptor 9 leading to strong stimulation of the immune system (Ballas et al., 2001). This combined adjuvant composition was similar to the one used in humanized mice models, where high-affinity antibodies were generated against selected antigens (Lee et al., 2014)

Included among the various strategies towards improving the anti-HIV immunogenicity of MVA based vectors (García-Arriaza and Esteban, 2014), there is the option to optimize the antigenic form expressed by the vector. We decided to follow this strategy and generated the recombinant vector MVA-GP120C14K, which is able to express correctly the fusion antigen GP120C14K so as to include the same within the immunization protocols to evaluate the contribution of the same to the immune responses against the HIV-1 envelope. We show that the insertion of the GP120C14K fusion antigen into the MVA genome did not alter the replication capacity of the virus, an important consideration for the large-scale manufacture of the viral stocks. The stability of the transgene cassette inserted into the viral genome was also confirmed after 9 consecutive passages in DF1 cells, another critical factor for the vector´s success as an agent for vaccination.

The immunogenicity (B and T cell responses) elicited by the adjuvanted GP120C14K recombinant protein and the MVA-GP120C14K vector in homologous (protein prime + protein boost) and heterologous (MVA prime + protein boost) protocols was established in mice when compared with the response obtained using the monomeric antigen GP120C.

Antibody responses in vivo:

One of the principal forms of protection against HIV-1 derives from the ability of vaccines to induce the adequate humoral immunity i.e., their ability to drive the development of potent anti-HIV antibody responses.

In our mice Study 1, the groups of mice immunized with the fusion antigen GP120C14K (as adjuvanted protein and MVA-GP120C14K) were able to induce high titers of binding antibodies, in the order of 10^6, against the GP120 protein of the HIV-1 clade C.

Recently, such high titers of anti-HIV-1 binding antibodies have been reported in rabbits immunized with native-like envelope trimer molecules (BG505 SOSIP) as MVA-expressed antigens and as adjuvanted recombinant proteins in various prime-boost combinations (Capucci et al., 2017).

The contribution of the fusion protein towards the development of a high titer of antibodies against the GP120 region can be appreciated from the fact that the adjuvanted protein on its own (prime and boost) is able to induce high titers (in the order of 10^6) of anti-GP120 binding antibodies, a magnitude that is 100000 fold higher when compared to the titers obtained with the use of the adjuvanted GP120C protein alone, and that is equivalent to those obtained when the MVA-GP120C14K was administered as the prime component.

Furthermore, it is noteworthy that in our modified ELISPOT assays, only the groups immunized with the GP120C14K antigen were able to demonstrate the presence of GP120C-specific IgG secreting B cells (GP120C14K P+P group in the spleen) and the GP120C-specific IgG1 secreting B cells (GP12014K M+P group in the draining lymph nodes), highlighting the contribution of the fusion antigen to the anti-HIV-1 Envelope antibody production capacities.

One of the most important determinations of the immunogenic capacity of an antigen lies in the quality of the antibody response generated, evaluated in terms of their ability to neutralize the viral strain. For example, Sanders et al., have previously reported the generation of autologous tier 2 neutralizing antibody responses in rabbits immunized with native-like SOSIP envelope trimers (Sanders et al., 2015).

However, immunized mice do not yield sufficient sera for conducting standard neutralization assays and elicit high background of non-specific neutralization and therefore, immunization assays using the fusion antigen need to be conducted in animal models that can permit a follow-up neutralisation analysis. The use of rabbits as models for such immunization assays can be considered as a logical next step, given the plethora of HIV immunogens being evaluated in this model for their ability to induce responses capable of virus neutralisation. We are currently conducting a rabbit study with a combination of MVA and protein vectors in order to set up neutralization values for different vaccination protocols.

CD8 T cell response improvements

While potent antibody responses generated by vaccination against HIV-1 are necessary for the neutralisation of the virus, T cell responses are equally important for their ability to drive long term qualitative antibody responses (through Tfh) and cellular responses able to destroy virally infected cells (through CD8 T cells).

There is a variety of evidence to indicate that virus-specific CTL ($CD8^+$ T cells) help control HIV-1 replication (for example: the coincidence between the decline in viremia and the appearance of specific $CD8^+$ T cells (Borrow et al., 1994), (Koup et al., 1994), the *ex vivo* elimination of HIV-1 infected $CD4^+$ T cells by $CD8^+$ T cells isolated from HIV controllers (Sáez-Cirión et al., 2007), or the $CD8^+$ T cell mediated viremia control in simian immunodeficiency virus infected rhesus macaques (Schmitz et al., 1999, Jin et al., 1999), etc).

In our mice Study 1, the group vaccinated with the fusion antigen GP120C14K delivered through MVA prime and boosted with adjuvanted protein exhibited the highest HIV Env-specific CD8 T cell responses in both organs analysed (splenocytes and lymph nodes), highlighting the capability of this prime-boost protocol to mount a strong T cell response against the HIV-1 envelope protein.

In addition to the magnitude, higher functionality has been reported to be a key characteristic of CD8 T cells among HIV-1 controllers (Betts et al., 2006), highlighting the importance of eliciting polyfunctional T cell responses by vaccine candidates. Here again, the group vaccinated with the MVA-GP120C14K delivered as a prime and boosted with adjuvanted protein elicited HIV-1 Env-specific CD8 T cell responses that

are more polyfunctional and therefore qualitatively superior when compared to the response obtained with the monomeric GP120C antigen group.

Our results suggest the capability of 14K fusion towards improving the HIV-1 Env-specific CD8 T cell responses quantitatively and qualitatively when compared to using the monomeric antigen GP120C.

Tfh and GC B cell responses in vivo:

It is well known that Tfh cells are indispensable to the survival, differentiation and proliferation of antigen specific B cells (Havenar-Daughton et al., 2017). While it is clear that the Tfh cells play a crucial role in the development of neutralizing antibodies, germinal centres and memory B cells (Crotty 2011), the importance of Tfh in the resistance to HIV infection is also under considerable scrutiny. Analysis of HIV infected patients who go on to develop bNAb responses against HIV-1 revealed higher percentages of circulating memory Tfh cells ($PD\text{-}1^{+}$ $CXCR3^{-}$ $CXCR5^{+}$) hinting a potential role of Tfh cells in the development of potent neutralizing responses against the virus (Locci et al., 2013).

Furthermore, recent evidence from HIV-1 controllers have shown a positive association between the presence of the resident anti-HIV-1 memory B cells (that possibly contribute to the long-term viremia control) and the HIV-1 Env-specific circulating Tfh cells, highlighting the critical role played by Tfh help in HIV-1 control and the need for inducing such responses through vaccination (Claireaux et al., 2018).

These evidences suggest the importance of stimulating HIV-1 Env-specific Tfh responses through vaccination in order to provoke adequate humoral responses against the virus. For instance, HIV-1 Env-specific Tfh cells has been also implied in protective efficacy observed in the RV144 trial: in one study, Schultz and colleagues have highlighted the potential role of vaccination induced Tfh cells in eliciting protective efficacies against HIV-1 by demonstrating that HIV-1 Env-specific Tfh cells in the peripheral blood provide help to cognate B and $CD8^{+}$ T cells. They further show that these Tfh cells were detected in higher frequencies among the ALVAC+AIDSVAX vaccinees of the RV144 trial when compared to those that were in the other vaccination regimens (Schultz et al., 2016).

In our analysis, mice immunized with the fusion antigen GP120C14K through MVA prime and protein boost showed the highest percentage of Env-specific Tfh cells in the early time point, and these levels were maintained until day 20 (only to be surpassed by the group immunized with the monomeric antigen with the same protocol at this time point). This pattern of obtaining a high percentage of Env-specific Tfh cells using the fusion antigen hints at the possible role that these cells might be playing in promoting favourable GC reactions towards qualitative humoral responses against HIV-1.

These results obtained might indicate the capacity of the fusion antigen, given its specific physio-chemical qualities, to stimulate a response profile that includes, among other unknown cell populations and mechanisms, the Tfh responses. As the GC B cells are known receivers of Tfh help, our model could hint at a possible collaboration between these two response groups that acts favourably towards raising humoral responses against the HIV-1 envelope.

In the case of HIV, for example, it has been reported that the quantity and quality of Env-specific Tfh cells in rhesus monkeys with $SHIV_{AD8}$ infection were influential in the development of Env-specific IgG-positive GC B cells, which translated to higher cross neutralizing humoral responses (Yamamoto et al., 2015).

Analysis of the GC B cell responses in the draining lymph nodes in our mice Study 1 revealed a high percentage of Env-specific GC B cell responses in the group immunized with the fusion antigen in the heterologous MVA prime + protein boost protocol (surpassed only by the homologous fusion protein only group in the early time point). Taken together with the results of the percentage of the Env-specific Tfh cells, this group shows the best indication of a favourable and HIV-1 Env-specific GC reaction.

Addition of a DNA priming step:

We sought to improve the cellular responses obtained against the HIV-1 envelope, given the good humoral responses observed with the use of the MVA prime and protein boost protocol employing the fusion antigen GP120C14K. Therefore, we decided to include a DNA priming step to the immunization assays with a view to improving the HIV-1 envelope specific CD8 T cell responses.

It has been known that the endogenous expression of peptides achieved though DNA driven expression of antigens lead to the establishment of major histocompatibility complex restricted CD8 T cell responses and that these DNA based immunizations act best as prime in prime-boost vaccination regimens (Koup and Douek, 2011). In the context of VACV based vaccinations against HIV-1 (both MVA and NYVAC vectors), the inclusion of a DNA priming component has led to an improvement in anti-HIV-1 cellular responses (Gómez et al., 2007a).

Furthermore, the central role played by SHIV-1 Env-specific CD8 T cells in the control of viremia through DNA/MVA vaccinations in macaques has also been reported (Amara et al., 2005). The role of a DNA priming step in increasing the HIV-1 Env-specific T cell responses has also been reported in human clinical trials where the combination of DNA priming step prior to a NYVAC boost resulted in the detection of high degree of T cell responses (in about 90% of participants) which was superior to the use of NYVAC vector alone (detection of T cell responses in 33% of participants) (Harari et al., 2008).

Previous work at the Esteban´s laboratory has shown that in the case of the Clade B fusion antigen GP120-14K, the inclusion of a DNA priming step for delivering the antigen prior to an MVA-based boost in immunization studies in mice augmented the HIV-1 Env-specific CD8 T cell response obtained (Vijayan et al., 2015). Encouraged by these results, we decided to include a DNA priming step followed by two booster doses (MVA and adjuvanted protein) to compare the immunogenicity of the GP120C14K antigen with that of the monomeric GP120C.

Overall, there was a definite improvement in the magnitude of the HIV-1 Env-specific CD8 T cell responses observed, highlighting the contribution of the addition of a DNA priming step to the immunization scheme. For example, in the case of the fusion antigen GP120C14K, the HIV-1 Env-specific CD8 T cell responses in the spleen of immunized mice showed almost a 10-fold increase with the inclusion of a DNA priming step to the M+P protocol. Although significantly lower than the response obtained with the monomeric antigen, the improvement in the cellular response against HIV-1 by the inclusion of the DNA priming step with the fusion antigen can definitely be considered as a positive step towards fine-tuning the immunization protocol.

With regards to the humoral response, the anti-HIV-1 Env antibody responses showed similar high end-point titers (10^6) in both the groups immunized with the fusion antigen GP120C14K and the monomeric GP120C, underlining the role of DNA priming event in improving the quantity of antibodies generated against the antigen. These antibody titers were similar to those observed with the immunizations using the fusion antigen without the DNA components (both P+P and M+P protocols).

However, we were further interested in analysing the quality of these humoral responses against HIV-1 as it has been reported that in mice immunized with DNA prime expressing the HIV envelope protein GP120 followed by the protein boost, there is increased Tfh differentiation and GC B cells (Hollister et al., 2014).

In the spleen of immunized animals, the HIV-1 Env-specific Tfh cells were consistently higher across the two time points analysed in the groups immunized with the fusion antigen compared with those obtained from the mice immunized with the monomeric antigen. In a similar fashion, the HIV-1 Env-specific GC B cells were also consistently higher in the draining lymph nodes of the groups immunized with the fusion antigen than those immunized with the monomeric GP120C. Taken together, these results highlight the significance of the DNA priming step in the improvement of the quality of the anti-HIV-Env humoral responses obtained using the vaccination regimen in mice.

Overall, the addition of an extra DNA priming step certainly increases the magnitude of the cellular responses directed towards HIV-1 envelope at least in the spleen of immunized animals, while augmenting the quality of humoral responses measured by the HIV-1 Env-specific Tfh and GC B cells obtained with the fusion antigen GP120C14K when compared with the monomeric antigen GP120C.

The pattern of immune responses observed with or without the use of DNA throws light on the distinct potential of the different platforms of expression or antigen presentation used in this study. In this regard, the key to future optimizations while using the fusion antigen could lie within the intelligent use of DNA, MVA and the adjuvanted fusion protein to arrive at an immunization protocol that can provide a profile of cellular / humoral responses in accordance with the requirements to protect against the HIV infection. This protocol should, in principle, be superior to the low immune response observed in a phase I clinical trial with the combination of DNA-C/MVA-C/protein (Joseph et al., 2017).

Summary

Based on the findings provided in this thesis, we propose the use of 14K fusion as a tool to oligomerize and improve the immunogenicity of the GP120C protein. We showed that the GP120C14K fusion protein is a soluble and stable oligomer which appears to be hexameric when analysed under native conditions. Also, the GP120C14K protein displayed favourable antigenic qualities when tested with some of the broadly neutralizing antibodies. A recombinant poxvirus vector expressing the fusion protein (with the partial furin cleavage site "REKR") MVA-GP120C14K was generated showing stable insertion of the encoding sequence into the MVA backbone and correct antigen expression across multiple passages.

The potential of the 14K fusion in improving both the vaccine induced cellular and humoral immunity against HIV-1 Evelope region was shown in prime-boost protocols *in vivo*. Evaluation of the immunogenicity of the fusion antigen in mice, revealed a higher and more polyfunctional HIV-1 Env-specific cellular response in the groups containing the fusion protein GP120C14K when compared with the monomeric counterpart GP120C. The GP120C14K protein alone or in combination with MVA-GP120C14K was able to elicit high tires of anti-HIV-1 Env antibodies revealing the improved humoral immunity raised by this antigen against HIV-1. Qualitative improvements to these humoral responses in terms of higher HIV-1 Env-specific Tfh cells and GC B cell reactions were also observed with the use of the fusion antigen.

Further studies *in vivo* revealed that the addition of a DNA priming step improves both the magnitude of the cellular responses (CD8 T cells) and the quality of the humoral responses (Tfh and GC B cells) specific against HIV-1 Env antigen and therefore can be explored as potential strategy to augment the immune responses elicited against the HIV-1 Envelope.

To facilitate interpretation of the findings, a relative comparison of the different HIV-1 Env-specific responses obtained with the fusion antigen GP120C14K and the monomeric GP120C under different protocols of immunization is provided in Table 5. The influence of the GP120C14K over the profile of immune cells is illustrated in Fig. 46. After vaccination with the GP120C14K in combined DNA/MVA/protein protocol, these immunogens activate Env-specific CD8+ T cells and promote induction of

antibodies through Tfh and GC B cells, leading to the production of immune modulators, all likely contributing to the control of HIV infection.

Immunization schedule	HIV-1 Env-specific response	GP120C14K versus GP120C
MVA prime + protein boost	CD8 T cells	1.48 fold increase
	Antibodies	3.2 fold increase
	Tfh cells	1.5 fold increase
	GC B cells	1.13 fold increase
DNA prime + MVA boost + protein boost	CD8 T cells	2.18 fold decrease
	Antibodies	Equal responses
	Tfh cells	1.16 fold increase
	GC B cells	1.2 fold increase

Table 5. Comparison of the immune responses elicited by the fusion antigen GP120C14K versus the monomeric GP120C under different immunization schemes. The fold-change values were calculated by dividing the specific response values of each of the groups from the early time point (10 days after final boost) analysis of spleen (CD8 T cells and Tfh cells), lymph nodes (GC B cells) and serum (Antibodies) from each experiment.

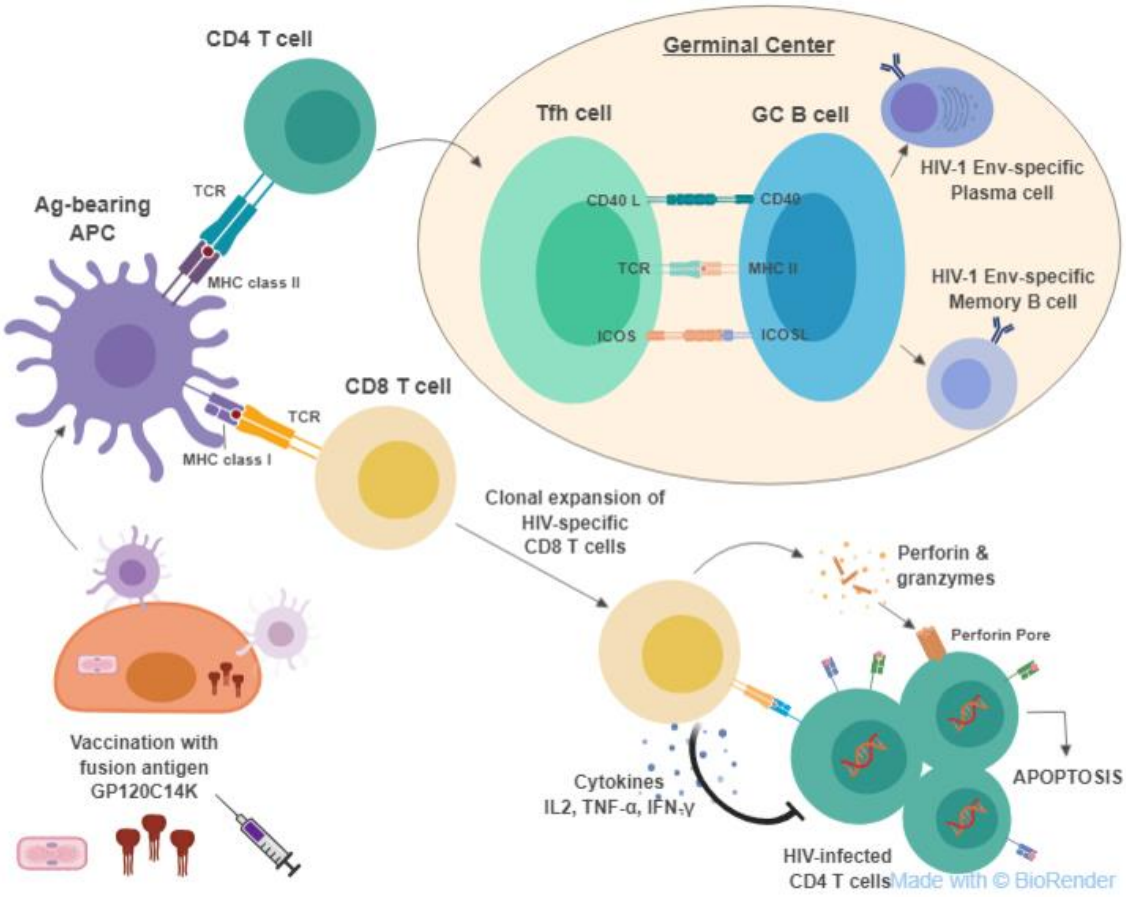

Fig. 46. Proposed mode of T and B cell-based immune action elicited by the vaccination regimen using the fusion antigen GP120C14K. In this work we showed that HIV-1 Env-specific responses such as CD8 T cells, as well as Tfh and GC B cells are induced by vaccination protocols with the fusion antigen delivered either through MVA/protein or DNA/MVA/protein protocols.

6. CONCLUSIONS

The following are the main conclusions of this work:

1. The fusion of 14K protein of vaccinia virus to the C-terminal end of HIV-1 Envelope GP120C protein produces an oligomeric fusion protein - GP120C14K.

2. The GP120C14K fusion protein was found to be a soluble and stable oligomer which appears to be hexameric when analysed under native conditions.

3. A recombinant poxvirus vector MVA-GP120C14K was generated with the correct insertion of the antigen GP120C14K into the MVA backbone and with stable antigen expression across multiple passages.

4. Studies in mice showed that the group immunized with the heterologous MVA-GP120C14K (prime) / GP120C14K (boost) protocol showed higher and more polyfunctional HIV-1 Env-specific cellular response when compared with the corresponding monomeric GP120C group

5. The GP120C14K protein alone or in heterologous combination with MVA-GP120C14K was able to elicit high tires of anti-GP120 antibodies in mice revealing the improved humoral immunity raised by this fusion antigen against HIV-1 envelope protein.

6. The quality of the humoral response against HIV-1 envelope was improved in mice primed with MVA-GP120C14K and boosted with GP120C14K protein, as measured by the greater proportion of Env-specific GC B and Tfh cells when compared to mice immunized with the monomeric antigen.

7. The addition of a DNA priming step to the heterologous MVA-GP120C14K + GP120C14K immunization augmented the magnitude of the HIV-1 Env-specific CD8 T cells.

8. The DNA priming step improved the quality of the humoral responses measured in terms of HIV-1 Env-specific Tfh and GC B cells elicited by the fusion antigen.

CONCLUSIONES

Las principales conclusiones de este trabajo son las siguientes:

1. La fusión de la proteína 14K del virus vaccinia con el extremo C-terminal de la proteína de la Envuelta GP120C del virus VIH-1 da lugar a una proteína de fusión oligomérica – GP120C14K.

2. La proteína de fusion GP120C14K forma un oligómero soluble y estable capaz de constituir un complejo hexamérico cuando se analiza bajo condiciones nativas.

3. Se ha generado el poxvirus recombinante MVA-GP120C14K mediante la correcta inserción del gen que codifica para el antígeno GP120C14K en el locus TK del genoma del virus MVA. Dicho antígeno insertado en el genoma viral se expresa de manera estable a lo largo de múltiples pases.

4. Estudios en ratón han demostrado que el grupo inmunizado con la combinación heteróloga MVA-GP120C14K en el "prime" y GP120C14K en el "boost" induce una respuesta celular específica para la Envuelta del VIH-1 más alta y polifuncional que el grupo correspondiente expresando la proteína GP120C monomérica.

5. La proteína GP120C14K sola o en combinación heteróloga con MVA-GP120C14K fue capaz de inducir altos títulos de anticuerpos específicos frente a GP120 en ratón indicando el efecto positivo de la proteína de fusion GP120C14K en la respuesta humoral frente a dicha proteína de la Envuelta del VIH-1.

6. La calidad de la respuesta humoral frente a la Envuelta del VIH-1 aumentó (mayor proporción de células B de los centros germinales y de células T foliculares específicas frente a la Envuelta) en aquellos animales que recibieron MVA-GP120C14K en el "prime" y GP120C14K en el "boost" con respecto a los animales inmunizados con la proteína GP120C monomérica.

7. La adición de un "priming" con DNA al protocolo heterólogo de inmunización MVA-GP120C14K + GP120C14K aumentó la magnitud de la respuesta de células T CD8 específicas de la Envuelta del VIH-1.

8. El "priming" con DNA mejoró la calidad de la respuesta humoral frente a la Envuelta del VIH-1 medida por la proporción de células B de los centros germinales y de células T foliculares específicas inducidas por el antígeno de fusión.

7. BIBLIOGRAPHY

ABAITUA, F., RODRÍGUEZ, J. R., GARZÓN, A., RODRÍGUEZ, D. & ESTEBAN, M. 2006. Improving recombinant MVA immune responses: potentiation of the immune responses to HIV-1 with MVA and DNA vectors expressing Env and the cytokines IL-12 and IFN-gamma. *Virus research,* 116**,** 11-20.

ABRISHAMI, V., ZALDÍVAR-PERAZA, A., DE LA ROSA-TREVÍN, J. M., VARGAS, J., OTÓN, J., MARABINI, R., SHKOLNISKY, Y., CARAZO, J. M. & SORZANO, C. O. S. 2013. A pattern matching approach to the automatic selection of particles from low-contrast electron micrographs. *Bioinformatics,* 29**,** 2460-2468.

AMARA, R. R., IBEGBU, C., VILLINGER, F., MONTEFIORI, D. C., SHARMA, S., NIGAM, P., XU, Y., MCCLURE, H. M. & ROBINSON, H. L. 2005. Studies using a viral challenge and CD8 T cell depletions on the roles of cellular and humoral immunity in the control of an SHIV-89.6 P challenge in DNA/MVA-vaccinated macaques. *Virology,* 343**,** 246-255.

ARTENSTEIN, A. W. & GRABENSTEIN, J. D. 2008. Smallpox vaccines for biodefense: need and feasibility. *Expert review of vaccines,* 7**,** 1225-1237.

BALLAS, Z. K., KRIEG, A. M., WARREN, T., RASMUSSEN, W., DAVIS, H. L., WALDSCHMIDT, M. & WEINER, G. J. 2001. Divergent therapeutic and immunologic effects of oligodeoxynucleotides with distinct CpG motifs. *The Journal of Immunology,* 167**,** 4878-4886.

BARRÉ-SINOUSSI, F., CHERMANN, J.-C., REY, F., NUGEYRE, M. T., CHAMARET, S., GRUEST, J., DAUGUET, C., AXLER-BLIN, C., VÉZINET-BRUN, F. & ROUZIOUX, C. 1983. Isolation of a T-lymphotropic retrovirus from a patient at risk for acquired immune deficiency syndrome (AIDS). *Science,* 220**,** 868-871.

BERTLEY, F. M., KOZLOWSKI, P. A., WANG, S.-W., CHAPPELLE, J., PATEL, J., SONUYI, O., MAZZARA, G., MONTEFIORI, D., CARVILLE, A. & MANSFIELD, K. G. 2004. Control of simian/human immunodeficiency virus viremia and disease progression after IL-2-augmented DNA-modified vaccinia virus Ankara nasal vaccination in nonhuman primates. *The Journal of Immunology,* 172**,** 3745-3757.

BETTS, M. R., NASON, M. C., WEST, S. M., DE ROSA, S. C., MIGUELES, S. A., ABRAHAM, J., LEDERMAN, M. M., BENITO, J. M., GOEPFERT, P. A. & CONNORS, M. 2006. HIV nonprogressors preferentially maintain highly functional HIV-specific CD8+ T cells. *Blood,* 107**,** 4781-4789.

BHANUPRAKASH, V., HOSAMANI, M., VENKATESAN, G., BALAMURUGAN, V., YOGISHARADHYA, R. & SINGH, R. K. 2012. Animal poxvirus vaccines: a comprehensive review. *Expert review of vaccines,* 11**,** 1355-1374.

BLASCO, R. & MOSS, B. 1991. Extracellular vaccinia virus formation and cell-to-cell virus transmission are prevented by deletion of the gene encoding the 37,000-Dalton outer envelope protein. *Journal of virology,* 65**,** 5910-5920.

BLATTNER, C., LEE, J. H., SLIEPEN, K., DERKING, R., FALKOWSKA, E., DE LA PEÑA, A. T., CUPO, A., JULIEN, J.-P., VAN GILS, M. & LEE, P. S. 2014. Structural delineation of a quaternary, cleavage-dependent epitope at the gp41-gp120 interface on intact HIV-1 Env trimers. *Immunity,* 40**,** 669-680.

BOIVIN, S., KOZAK, S. & MEIJERS, R. 2013. Optimization of protein purification and characterization using Thermofluor screens. *Protein expression and purification,* 91**,** 192-206.

BORROW, P., LEWICKI, H., HAHN, B. H., SHAW, G. M. & OLDSTONE, M. 1994. Virus-specific CD8+ cytotoxic T-lymphocyte activity associated with control of viremia in primary human immunodeficiency virus type 1 infection. *Journal of virology,* 68**,** 6103-6110.

BUCHBINDER, S. P., MEHROTRA, D. V., DUERR, A., FITZGERALD, D. W., MOGG, R., LI, D., GILBERT, P. B., LAMA, J. R., MARMOR, M. & DEL RIO, C. 2008. Efficacy assessment of a cell-mediated immunity HIV-1 vaccine (the Step Study): a double-

blind, randomised, placebo-controlled, test-of-concept trial. *The Lancet,* 372**,** 1881-1893.
BUONAGURO, L., TORNESELLO, M. & BUONAGURO, F. 2007. Human immunodeficiency virus type 1 subtype distribution in the worldwide epidemic: pathogenetic and therapeutic implications. *Journal of virology,* 81**,** 10209-10219.
BURTON, D. R., DESROSIERS, R. C., DOMS, R. W., FEINBERG, M. B., GALLO, R. C., HAHN, B., HOXIE, J. A., HUNTER, E., KORBER, B. & LANDAY, A. 2004. A sound rationale needed for phase III HIV-1 vaccine trials. American Association for the Advancement of Science.
BURTON, D. R. & MASCOLA, J. R. 2015. Antibody responses to envelope glycoproteins in HIV-1 infection. *Nature immunology,* 16**,** 571.
CAPUCCI, S., WEE, E. G., SCHIFFNER, T., LABRANCHE, C. C., BORTHWICK, N., CUPO, A., DODD, J., DEAN, H., SATTENTAU, Q. & MONTEFIORI, D. 2017. HIV-1-neutralizing antibody induced by simian adenovirus-and poxvirus MVA-vectored BG505 native-like envelope trimers. *PloS one,* 12**,** e0181886.
CARROLL, M. & MOSS, B. 1995. E. coli beta-glucuronidase (GUS) as a marker for recombinant vaccinia viruses. *BioTechniques,* 19**,** 352.
CARTER, G. C., RODGER, G., MURPHY, B. J., LAW, M., KRAUSS, O., HOLLINSHEAD, M. & SMITH, G. L. 2003. Vaccinia virus cores are transported on microtubules. *Journal of General Virology,* 84**,** 2443-2458.
CASTILLO-MENENDEZ, L. R., WITT, K., ESPY, N., PRINCIOTTO, A., MADANI, N., PACHECO, B., FINZI, A. & SODROSKI, J. 2018. Comparison of Uncleaved and Mature Human Immunodeficiency Virus Membrane Envelope Glycoprotein Trimers. *Journal of virology,* 92**,** e00277-18.
CHAKRABARTI, B. K., PANCERA, M., PHOGAT, S., O'DELL, S., MCKEE, K., GUENAGA, J., ROBINSON, J., MASCOLA, J. & WYATT, R. T. 2011. HIV type 1 Env precursor cleavage state affects recognition by both neutralizing and nonneutralizing gp41 antibodies. *AIDS research and human retroviruses,* 27**,** 877-887.
CHAKRABARTI, S., BRECHLING, K. & MOSS, B. 1985. Vaccinia virus expression vector: coexpression of beta-galactosidase provides visual screening of recombinant virus plaques. *Molecular and Cellular Biology,* 5**,** 3403-3409.
CHAN, D. C. & KIM, P. S. 1998. HIV entry and its inhibition. *Cell,* 93**,** 681-684.
CHANG, T.-H., CHANG, S.-J., HSIEH, F.-L., KO, T.-P., LIN, C.-T., HO, M.-R., WANG, I., HSU, S.-T. D., GUO, R.-T. & CHANG, W. 2013. Crystal structure of vaccinia viral A27 protein reveals a novel structure critical for its function and complex formation with A26 protein. *PLoS pathogens,* 9**,** e1003563.
CHECKLEY, M. A., LUTTGE, B. G. & FREED, E. O. 2011. HIV-1 envelope glycoprotein biosynthesis, trafficking, and incorporation. *Journal of molecular biology,* 410**,** 582-608.
CHUNG, C.-S., HSIAO, J.-C., CHANG, Y.-S. & CHANG, W. 1998. A27L protein mediates vaccinia virus interaction with cell surface heparan sulfate. *Journal of virology,* 72**,** 1577-1585.
CHURCHYARD, G. J., MORGAN, C., ADAMS, E., HURAL, J., GRAHAM, B. S., MOODIE, Z., GROVE, D., GRAY, G., BEKKER, L.-G. & MCELRATH, M. J. 2011. A phase IIA randomized clinical trial of a multiclade HIV-1 DNA prime followed by a multiclade rAd5 HIV-1 vaccine boost in healthy adults (HVTN204). *PloS one,* 6**,** e21225.
CIHLAR, T. & FORDYCE, M. 2016. Current status and prospects of HIV treatment. *Current opinion in virology,* 18**,** 50-56.
CLAIREAUX, M., GALPERIN, M., BENATI, D., NOUËL, A., MUKHOPADHYAY, M., KLINGLER, J., DE TRUCHIS, P., ZUCMAN, D., HENDOU, S. & BOUFASSA, F. 2018. A High Frequency of HIV-Specific Circulating Follicular Helper T Cells Is Associated with Preserved Memory B Cell Responses in HIV Controllers. *mBio,* 9**,** e00317-18.
COLLADO, M., RODRíGUEZ, D., RODRíGUEZ, J. R., VÁZQUEZ, I., GONZALO, R. M. & ESTEBAN, M. 2000. Chimeras between the human immunodeficiency virus (HIV-1)

Env and vaccinia virus immunogenic proteins p14 and p39 generate in mice broadly reactive antibodies and specific activation of CD8+ T cell responses to Env. *Vaccine,* 18**,** 3123-3133.

CRAIGIE, R. & BUSHMAN, F. D. 2012. Hiv dna integration. *Cold Spring Harbor perspectives in medicine,* 2**,** a006890.

CURRIER, J. R., NGAUY, V., DE SOUZA, M. S., RATTO-KIM, S., COX, J. H., POLONIS, V. R., EARL, P., MOSS, B., PEEL, S. & SLIKE, B. 2010. Phase I safety and immunogenicity evaluation of MVA-CMDR, a multigenic, recombinant modified vaccinia Ankara-HIV-1 vaccine candidate. *PloS one,* 5**,** e13983.

CYRKLAFF, M., RISCO, C., FERNÁNDEZ, J. J., JIMÉNEZ, M. V., ESTÉBAN, M., BAUMEISTER, W. & CARRASCOSA, J. L. 2005. Cryo-electron tomography of vaccinia virus. *Proceedings of the National Academy of Sciences of the United States of America,* 102**,** 2772-2777.

DALLO, S., RODRIGUEZ, J. F. & ESTEBAN, M. 1987. A 14K envelope protein of vaccinia virus with an important role in virus-host cell interactions is altered during virus persistence and determines the plaque size phenotype of the virus. *Virology,* 159**,** 423-432.

DE LA ROSA-TREVÍN, J., OTÓN, J., MARABINI, R., ZALDIVAR, A., VARGAS, J., CARAZO, J. & SORZANO, C. 2013. Xmipp 3.0: an improved software suite for image processing in electron microscopy. *Journal of structural biology,* 184**,** 321-328.

DOMS, R., BLUMENTHAL, R. & MOSS, B. 1990. Fusion of intra-and extracellular forms of vaccinia virus with the cell membrane. *Journal of virology,* 64**,** 4884-4892.

ELENA GÓMEZ, C., PERDIGUERO, B., GARCÍA-ARRIAZA, J. & ESTEBAN, M. 2012. Poxvirus vectors as HIV/AIDS vaccines in humans. *Human vaccines & immunotherapeutics,* 8**,** 1192-1207.

ESTEBAN, M. 1984. Defective vaccinia virus particles in interferon-treated infected cells. *Virology,* 133**,** 220-227.

ESTEBAN, M., FLORES, L. & HOLOWCZAK, J. A. 1977. Model for vaccinia virus DNA replication. *Virology,* 83**,** 467-473.

ESTEBAN, M. & METZ, D. 1973. Early virus protein synthesis in vaccinia virus-infected cells. *Journal of General Virology,* 19**,** 201-216.

ESTEBAN, M., SOLOSKI, M., CABRERA, C. & HOLOWCZAK, J. Replication of vaccinia DNA and studies on the structure of the viral chromosome. Cold Spring Harbor symposia on quantitative biology, 1979. Cold Spring Harbor Laboratory Press, 789-799.

FALIVENE, J., ZAJAC, M. P. D. M., PASCUTTI, M. F., RODRÍGUEZ, A. M., MAETO, C., PERDIGUERO, B., GÓMEZ, C. E., ESTEBAN, M., CALAMANTE, G. & GHERARDI, M. M. 2012. Improving the MVA vaccine potential by deleting the viral gene coding for the IL-18 binding protein. *PloS one,* 7**,** e32220.

FOUDA, G. G., AMOS, J. D., WILKS, A. B., POLLARA, J., RAY, C. A., CHAND, A., KUNZ, E. L., LIEBL, B. E., WHITAKER, K. & CARVILLE, A. 2013. Mucosal immunization of lactating female rhesus monkeys with a transmitted/founder HIV-1 envelope induces strong Env-specific IgA antibody responses in breast milk. *Journal of virology,* 87**,** 6986-6999.

FRANKEL, A. D. & YOUNG, J. A. 1998. HIV-1: fifteen proteins and an RNA. Annual Reviews 4139 El Camino Way, PO Box 10139, Palo Alto, CA 94303-0139, USA.

GALLO, R. C., SARIN, P. S., GELMANN, E., ROBERT-GUROFF, M., RICHARDSON, E., KALYANARAMAN, V., MANN, D., SIDHU, G. D., STAHL, R. E. & ZOLLA-PAZNER, S. 1983. Isolation of human T-cell leukemia virus in acquired immune deficiency syndrome (AIDS). *Science,* 220**,** 865-867.

GAO, F., CHEN, Y., LEVY, D. N., CONWAY, J. A., KEPLER, T. B. & HUI, H. 2004. Unselected mutations in the human immunodeficiency virus type 1 genome are mostly nonsynonymous and often deleterious. *Journal of virology,* 78**,** 2426-2433.

GARCES, F., SOK, D., KONG, L., MCBRIDE, R., KIM, H. J., SAYE-FRANCISCO, K. F., JULIEN, J.-P., HUA, Y., CUPO, A. & MOORE, J. P. 2014. Structural evolution of glycan recognition by a family of potent HIV antibodies. *Cell,* 159**,** 69-79.

GARCÍA-ARRIAZA, J. & ESTEBAN, M. 2014. Enhancing poxvirus vectors vaccine immunogenicity. *Human vaccines & immunotherapeutics,* 10**,** 2235-2244.

GARCÍA-ARRIAZA, J., GÓMEZ, C. E., SORZANO, C. Ó. S. & ESTEBAN, M. 2014. Deletion of the vaccinia virus N2L gene encoding an inhibitor of IRF3 improves the immunogenicity of modified vaccinia virus Ankara expressing HIV-1 antigens. *Journal of virology,* 88**,** 3392-3410.

GARCÍA-ARRIAZA, J., NÁJERA, J. L., GÓMEZ, C. E., SORZANO, C. O. S. & ESTEBAN, M. 2010. Immunogenic profiling in mice of a HIV/AIDS vaccine candidate (MVA-B) expressing four HIV-1 antigens and potentiation by specific gene deletions. *PLoS One,* 5**,** e12395.

GARCÍA-ARRIAZA, J., NÁJERA, J. L., GÓMEZ, C. E., TEWABE, N., SORZANO, C. O. S., CALANDRA, T., ROGER, T. & ESTEBAN, M. 2011. A candidate HIV/AIDS vaccine (MVA-B) lacking vaccinia virus gene C6L enhances memory HIV-1-specific T-cell responses. *PloS one,* 6**,** e24244.

GARCÍA, F., DE QUIRÓS, J. C. L. B., GÓMEZ, C. E., PERDIGUERO, B., NÁJERA, J. L., JIMÉNEZ, V., GARCÍA-ARRIAZA, J., GUARDO, A. C., PÉREZ, I. & DÍAZ-BRITO, V. 2011. Safety and immunogenicity of a modified pox vector-based HIV/AIDS vaccine candidate expressing Env, Gag, Pol and Nef proteins of HIV-1 subtype B (MVA-B) in healthy HIV-1-uninfected volunteers: A phase I clinical trial (RISVAC02). *Vaccine,* 29**,** 8309-8316.

GASTINEL, L. N., SIMISTER, N. E. & BJORKMAN, P. J. 1992. Expression and crystallization of a soluble and functional form of an Fc receptor related to class I histocompatibility molecules. *Proceedings of the National Academy of Sciences,* 89**,** 638-642.

GAVIN, A. L., HOEBE, K., DUONG, B., OTA, T., MARTIN, C., BEUTLER, B. & NEMAZEE, D. 2006. Adjuvant-enhanced antibody responses in the absence of toll-like receptor signaling. *Science,* 314**,** 1936-1938.

GILBERT, P. B., PETERSON, M. L., FOLLMANN, D., HUDGENS, M. G., FRANCIS, D. P., GURWITH, M., HEYWARD, W. L., JOBES, D. V., POPOVIC, V. & SELF, S. G. 2005. Correlation between immunologic responses to a recombinant glycoprotein 120 vaccine and incidence of HIV-1 infection in a phase 3 HIV-1 preventive vaccine trial. *The Journal of infectious diseases,* 191**,** 666-677.

GOMEZ, C. & ESTEBAN, M. 2001. Recombinant proteins produced by vaccinia virus vectors can be incorporated within the virion (IMV form) into different compartments. *Archives of virology,* 146**,** 875-892.

GÓMEZ, C. E., NÁJERA, J. L., JIMÉNEZ, E. P., JIMÉNEZ, V., WAGNER, R., GRAF, M., FRACHETTE, M.-J., LILJESTRÖM, P., PANTALEO, G. & ESTEBAN, M. 2007a. Head-to-head comparison on the immunogenicity of two HIV/AIDS vaccine candidates based on the attenuated poxvirus strains MVA and NYVAC co-expressing in a single locus the HIV-1BX08 gp120 and HIV-1IIIB Gag-Pol-Nef proteins of clade B. *Vaccine,* 25**,** 2863-2885.

GÓMEZ, C. E., NÁJERA, J. L., JIMÉNEZ, V., BIELER, K., WILD, J., KOSTIC, L., HEIDARI, S., CHEN, M., FRACHETTE, M.-J. & PANTALEO, G. 2007b. Generation and immunogenicity of novel HIV/AIDS vaccine candidates targeting HIV-1 Env/Gag-Pol-Nef antigens of clade C. *Vaccine,* 25**,** 1969-1992.

GÓMEZ, C. E., NÁJERA, J. L., PERDIGUERO, B., GARCÍA-ARRIAZA, J., SORZANO, C. O. S., JIMÉNEZ, V., GONZÁLEZ-SANZ, R., JIMÉNEZ, J. L., MUÑOZ-FERNÁNDEZ, M. A. & DE QUIRÓS, J. C. L. B. 2011. The HIV/AIDS vaccine candidate MVA-B administered as a single immunogen in humans triggers robust, polyfunctional, and selective effector memory T cell responses to HIV-1 antigens. *Journal of virology,* 85**,** 11468-11478.

GÓMEZ, C. E., NÁJERA, J. L., SÁNCHEZ, R., JIMÉNEZ, V. & ESTEBAN, M. 2009. Multimeric soluble CD40 ligand (sCD40L) efficiently enhances HIV specific cellular immune responses during DNA prime and boost with attenuated poxvirus vectors MVA and NYVAC expressing HIV antigens. *Vaccine,* 27**,** 3165-3174.

GÓMEZ, C. E., PERDIGUERO, B., CEPEDA, M. V., MINGORANCE, L., GARCÍA-ARRIAZA, J., VANDERMEEREN, A., SORZANO, C. Ó. S. & ESTEBAN, M. 2013. High, broad, polyfunctional, and durable T cell immune responses induced in mice by a novel hepatitis C virus (HCV) vaccine candidate (MVA-HCV) based on modified vaccinia virus Ankara expressing the nearly full-length HCV genome. *Journal of virology,* 87**,** 7282-7300.

GÓMEZ, C. E., PERDIGUERO, B., GARCÍA-ARRIAZA, J., CEPEDA, V., SÁNCHEZ-SORZANO, C. Ó., MOTHE, B., JIMÉNEZ, J. L., MUÑOZ-FERNÁNDEZ, M. Á., GATELL, J. M. & DE QUIRÓS, J. C. L. B. 2015. A phase I randomized therapeutic MVA-B vaccination improves the magnitude and quality of the T cell immune responses in HIV-1-infected subjects on HAART. *PloS one,* 10**,** e0141456.

GÓMEZ, C. E., PERDIGUERO, B., SÁNCHEZ-CORZO, C., SORZANO, C. O. S. & ESTEBAN, M. 2017. Immune Modulation of NYVAC-Based HIV Vaccines by Combined Deletion of Viral Genes that Act on Several Signalling Pathways. *Viruses,* 10**,** 7.

GONG, S., LAI, C. & ESTEBAN, M. 1990. Vaccinia virus induces cell fusion at acid pH and this activity is mediated by the N-terminus of the 14-kDa virus envelope protein. *Virology,* 178**,** 81-91.

GORNY, M., XU, J.-Y., KARWOWSKA, S., BUCHBINDER, A. & ZOLLA-PAZNER, S. 1993. Repertoire of neutralizing human monoclonal antibodies specific for the V3 domain of HIV-1 gp120. *The Journal of Immunology,* 150**,** 635-643.

GORNY, M. K., XU, J.-Y., GIANAKAKOS, V., KARWOWSKA, S., WILLIAMS, C., SHEPPARD, H. W., HANSON, C. V. & ZOLLA-PAZNER, S. 1991. Production of site-selected neutralizing human monoclonal antibodies against the third variable domain of the human immunodeficiency virus type 1 envelope glycoprotein. *Proceedings of the National Academy of Sciences,* 88**,** 3238-3242.

GOULDING, J., TAHILIANI, V. & SALEK-ARDAKANI, S. 2011. OX40: OX40L axis: emerging targets for improving poxvirus-based CD8+ T-cell vaccines against respiratory viruses. *Immunological reviews,* 244**,** 149-168.

GRAY, G. E., ALLEN, M., MOODIE, Z., CHURCHYARD, G., BEKKER, L.-G., NCHABELENG, M., MLISANA, K., METCH, B., DE BRUYN, G. & LATKA, M. H. 2011. Safety and efficacy of the HVTN 503/Phambili study of a clade-B-based HIV-1 vaccine in South Africa: a double-blind, randomised, placebo-controlled test-of-concept phase 2b study. *The Lancet infectious diseases,* 11**,** 507-515.

GREEN, M. & SAMBROOK, J. 2012. Molecular Cloning: A Laboratory Manual. Cold Spring Harbor Lab Press. Cold Spring Harbor, NY.

GUARDO, A. C., GÓMEZ, C. E., DÍAZ-BRITO, V., PICH, J., ARNAIZ, J. A., PERDIGUERO, B., GARCÍA-ARRIAZA, J., GONZÁLEZ, N., SORZANO, C. O. & JIMÉNEZ, L. 2017. Safety and vaccine-induced HIV-1 immune responses in healthy volunteers following a late MVA-B boost 4 years after the last immunization. *PloS one,* 12**,** e0186602.

GUDMUNDSDOTTER, L., NILSSON, C., BRAVE, A., HEJDEMAN, B., EARL, P., MOSS, B., ROBB, M., COX, J., MICHAEL, N. & MAROVICH, M. 2009. Recombinant Modified Vaccinia Ankara (MVA) effectively boosts DNA-primed HIV-specific immune responses in humans despite pre-existing vaccinia immunity. *Vaccine,* 27**,** 4468-4474.

GUENAGA, J., DE VAL, N., TRAN, K., FENG, Y., SATCHWELL, K., WARD, A. B. & WYATT, R. T. 2015. Well-ordered trimeric HIV-1 subtype B and C soluble spike mimetics generated by negative selection display native-like properties. *PLoS pathogens,* 11**,** e1004570.

HAMEL, K. M., LIARSKI, V. M. & CLARK, M. R. 2012. Germinal center B-cells. *Autoimmunity,* 45**,** 333-347.

HAMMER, S. M., SOBIESZCZYK, M. E., JANES, H., KARUNA, S. T., MULLIGAN, M. J., GROVE, D., KOBLIN, B. A., BUCHBINDER, S. P., KEEFER, M. C. & TOMARAS, G. D. 2013. Efficacy trial of a DNA/rAd5 HIV-1 preventive vaccine. *New England Journal of Medicine,* 369**,** 2083-2092.

HARARI, A., BART, P.-A., STÖHR, W., TAPIA, G., GARCIA, M., MEDJITNA-RAIS, E., BURNET, S., CELLERAI, C., ERLWEIN, O. & BARBER, T. 2008. An HIV-1 clade C DNA prime, NYVAC boost vaccine regimen induces reliable, polyfunctional, and long-lasting T cell responses. *Journal of experimental medicine,* 205**,** 63-77.

HAVENAR-DAUGHTON, C., LEE, J. H. & CROTTY, S. 2017. Tfh cells and HIV bnAbs, an immunodominance model of the HIV neutralizing antibody generation problem. *Immunological reviews,* 275**,** 49-61.

HEMELAAR, J. 2012. The origin and diversity of the HIV-1 pandemic. *Trends in molecular medicine,* 18**,** 182-192.

HO, Y., HSIAO, J.-C., YANG, M.-H., CHUNG, C.-S., PENG, Y.-C., LIN, T.-H., CHANG, W. & TZOU, D.-L. M. 2005. The oligomeric structure of vaccinia viral envelope protein A27L is essential for binding to heparin and heparan sulfates on cell surfaces: a structural and functional approach using site-specific mutagenesis. *Journal of molecular biology,* 349**,** 1060-1071.

HOLLISTER, K., CHEN, Y., WANG, S., WU, H., MONDAL, A., CLEGG, N., LU, S. & DENT, A. 2014. The role of follicular helper T cells and the germinal center in HIV-1 gp120 DNA prime and gp120 protein boost vaccination. *Human vaccines & immunotherapeutics,* 10**,** 1985-1992.

HUGHES, A. L., IRAUSQUIN, S. & FRIEDMAN, R. 2010. The evolutionary biology of poxviruses. *Infection, Genetics and Evolution,* 10**,** 50-59.

JIN, X., BAUER, D. E., TUTTLETON, S. E., LEWIN, S., GETTIE, A., BLANCHARD, J., IRWIN, C. E., SAFRIT, J. T., MITTLER, J. & WEINBERGER, L. 1999. Dramatic rise in plasma viremia after CD8+ T cell depletion in simian immunodeficiency virus–infected macaques. *Journal of Experimental Medicine,* 189**,** 991-998.

JOKLIK, W. 1962. The purification of four strains of poxvirus. *Virology,* 18**,** 9-18.

JOKLIK, W. K. & BECKER, Y. 1964. The replication and coating of vaccinia DNA. *Journal of molecular biology,* 10**,** 452-474.

JOSEPH, S., QUINN, K., GREENWOOD, A., COPE, A. V., MCKAY, P. F., HAYES, P. J., KOPYCINSKI, J. T., GILMOUR, J., MILLER, A. N. & GELDMACHER, C. 2017. A comparative phase I study of combination, homologous subtype-C DNA, MVA, and Env gp140 protein/adjuvant HIV vaccines in two immunization regimes. *Frontiers in immunology,* 8**,** 149.

JULIEN, J.-P., SOK, D., KHAYAT, R., LEE, J. H., DOORES, K. J., WALKER, L. M., RAMOS, A., DIWANJI, D. C., PEJCHAL, R. & CUPO, A. 2013. Broadly neutralizing antibody PGT121 allosterically modulates CD4 binding via recognition of the HIV-1 gp120 V3 base and multiple surrounding glycans. *PLoS pathogens,* 9**,** e1003342.

KLEIN, J. S. & BJORKMAN, P. J. 2010. Few and far between: how HIV may be evading antibody avidity. *PLoS pathogens,* 6**,** e1000908.

KOLIBAB, K., YANG, A., DERRICK, S. C., WALDMANN, T. A., PERERA, L. P. & MORRIS, S. L. 2010. Highly persistent and effective prime/boost regimens against tuberculosis that use a multivalent modified vaccine virus Ankara-based tuberculosis vaccine with interleukin-15 as a molecular adjuvant. *Clinical and Vaccine Immunology,* 17**,** 793-801.

KOOL, M., FIERENS, K. & LAMBRECHT, B. N. 2012. Alum adjuvant: some of the tricks of the oldest adjuvant. *Journal of medical microbiology,* 61**,** 927-934.

KOPPENSTEINER, H., BRACK-WERNER, R. & SCHINDLER, M. 2012. Macrophages and their relevance in Human Immunodeficiency Virus Type I infection. *Retrovirology,* 9**,** 82.

KOUP, R., SAFRIT, J. T., CAO, Y., ANDREWS, C. A., MCLEOD, G., BORKOWSKY, W., FARTHING, C. & HO, D. D. 1994. Temporal association of cellular immune responses with the initial control of viremia in primary human immunodeficiency virus type 1 syndrome. *Journal of virology,* 68**,** 4650-4655.

KOUP, R. A. & DOUEK, D. C. 2011. Vaccine design for CD8 T lymphocyte responses. *Cold Spring Harbor perspectives in medicine,* 1**,** a007252.

KOVACS, J. M., NKOLOLA, J. P., PENG, H., CHEUNG, A., PERRY, J., MILLER, C. A., SEAMAN, M. S., BAROUCH, D. H. & CHEN, B. 2012. HIV-1 envelope trimer elicits more potent neutralizing antibody responses than monomeric gp120. *Proceedings of the National Academy of Sciences,* 109**,** 12111-12116.

KOVACS, J. M., NOELDEKE, E., HA, H. J., PENG, H., RITS-VOLLOCH, S., HARRISON, S. C. & CHEN, B. 2014. Stable, uncleaved HIV-1 envelope glycoprotein gp140 forms a tightly folded trimer with a native-like structure. *Proceedings of the National Academy of Sciences,* 111**,** 18542-18547.

KWONG, P. D., DOYLE, M. L., CASPER, D. J., CICALA, C., LEAVITT, S. A., MAJEED, S., STEENBEKE, T. D., VENTURI, M., CHAIKEN, I. & FUNG, M. 2002. HIV-1 evades antibody-mediated neutralization through conformational masking of receptor-binding sites. *Nature,* 420**,** 678.

LEE, E.-C., LIANG, Q., ALI, H., BAYLISS, L., BEASLEY, A., BLOOMFIELD-GERDES, T., BONOLI, L., BROWN, R., CAMPBELL, J. & CARPENTER, A. 2014. Complete humanization of the mouse immunoglobulin loci enables efficient therapeutic antibody discovery. *Nature biotechnology,* 32**,** 356.

LEE, J. H., ANDRABI, R., SU, C.-Y., YASMEEN, A., JULIEN, J.-P., KONG, L., WU, N. C., MCBRIDE, R., SOK, D. & PAUTHNER, M. 2017. A broadly neutralizing antibody targets the dynamic HIV envelope trimer apex via a long, rigidified, and anionic β-hairpin structure. *Immunity,* 46**,** 690-702.

LI, Y., O'DELL, S., WALKER, L. M., WU, X., GUENAGA, J., FENG, Y., SCHMIDT, S. D., MCKEE, K., LOUDER, M. K. & LEDGERWOOD, J. E. 2011. Mechanism of neutralization by the broadly neutralizing HIV-1 monoclonal antibody VRC01. *Journal of virology,* 85**,** 8954-8967.

LIU, Y., PAN, J., CAI, Y., GRIGORIEFF, N., HARRISON, S. C. & CHEN, B. 2017. Conformational states of a soluble, uncleaved HIV-1 envelope trimer. *Journal of virology,* 91**,** e00175-17.

LOCCI, M., HAVENAR-DAUGHTON, C., LANDAIS, E., WU, J., KROENKE, M. A., ARLEHAMN, C. L., SU, L. F., CUBAS, R., DAVIS, M. M. & SETTE, A. 2013. Human circulating PD-1+ CXCR3− CXCR5+ memory Tfh cells are highly functional and correlate with broadly neutralizing HIV antibody responses. *Immunity,* 39**,** 758-769.

MALYALA, P. & SINGH, M. 2008. Endotoxin limits in formulations for preclinical research. *Journal of pharmaceutical sciences,* 97**,** 2041-2044.

MAYR, A., STICKL, H., MÜLLER, H., DANNER, K. & SINGER, H. 1978. The smallpox vaccination strain MVA: marker, genetic structure, experience gained with the parenteral vaccination and behavior in organisms with a debilitated defence mechanism (author's transl). *Zentralblatt fur Bakteriologie, Parasitenkunde, Infektionskrankheiten und Hygiene. Erste Abteilung Originale. Reihe B: Hygiene, Betriebshygiene, praventive Medizin,* 167**,** 375-390.

MCFADDEN, G. 2005. Poxvirus tropism. *Nature Reviews Microbiology,* 3**,** 201.

MCKAY, P. F., COPE, A. V., MANN, J. F., JOSEPH, S., ESTEBAN, M., TATOUD, R., CARTER, D., REED, S. G., WEBER, J. & SHATTOCK, R. J. 2014. Glucopyranosyl lipid A adjuvant significantly enhances HIV specific T and B cell responses elicited by a DNA-MVA-protein vaccine regimen. *PloS one,* 9**,** e84707.

MCLELLAN, J. S., PANCERA, M., CARRICO, C., GORMAN, J., JULIEN, J.-P., KHAYAT, R., LOUDER, R., PEJCHAL, R., SASTRY, M. & DAI, K. 2011. Structure of HIV-1 gp120 V1/V2 domain with broadly neutralizing antibody PG9. *Nature,* 480**,** 336.

MERCER, A., SCHMIDT, A. & WEBER, O. 2007. *Poxviruses*, Springer Science & Business Media.

METZ, D. & ESTEBAN, M. 1972. Interferon inhibits viral protein synthesis in L cells infected with vaccinia virus. *Nature,* 238**,** 385.

MOORE, P. L., CROOKS, E. T., PORTER, L., ZHU, P., CAYANAN, C. S., GRISE, H., CORCORAN, P., ZWICK, M. B., FRANTI, M. & MORRIS, L. 2006. Nature of nonfunctional envelope proteins on the surface of human immunodeficiency virus type 1. *Journal of virology,* 80**,** 2515-2528.

MOSS, B. 1996. Genetically engineered poxviruses for recombinant gene expression, vaccination, and safety. *Proceedings of the National Academy of Sciences,* 93**,** 11341-11348.

MOSS, B. 2012. Poxvirus cell entry: how many proteins does it take? *Viruses,* 4**,** 688-707.

MOSS, B. 2013. Poxvirus DNA replication. *Cold Spring Harbor perspectives in biology,* 5**,** a010199.

MOSS, B., KNIPE, D. M. & HOWLEY, P. M. (eds.) 2007. *Poxviridae: The viruses and their replication,* Philadelphia: Lippincott-Raven.

MOTHE, B., CLIMENT, N., PLANA, M., ROSÀS, M., JIMÉNEZ, J. L., MUÑOZ-FERNÁNDEZ, M. Á., PUERTAS, M. C., CARRILLO, J., GONZALEZ, N. & LEÓN, A. 2015. Safety and immunogenicity of a modified vaccinia Ankara-based HIV-1 vaccine (MVA-B) in HIV-1-infected patients alone or in combination with a drug to reactivate latent HIV-1. *Journal of Antimicrobial Chemotherapy,* 70**,** 1833-1842.

MOUQUET, H., SCHARF, L., EULER, Z., LIU, Y., EDEN, C., SCHEID, J. F., HALPER-STROMBERG, A., GNANAPRAGASAM, P. N., SPENCER, D. I. & SEAMAN, M. S. 2012. Complex-type N-glycan recognition by potent broadly neutralizing HIV antibodies. *Proceedings of the National Academy of Sciences,* 109**,** E3268-E3277.

MUNRO, J. B., GORMAN, J., MA, X., ZHOU, Z., ARTHOS, J., BURTON, D. R., KOFF, W. C., COURTER, J. R., SMITH, A. B. & KWONG, P. D. 2014. Conformational dynamics of single HIV-1 envelope trimers on the surface of native virions. *Science,* 346**,** 759-763.

NIESSL, J. & KAUFMANN, D. E. 2018. Harnessing T Follicular Helper Cell Responses for HIV Vaccine Development. *Viruses,* 10.

PALMER, S., JOSEFSSON, L. & COFFIN, J. 2011. HIV reservoirs and the possibility of a cure for HIV infection. *Journal of internal medicine,* 270**,** 550-560.

PANCERA, M., SHAHZAD-UL-HUSSAN, S., DORIA-ROSE, N. A., MCLELLAN, J. S., BAILER, R. T., DAI, K., LOESGEN, S., LOUDER, M. K., STAUPE, R. P. & YANG, Y. 2013. Structural basis for diverse N-glycan recognition by HIV-1–neutralizing V1–V2–directed antibody PG16. *Nature Structural and Molecular Biology,* 20**,** 804.

PANCERA, M., ZHOU, T., DRUZ, A., GEORGIEV, I. S., SOTO, C., GORMAN, J., HUANG, J., ACHARYA, P., CHUANG, G.-Y. & OFEK, G. 2014. Structure and immune recognition of trimeric pre-fusion HIV-1 Env. *Nature,* 514**,** 455.

PANTALEO, G., ESTEBAN, M., JACOBS, B. & TARTAGLIA, J. 2010. Poxvirus vector-based HIV vaccines. *Current Opinion in HIV and AIDS,* 5**,** 391-396.

PAOLETTI, E. 1996. Applications of pox virus vectors to vaccination: an update. *Proceedings of the National Academy of Sciences,* 93**,** 11349-11353.

PASTORET, P.-P. & VANDERPLASSCHEN, A. 2003. Poxviruses as vaccine vectors. *Comparative immunology, microbiology and infectious diseases,* 26**,** 343-355.

PERDIGUERO, B., GÓMEZ, C. E., NÁJERA, J. L., SORZANO, C. O. S., DELALOYE, J., GONZÁLEZ-SANZ, R., JIMÉNEZ, V., ROGER, T., CALANDRA, T. & PANTALEO, G. 2012. Deletion of the viral anti-apoptotic gene F1L in the HIV/AIDS vaccine candidate MVA-C enhances immune responses against HIV-1 antigens. *PloS one,* 7**,** e48524.

PETERS, B. S., JAOKO, W., VARDAS, E., PANAYOTAKOPOULOS, G., FAST, P., SCHMIDT, C., GILMOUR, J., BOGOSHI, M., OMOSA-MANYONYI, G. & DALLY, L. 2007. Studies of a prophylactic HIV-1 vaccine candidate based on modified vaccinia virus Ankara (MVA) with and without DNA priming: effects of dosage and route on safety and immunogenicity. *Vaccine,* 25**,** 2120-2127.

PITISUTTITHUM, P., GILBERT, P., GURWITH, M., HEYWARD, W., MARTIN, M., VAN GRIENSVEN, F., HU, D., TAPPERO, J. W. & GROUP, B. V. E. 2006. Randomized, double-blind, placebo-controlled efficacy trial of a bivalent recombinant glycoprotein 120 HIV-1 vaccine among injection drug users in Bangkok, Thailand. *The Journal of infectious diseases,* 194**,** 1661-1671.

RAMÍREZ, J. C., GHERARDI, M. M. & ESTEBAN, M. 2000. Biology of attenuated modified vaccinia virus Ankara recombinant vector in mice: virus fate and activation of B-and T-cell immune responses in comparison with the Western Reserve strain and advantages as a vaccine. *Journal of virology,* 74**,** 923-933.

RERKS-NGARM, S., PITISUTTITHUM, P., NITAYAPHAN, S., KAEWKUNGWAL, J., CHIU, J., PARIS, R., PREMSRI, N., NAMWAT, C., DE SOUZA, M. & ADAMS, E. 2009. Vaccination with ALVAC and AIDSVAX to prevent HIV-1 infection in Thailand. *New England Journal of Medicine,* 361**,** 2209-2220.

RINGE, R. P., SANDERS, R. W., YASMEEN, A., KIM, H. J., LEE, J. H., CUPO, A., KORZUN, J., DERKING, R., VAN MONTFORT, T. & JULIEN, J.-P. 2013. Cleavage strongly influences whether soluble HIV-1 envelope glycoprotein trimers adopt a native-like conformation. *Proceedings of the National Academy of Sciences,* 110**,** 18256-18261.

RODRÍGUEZ, A. M., PASCUTTI, M. F., MAETO, C., FALIVENE, J., HOLGADO, M. P., TURK, G. & GHERARDI, M. M. 2012. IL-12 and GM-CSF in DNA/MVA immunizations against HIV-1 CRF12_BF Nef induced T-cell responses with an enhanced magnitude, breadth and quality. *PloS one,* 7**,** e37801.

RODRIGUEZ, J.-R., RODRIGUEZ, D. & ESTEBAN, M. 1991. Structural properties of HIV-1 Env fused with the 14-kDa vaccinia virus envelope protein. *Virology,* 181**,** 742-748.

RODRIGUEZ, J., PAEZ, E. & ESTEBAN, M. 1987. A 14,000-Mr envelope protein of vaccinia virus is involved in cell fusion and forms covalently linked trimers. *Journal of virology,* 61**,** 395-404.

RODRIGUEZ, J. F. & ESTEBAN, M. 1987. Mapping and nucleotide sequence of the vaccinia virus gene that encodes a 14-kilodalton fusion protein. *Journal of virology,* 61**,** 3550-3554.

RODRIGUEZ, J. F. & SMITH, G. L. 1990. IPTG-dependent vaccinia virus: identification of a virus protein enabling virion envelopment by Golgi membrane and egress. *Nucleic acids research,* 18**,** 5347-5351.

RODRIGUEZ, J. R., RISCO, C., CARRASCOSA, J. L., ESTEBAN, M. & RODRÍGUEZ, D. 1997. Characterization of early stages in vaccinia virus membrane biogenesis: implications of the 21-kilodalton protein and a newly identified 15-kilodalton envelope protein. *Journal of virology,* 71**,** 1821-1833.

ROEDERER, M., NOZZI, J. L. & NASON, M. C. 2011. SPICE: Exploration and analysis of post-cytometric complex multivariate datasets. *Cytometry Part A,* 79**,** 167-174.

ROLLAND, M., TOVANABUTRA, S., FRAHM, N., GILBERT, P. B., SANDERS-BUELL, E., HEATH, L., MAGARET, C. A., BOSE, M., BRADFIELD, A. & O'SULLIVAN, A. 2011. Genetic impact of vaccination on breakthrough HIV-1 sequences from the STEP trial. *Nature medicine,* 17**,** 366.

SÁEZ-CIRIÓN, A., LACABARATZ, C., LAMBOTTE, O., VERSMISSE, P., URRUTIA, A., BOUFASSA, F., BARRÉ-SINOUSSI, F., DELFRAISSY, J.-F., SINET, M. & PANCINO, G. 2007. HIV controllers exhibit potent CD8 T cell capacity to suppress HIV infection ex vivo and peculiar cytotoxic T lymphocyte activation phenotype. *Proceedings of the National Academy of Sciences,* 104**,** 6776-6781.

SANDERS, R. W. & MOORE, J. P. 2014. HIV: A stamp on the envelope. *Nature,* 514**,** 437.

SANDERS, R. W., VAN GILS, M. J., DERKING, R., SOK, D., KETAS, T. J., BURGER, J. A., OZOROWSKI, G., CUPO, A., SIMONICH, C. & GOO, L. 2015. HIV-1 neutralizing antibodies induced by native-like envelope trimers. *Science,* 349**,** aac4223.

SANDERSON, C. M., HOLLINSHEAD, M. & SMITH, G. L. 2000. The vaccinia virus A27L protein is needed for the microtubule-dependent transport of intracellular mature virus particles. *Journal of General Virology,* 81**,** 47-58.

SAROV, I. & JOKLIK, W. K. 1972. Characterization of intermediates in the uncoating of vaccinia virus DNA. *Virology,* 50**,** 593-602.

SCHERES, S. H. 2012a. A Bayesian view on cryo-EM structure determination. *Journal of molecular biology,* 415**,** 406-418.

SCHERES, S. H. 2012b. RELION: implementation of a Bayesian approach to cryo-EM structure determination. *Journal of structural biology,* 180**,** 519-530.

SCHERES, S. H., NÚÑEZ-RAMÍREZ, R., SORZANO, C. O., CARAZO, J. M. & MARABINI, R. 2008. Image processing for electron microscopy single-particle analysis using XMIPP. *Nature protocols,* 3**,** 977.

SCHMITZ, J. E., KURODA, M. J., SANTRA, S., SASSEVILLE, V. G., SIMON, M. A., LIFTON, M. A., RACZ, P., TENNER-RACZ, K., DALESANDRO, M. & SCALLON, B. J. 1999. Control of viremia in simian immunodeficiency virus infection by CD8+ lymphocytes. *Science,* 283**,** 857-860.

SCHULTZ, B. T., TEIGLER, J. E., PISSANI, F., OSTER, A. F., KRANIAS, G., ALTER, G., MAROVICH, M., ELLER, M. A., DITTMER, U. & ROBB, M. L. 2016. Circulating HIV-specific interleukin-21+ CD4+ T cells represent peripheral Tfh cells with antigen-dependent helper functions. *Immunity,* 44**,** 167-178.

SHARMA, S. K., DE VAL, N., BALE, S., GUENAGA, J., TRAN, K., FENG, Y., DUBROVSKAYA, V., WARD, A. B. & WYATT, R. T. 2015. Cleavage-independent HIV-1 Env trimers engineered as soluble native spike mimetics for vaccine design. *Cell reports,* 11**,** 539-550.

SHARP, P. M. & HAHN, B. H. 2011. Origins of HIV and the AIDS pandemic. *Cold Spring Harbor perspectives in medicine,* 1**,** a006841.

SMITH, G. 1990. Vaccinia: virus, vector and vaccine. *Control of Virus Diseases***,** 77-122.

SMITH, G. L., VANDERPLASSCHEN, A. & LAW, M. 2002. The formation and function of extracellular enveloped vaccinia virus. *Journal of General Virology,* 83**,** 2915-2931.

STARCICH, B. R., HAHN, B. H., SHAW, G. M., MCNEELY, P. D., MODROW, S., WOLF, H., PARKS, E. S., PARKS, W. P., JOSEPHS, S. F. & GALLO, R. C. 1986. Identification and characterization of conserved and variable regions in the envelope gene of HTLV-III/LAV, the retrovirus of AIDS. *Cell,* 45**,** 637-648.

STARK, H. 2010. GraFix: stabilization of fragile macromolecular complexes for single particle cryo-EM. *Methods in enzymology*. Elsevier.

STEINMAN, R., GRANELLI-PIPERNO, A., POPE, M., TRUMPFHELLER, C., IGNATIUS, R., ARRODE, G., RACZ, P. & TENNER-RACZ, K. 2003. The interaction of immunodeficiency viruses with dendritic cells. *Dendritic Cells and Virus Infection.* Springer.

STICKL, H., HOCHSTEIN-MINTZEL, V., MAYR, A., HUBER, H. C., SCHÄFER, H. & HOLZNER, A. 1974. MVA-stufenimpfung gegen Pocken. *DMW-Deutsche Medizinische Wochenschrift,* 99**,** 2386-2392.

TARTAGLIA, J., PERKUS, M. E., TAYLOR, J., NORTON, E. K., AUDONNET, J.-C., COX, W. I., DAVIS, S. W., VAN DER HOEVEN, J., MEIGNIER, B. & RIVIERE, M. 1992. NYVAC: a highly attenuated strain of vaccinia virus. *Virology,* 188**,** 217-232.

VAN DIJK, J. & SMIT, J. 2000. Size-exclusion chromatography–multiangle laser light scattering analysis of β-lactoglobulin and bovine serum albumin in aqueous solution with added salt. *Journal of Chromatography A,* 867**,** 105-112.

VARGAS, J., ALVAREZ-CABRERA, A.-L., MARABINI, R., CARAZO, J. M. & SORZANO, C. O. S. 2014. Efficient initial volume determination from electron microscopy images of single particles. *Bioinformatics,* 30**,** 2891-2898.

VÁZQUEZ, M.-I. & ESTEBAN, M. 1999. Identification of functional domains in the 14-kilodalton envelope protein (A27L) of vaccinia virus. *Journal of virology,* 73**,** 9098-9109.

VÁZQUEZ, M.-I., RIVAS, G., CREGUT, D., SERRANO, L. & ESTEBAN, M. 1998. The vaccinia virus 14-kilodalton (A27L) fusion protein forms a triple coiled-coil structure and interacts with the 21-kilodalton (A17L) virus membrane protein through a C-terminal α-helix. *Journal of virology,* 72**,** 10126-10137.

VICTORA, G. D. & NUSSENZWEIG, M. C. 2012. Germinal centers. *Annual review of immunology,* 30**,** 429-457.

VIJAYAN, A., GARCÍA-ARRIAZA, J., RAMAN, S. C., CONESA, J. J., CHICHÓN, F. J., SANTIAGO, C., SORZANO, C. Ó. S., CARRASCOSA, J. L. & ESTEBAN, M. 2015. A chimeric HIV-1 gp120 fused with vaccinia virus 14K (A27) protein as an HIV immunogen. *PloS one,* 10**,** e0133595.

VIJAYAN, A., GÓMEZ, C. E., ESPINOSA, D. A., GOODMAN, A. G., SANCHEZ-SAMPEDRO, L., SORZANO, C. O. S., ZAVALA, F. & ESTEBAN, M. 2012. Adjuvant-like effect of vaccinia virus 14K protein: a case study with malaria vaccine based on the circumsporozoite protein. *The Journal of Immunology,* 188**,** 6407-6417.

VIJAYAN, A., MEJÍAS-PÉREZ, E., ESPINOSA, D. A., RAMAN, S. C., SORZANO, C. O. S., ZAVALA, F. & ESTEBAN, M. 2017. A prime/boost PfCS14KM/MVA-sPfCSM vaccination protocol generates robust CD8+ T cell and antibody responses to Plasmodium falciparum circumsporozoite protein and protects mice against malaria. *Clinical and Vaccine Immunology,* 24**,** e00494-16.

VINUESA, C. G., LINTERMAN, M. A., YU, D. & MACLENNAN, I. C. 2016. Follicular helper T cells. *Annual review of immunology,* 34**,** 335-368.

VOS, J. C. & STUNNENBERG, H. G. 1988. Derepression of a novel class of vaccinia virus genes upon DNA replication. *The EMBO journal,* 7**,** 3487-3492.

WALKER, B. D. & BURTON, D. R. 2008. Toward an AIDS vaccine. *science,* 320**,** 760-764.

WYATT, L. S., CARROLL, M. W., CZERNY, C.-P., MERCHLINSKY, M., SISLER, J. R. & MOSS, B. 1998. Marker rescue of the host range restriction defects of modified vaccinia virus Ankara. *Virology,* 251**,** 334-342.

YAMAMOTO, T., LYNCH, R. M., GAUTAM, R., MATUS-NICODEMOS, R., SCHMIDT, S. D., BOSWELL, K. L., DARKO, S., WONG, P., SHENG, Z. & PETROVAS, C. 2015. Quality and quantity of TFH cells are critical for broad antibody development in SHIVAD8 infection. *Science translational medicine,* 7**,** 298ra120-298ra120.